SEPARATION OF COPPER-OXIDE NANOPARTICLES FROM NANOPARTICLE ENHANCED PHASE CHANGE MATERIAL

by

MOHAMMED HAROON SHEIKH

M.A.R. SHARIF, COMMITTEE CHAIR
A. HAQUE
D. Li

A THESIS

Submitted in partial fulfillment of the requirements for the degree of Master of Science
in the Department of Aerospace Engineering and Mechanics
in the Graduate School of
The University of Alabama

TUSCALOOSA, ALABAMA

2013

ABSTRACT

Phase change materials (PCM) are used in many energy storage applications. Energy is stored (latent heat of fusion) by melting the PCM and is released during re-solidification. Dispersing highly-conductive nanoparticles into the PCM enhances the effective thermal conductivity of the PCM, which in turn significantly improves the energy storage capability of the PCM. The resulting colloidal mixture with the nanoparticles in suspension is referred to as nanoparticle enhanced phase change materials (NEPCM). A commonly used PCM for energy storage application is the family of paraffins (C_nH_{2n+2}). Mixing copper oxide (CuO) nanoparticles in the paraffin produces an effective & highly efficient NEPCM for energy storage. However, after long term application cycles, the efficiency of the NEPCM may deteriorate and it may need replacement with fresh supply. Disposal of the used NECPM containing the nanoparticles is a matter of concern. Used NEPCM containing nanoparticles cannot be discarded directly into the environment because of various short term health hazards for humans and all living beings and un-identified long term environmental and health hazards due to nanoparticles. This problem will be considerable when widespread use of NEPCM is practiced. It is thus important to develop technologies to separate the nanoparticles before the disposal of the NEPCM. This is the motivation behind this study. The primary objective of this research work is to develop methods for the separation and reclamation of the nanoparticles from the NEPCM before its disposal.

It is aimed to find or design separation methods which are simple, safe, and economical. The specific NEPCM considered in this study is a colloidal mixture of dodecane ($C_{12}H_{26}$) and CuO nanoparticles (1% - 5% mass fraction and 5-15 nm size distribution). The nanoparticles are coated with a surfactant or stabilizing ligands for suspension stability in the mixture for a

long period of time. Various methods for separating the nanoparticles from the NEPCM are explored. The identified methods include; (i) distillation under atmospheric and reduced pressure, (ii) high speed centrifugation, (iii) destabilization of the nanoparticles by adding chemical agents thereby inducing gravitational precipitation, (iv) silica-column chromatography, (v) silica adsorption and (vi) nanofiltration These different nanoparticle separation methods have been pursued and the results are presented with detailed process description, analysis, and conclusion.

DEDICATION

This thesis is dedicated to my parents.

LIST OF ABBREVIATIONS AND SYMBOLS

NP	Nanoparticle
NEPCM	Nano Enhanced Phase Change Material
PCM	Phase Change Material
UV	Ultra Violet
Wt	Weight
Ø	Weight %

ACKNOWLEDGMENTS

I would like express my gracious gratitude to Dr. M.A.R. Sharif, the chairman of the thesis committee for selecting me to work on this project and for his continued guidance, support and encouragement which played a phenomenal role in success of this project.

Additional appreciation is given to the advisory committee which consists of Dr. Anwarul Haque for sharing lab facility and valuable inputs and Dr. Dawen Li for encouragement and guidance. Also I would like to thank Dr. Hank Heath from Biology department for his continuous co-operation and tireless support while conducting experiments at his facilities. This section would be far from complete without recognizing Dr. Paul Rupar for allowing us to use his lab facilities and resources as well as for his valuable guidance. I would also like to thank Dr. Jay Khodadadi, Dr. German Mills, and Dr. Robert Jackson from Auburn University for their timely and valuable inputs for improvement and betterment of this work.

Also I would like to take this opportunity to thank all of my friends, NEPCM group colleagues, UA students and critics for their support and encouragement. Also Dr. Kim Lacky at Biology department and Johnny Goodwin and Rob Holler at UA central analytical facility deserve special thanks for their kind co-operation. Gratitude is given to the U.S. Department of Energy for providing funding for this project under the EPSCoR/DOE implement Award Number DE-SC0002470.

The greatest thanks of all goes to my family for their unconditional love, continuous support and un-wearying faith in me from thousands of miles.

CONTENTS

LIST OF TABLES

LIST OF FIGURES

CHAPTER 1

INTRODUCTION

1.1 Phase Change Materials

Ideally all materials exist in three phases; solid, liquid, and gaseous and can change phases depending on the subjected temperature. Thereby all materials are phase change materials. However, in the context of the research presented in this work, Phase Change Materials (PCM) are those materials having relatively low melting points which are melted and solidified easily, such as water, paraffins, salts, fatty acids, esters etc. These materials, with the capability of storing and releasing large amount of heat energy with a slight or no temperature change are widely used as thermal energy storage materials. Thermal or heat energy can be stored either as a sensible heat or latent heat. Sensible heat storage stores/releases thermal energy passively and requires a much larger volume of material to store same amount of energy in comparison to latent heat storage. A PCM changes its phase from solid to liquid as the temperature increases and reaches the melting point and as it melts, the PCM absorbs the heat energy as the latent heat of fusion and the process is endothermic. Similarly, when the temperature decreases and reaches the solidifying temperature, the material changes phase from liquid to solid and the PCM releases the latent heat through an exothermic process [1].

Latent heat storage is an attractive energy storage option. One of the major advantages of the PCM system is the (almost) isothermal release or gain of thermal energy. A PCM is a constant temperature heat source, meaning the PCM stores/absorbs heat energy in the form of latent heat of fusion and then releases thermal energy during solidification; with slight or no

change of temperature. A PCM offers high energy storage density as their latent heat of fusion of PCM is 50-100 times more than the sensible heat [2]. PCM can regenerate thermal energy at high temperature at a melting point slightly lower than the temperature of waste heat. Melting and solidifying processes of the PCM can be repeated for many cycles offering economic benefits. Due to advantages offered by PCM latent heat thermal energy storage, such as low (negligible) temperature variation during phase change cycles, small unit size and high storage density, and relatively constant heat transfer fluid temperature during discharge process, it has been applied to numerous low temperature applications such as solar energy storage, smart housing, heat management of electronics, agricultural greenhouse, and industrial waste heat recovery. Due to the widespread concern about recent energy crisis, PCMs are attracting much attention due to their energy saving energy potential [1-5].

Thermal energy storage (TES), also commonly called heat and cold storage allows the storage of heat or cold to be used later. Hence to be able to retrieve the heat or cold after some elapsed time, the method of storage needs to be reversible. This reversibility is offered by PCMs where they store heat energy by changing phase from solid to liquid via charging process and gives away heat through discharging process leading to PCM freezing. Depending upon the temperature requirement, PCMs can be used for number of applications. Also being quasi-isothermal phase change process it is particularly attractive for transport of temperature sensitive products as it aids to the simplicity of the storage system [6-8].

As the demand for air conditioning increased greatly over the years, large demands of electric power and limited reserves of fossil fuels have led to a surge of interest with efficient energy storage applications. Electrical energy consumption varies significantly during the day and night according to the demand by the industrial, commercial, and residential activities. In hot and cold climate countries, the major part of the load variation is due to the air conditioning and space heating which leads to a differential pricing system for peak and off peak periods

of energy use. Recent discussions on topics like global warming and heat waves along with the increasing demands for cooling systems have brought attention once again to energy efficient systems utilizing renewable energy sources. Hence due to the increase in greenhouse gas emissions and energy crisis, the utilization of renewable energy sources and thermal energy storage are crucial current topics. The thermal energy storage has wide range of applications, e.g., solar energy storage, waste heat recovery, smart housing, temperature control greenhouses, textiles, heat regulation of electronics and so on [4,9-14,16,17].

1.2 Types of Thermal Energy Storage Systems:

To assist and solve the energy related problems thermal energy storage (TES) systems have been developed. The selection of TES is generally dependent on the storage period required, i.e., diurnal or seasonal, economic viability, operating conditions, etc. [1,9].

Three types of TES systems are common in practice:

1) Sensible TES (e.g., water, rock),

2) Latent TES (e.g., water/ice, salt hydrates),

3) Thermo chemical TES (e.g., inorganic substances).

The most common way of thermal energy storage is as **sensible heat storage**. In this case heat transferred to the storage medium leads to a temperature increase of the storage medium as shown in Fig. 1.1. A sensor can detect this temperature increase and the heat stored is thus called sensible heat. In sensible heat storage system, energy is stored or extracted by heating or cooling a liquid or a solid, which *does not change its phase* during the process. A variety of substances like water, heat transfer oils and certain inorganic molten salts, and solids like rocks, pebbles, and refractory are used. The choice of the substances used largely depends upon the temperature level of the application [1].

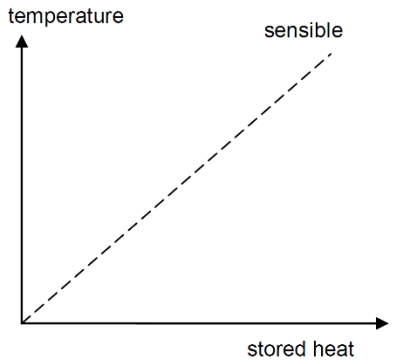

Fig. 1.1. Heat storage as sensible heat leads to a temperature increase when heat is stored.

In case of **latent heat storage** the material (PCM) stores or releases heat by changing its phase at constant temperature. PCM has low temperature range and high energy density of melting – solidification compared to the sensible heat storage. Also PCM can store about 3 to 4 times more heat per volume than is stored as sensible heat in solids or liquids in a temperature interval of 20°C [18]. This can be a significant advantage in many applications like in domestic space heating. As per requirement with the selection of suitable material the phase change by melting and solidification can store large amounts of heat or cold. Also melting is characterized by a small volume change, usually less than 10%. Hence a container can fit the phase with the larger volume, usually the liquid, so the pressure is not changed significantly and consequently melting and solidification of the storage material proceed at a constant temperature. While heat is transferred to the storage material upon melting, the material maintains its temperature constant at the melting temperature, also called phase change temperature [9].

The storage of heat of melting takes place at constant temperature and is referred as latent heat and the process is known as latent heat storage. Due to the small volume change, the stored heat is equal to the enthalpy difference between the solid and liquid phase. This

enthalpy change is known as melting enthalpy, or heat of fusion, or solid-liquid phase change enthalpy [8,9].

In **thermochemical** systems of heat storage, heat is stored or released by using reversible endothermic chemical reactions. The reactions involve the breaking and forming of bonds such that a great deal of energy can be stored. Although not currently viable, a variety of reactions are being explored [9].

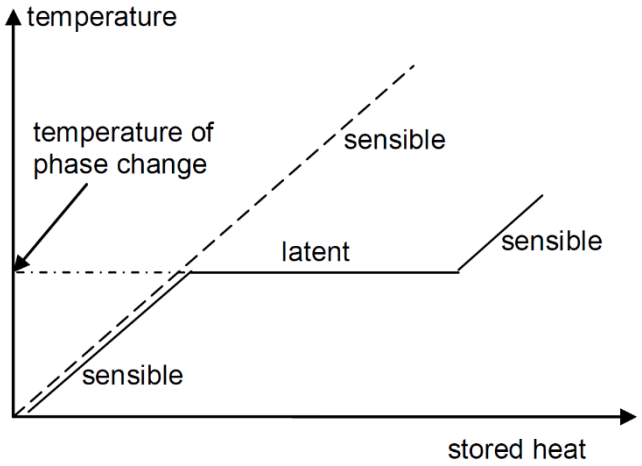

Fig. 1.2. Heat storage as Latent heat storage showing phase change temperature

1.3 Classification of Phase Change Materials:

According to the phase change states, PCMs are divided into three categories: solid-solid, solid-liquid and liquid-gas. In general, the term "latent heat" refers to the heat of solid-solid, solid-liquid, and liquid-vapor phase changes as shown in Fig 1.3. However, the terms "latent heat storage" and "phase change material" are commonly only used for the first two kinds of phase changes and not for liquid-vapor phase changes because liquid-vapor (gas) PCMs have no practical application due to larger volume change during phase change which leads to a storage problem. In a liquid-vapor phase change, the phase change temperature strongly depends on the boundary conditions, and therefore the phase change is not just used for

storage of heat alone. Usually it is connected with a pressure and a temperature difference between charging and discharging [10-17,19,20].

1.4 Materials Used as PCM:

There are large numbers of phase change materials that melt and solidify at a wide range of temperatures, making them attractive for number of energy storage applications. A material to be used as PCM should possess some desirable thermo-physical, kinetic and chemical properties. Based on the information available from different studies [6,21-28] the essential characteristics of a good PCM are:

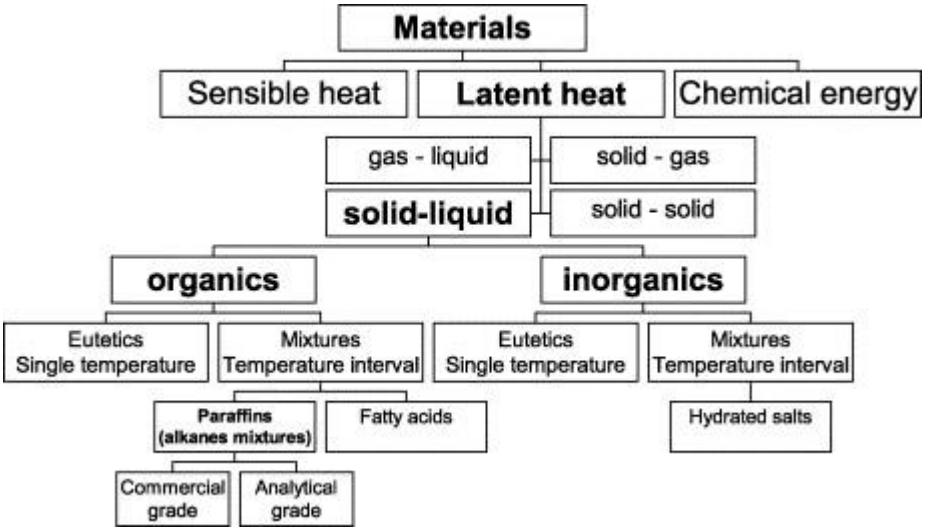

Fig. 1.3 Classification of PCM [20, 24]

- **Thermo physical Properties:**

- High latent heat of fusion per unit volume
- High thermal conductivity of both solid and liquid phases
- Melting temperature in desired operating temperature range
- Small volume change on phase transformation
- Small vapor pressure at operating temperature
- Congruent melting for a constant storage capacity of material with each cycle
- High specific heat to provide additional significant sensible heat storage
- High density

- **Chemical Properties:**

- Freeze/melt cycle reversibility
- Non-corrosiveness
- Non-toxic, non-flammable, and non-explosive

- **Nucleation and crystal growth Requirements:**
  - High nucleation rate to avoid sub-cooling of the liquid phase during solidification, assuring phase change cycle occurs at same temperature
  - High rate of crystal growth, so that system can meet the demand for heat recovery from the storage system

- **Economics:**

- Abundant and easily available
- Cost effective
- Easy recycling and treatment

In general, materials to be used for phase change thermal energy storage must have a large latent heat and high thermal conductivity. They should possess a melting temperature lying in the practical range of operation, melt congruently with minimum sub-cooling and be chemically stable, low in cost, non-toxic, and non-corrosive. The materials exhibiting most of these properties can be used as PCM. As shown in Fig. 1.4, PCMs are primarily divided into organic and inorganic materials. Organic materials are further classified as paraffin and non-paraffin (fatty acids, eutectics and mixtures). Experimental evidences of melting and freezing cycles using these materials/material composites showed that they crystallize with little or no sub-cooling and are chemically and thermally very stable and non-corrosive [7,29]. However, they suffer from some inherent disadvantages like flammability, low thermal conductivity and low phase change enthalpy. Inorganic materials are further classified as eutectics and compounds.

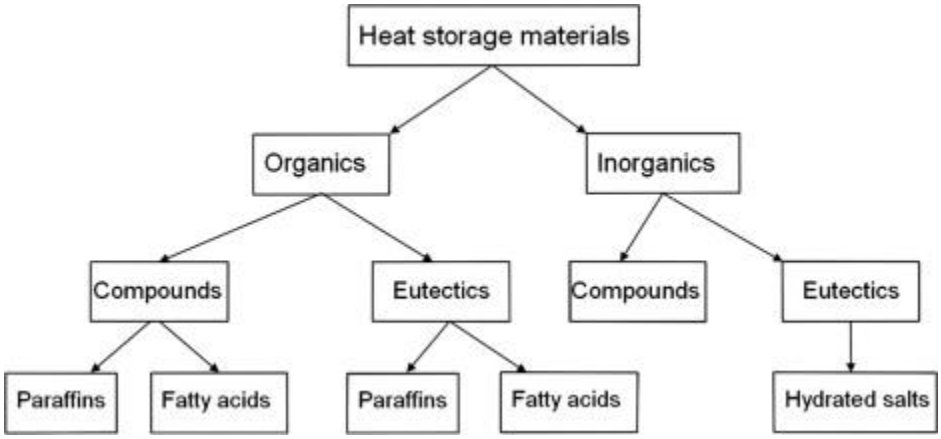

Fig.1.4 Families of phase change heat storage materials [6,9,22]

Inorganic materials cover a wide temperature range. Compared to organic materials, inorganic materials usually have similar melting enthalpies per unit mass, but higher ones per unit volume due to their high density also they are non-flammable. Their main disadvantages are sub-cooling, phase segregation, incompatibility with metals since severe corrosion can be developed in some PCM-metal combinations [9]. Materials that have been studied to work as PCM during the last 40 years are salt hydrates, paraffin waxes, fatty acids, and eutectics of organic and non-organic compounds.

1.5 Paraffins as PCM:

Depending upon the applications and corresponding temperature requirements, a major field of research in area of energy storage is the development of PCMs which maintains good heat storage when required, followed by heat release. Based on their melting temperature there are variety of materials which qualify as PCM [7]. For different applications, temperature requirements varies like low temperature (e.g., freezing for food storage), medium temperature (e.g., house heating – cooling) and high temperature (e.g., for cooking) hence suitability of a PCM is governed by its phase change temperature. The paraffins are a mixture

of pure alkanes which have quite a range of the phase change temperature. Some paraffins are an attractive alternative to chilled water for comfort cooling applications because they enable cold storage with high energy density. Paraffin waxes were found to have melting temperature from -12°C to 71°C with a latent heat of 128 kJ/kg to 198 kJ/kg [30]. The phase change or melting temperature is normally a function of the molecular properties. For paraffins it is found that molecular weight and hence number of carbon atoms is a linear function of melting temperature [7,9]. Also by mixing different paraffins, different non-paraffins, or paraffins with non-paraffins different melting temperature can be obtained [29,30].

Paraffins (alkanes) are the saturated hydrocarbons which consists of hydrogen and carbon atoms only and are held together by single bonds in a non-cyclic or linear (can be branched) chain form. The alkanes with cyclic structure are known as cycloalkanes. The non-cyclic alkanes have the general chemical formula as C_nH_{2n+2} where n being the number of carbon atoms. The physical and chemical properties of alkanes are mainly governed by the number of carbon atoms and corresponding hydrogen atoms. Hence according to the number of the constituent atoms and eventually their molecular weight, alkanes are found in gaseous, liquid, and solid states offering different melting points to be used as phase change temperatures, as shown in table below [31-33].

As it is explained earlier, alkanes with liquid-gas mode of phase change are not efficient as an energy storage medium due to high volumetric expansion leading to storage issues. Hence further discussions would pertain to the non-gaseous alkanes only. From the Table 1 it is evident that for alkanes in general, as the number of carbon atoms increases thereby subsequent increase in number of hydrogen atoms, their thermo-chemical properties vary in direct relation.

For example alkane with lower carbon atoms, e.g., pentane with 5 carbon atoms has melting temperature and density lower than that of hexane and all the other alkanes with higher carbon content. As carbon content of an alkane increases its properties as well as its state changes and for higher carbon content (higher than 16 C atoms) alkane exists as solid.

Table 1: Properties of alkanes used as PCM

Alkane	Formula	No. of Carbon atoms	Boiling point (°C)	Melting point [°C]	Density ($g \cdot cm^{-3}$) (at 20 °C)	State (at 20 °C)
Methane	CH_4	1	-162	-182	gas	gas
Ethane	C_2H_6	2	-89	-183	gas	gas
Propane	C_3H_8	3	-42	-188	gas	gas
Butane	C_4H_{10}	4	0	-138	gas	gas
Pentane	C_5H_{12}	5	36	-130	0.626	liquid
Hexane	C_6H_{14}	6	69	-95	0.659	liquid
Heptane	C_7H_{16}	7	98	-91	0.684	liquid
Octane	C_8H_{18}	8	126	-57	0.703	liquid
Nonane	C_9H_{20}	9	151	-54	0.718	liquid
Decane	$C_{10}H_{22}$	10	174	-30	0.73	liquid
Undecane	$C_{11}H_{24}$	11	196	-26	0.74	liquid
Dodecane	$C_{12}H_{26}$	12	216	-10	0.749	liquid
Hexadecane	$C_{16}H_{34}$	16	281	18	0.773	solid-liquid
Icosane	$C_{20}H_{42}$	20	343	37	0.7886	solid
Triacontane	$C_{30}H_{62}$	30	450	66	0.81	solid
Tetracontane	$C_{40}H_{82}$	40	525	82	0.817	solid
Pentacontane	$C_{50}H_{102}$	50	575	91	0.823	solid
Hexacontane	$C_{60}H_{122}$	60	625	100	0.827	solid

Vapor pressure of a liquid is the pressure at which liquid boils at a particular temperature and hence the vapor pressure is a function of the liquid temperature. Vapor pressure is determined by the kinetic energy of molecules which is related to temperature, mass, and velocity of molecules. When the liquid is heated and the temperature reaches the boiling point, the average kinetic energy of the liquid particle is sufficient to overcome the forces of attraction that holds molecules in the liquid state. This results in breaking of molecules away from liquid to form a gaseous phase. Molecules with the most independence in individual

Brownian motions achieve sufficient kinetic energy to escape into the vapor phase at lower temperatures. The vapor pressure will be higher and therefore the compound will boil at lower temperature. The molecules that bond with each other through a variety of intermolecular forces or interact strongly with each other cannot move easily or rapidly and therefore do not achieve the kinetic energy necessary to escape the liquid state. Hence the molecules with strong intermolecular forces will have higher boiling points. This is mainly due to the greater intermolecular London attractive forces which increases as the number of electrons per molecule, molecular polarity and contact between chains increases with increasing chain length [34] This explains the change in state of molecule due to change in number of carbon atoms present in case of alkanes.

Fig. 1.5 shows variation of melting temperature and density of alkanes with respect to number of carbon atoms. Evidently, alkanes offer wide range of phase change temperatures and qualify to be used as phase change material for thermal energy storage applications.

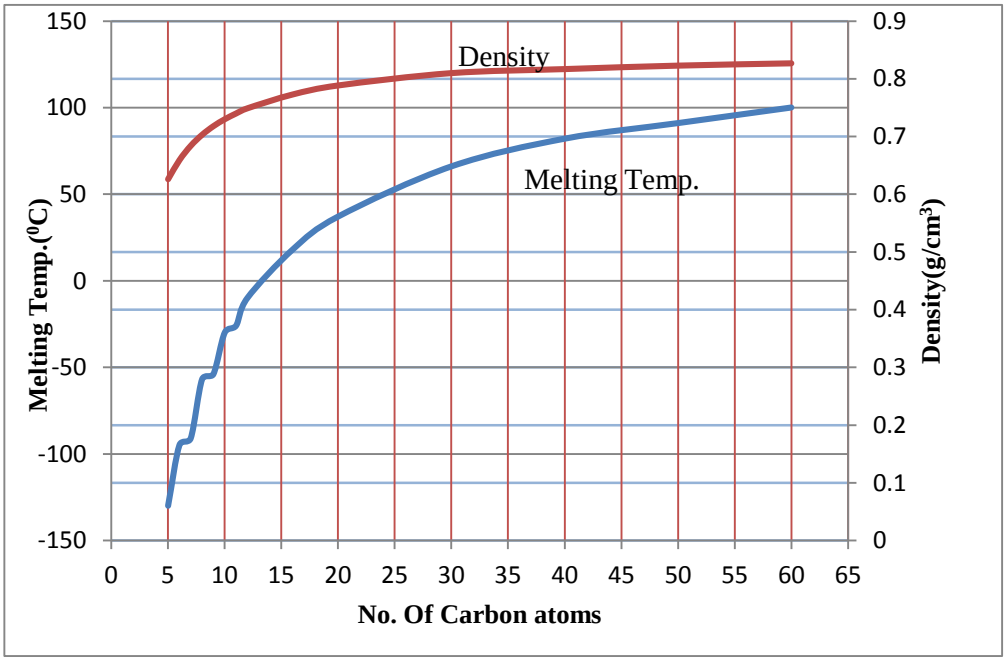

Fig.1.5 Alkane Melting point and Density variation with number of Carbon atoms

Alkanes are also referred as thermo-adjustable, because the phase change temperature of alkane can be changed by varying the number of carbon atoms. Thus, it is possible to vary the

number of carbon atoms or form different molecular alloys to obtain a continuous variation of phase change temperature within certain ranges. Hence, with varying phase transition temperature requirement according to specific applications, alkanes offer all possible temperature ranges either as basic available form or as a tailored alloy.

In this research, dodecane ($C_{12}H_{26}$) with phase transition temperature of -10°C was selected as the base fluid. Being liquid at room temperature dodecane can be stored conveniently and possess most of the required properties of phase change material like; inert, non-poisonous, chemically stable, etc. However, thermal conductivity of dodecane, and alkanes in general, is not very attractive (~0.2 W/m°C) to be considered as an efficient phase change material. This low thermal conductivity value limits applications of alkanes for high temperature LHS systems. To store a certain amount of heat, the low thermal conductivity of paraffin results in higher volume requirement than the material with higher thermal conductivity. Therefore, to make paraffin suitable for applications requiring higher thermal conductivity, different approaches have been adopted, e.g., suspension of metal rods, suspension of metal plates, and suspension of metal nanoparticles [9,35-37]

CHAPTER 2

NANOPARTICLES

2.1 Nanoparticle Basics

A nanoparticle is an ultrafine particle whose size is measured in nanometers (nm) which in metric system is same as one-billionth of a meter (10^{-9}m). In general, nanoparticles refer to ultrafine particles whose sizes are in the range of 1 nm to several hundred nanometers depending on materials, fields and applications [38-40].

There is no accepted international definition of a nanoparticle and term ‘nanoparticle’ is utilized to refer to particles of size < 100 nm or < 50 nm, at times for any particle 10 nm or less and occasionally < 1 μm. Based on size (diameter) range they also known as fine particles covering 100-2,500 nm range while ultrafine particles have dimensions 1-100 nm [41,42]. One definition given in the new PAS71 document developed in the UK is: "a particle having one or more dimensions of the order of 100 nm or less".

"Novel properties that differentiate nanoparticles from the bulk materials, are typically develop at a critical length scale of under 100 nm. “The "novel properties" mentioned are entirely dependent on the facts that at the nano-scale, the physics of nanoparticles, meaning their properties, are different from the properties of the bulk material. This makes the size of particles or the scale of its features the most important attribute of nanoparticles. The properties of many conventional materials change when formed from nanoparticles. This is typically because nanoparticles have a greater surface area per unit weight than larger particles; this causes them to be more reactive to certain other molecules.

Nanoparticles are of great scientific interest as they are effectively a bridge between bulk materials and atomic or molecular-structures. A bulk material should have constant physical properties regardless of its size, but at the nano-scale size-dependent properties are often observed. Thus, the properties like melting point, dielectric constant, thermal behavior, optical behavior, mechanical behavior of materials change as their size approaches the nano-scale and as the percentage of atoms at the surface of a material becomes significant. At nano-scale, materials exhibit various sizes dependent properties like quantum confinement effect is observed in semiconductor particles, super-paramagnetism is evident in magnetic materials and surface plasmon resonance is observed in some metal particles. For bulk materials larger than one micrometer (or micron), the percentage of atoms at the surface is insignificant in relation to the number of atoms in the bulk of the material. The interesting and sometimes unexpected properties of nanoparticles are therefore largely due to the large surface area of the material, which dominates the contributions made by the small bulk of the material [38-42].

Due to their unique properties nanoparticles of different materials have been used in wide range of applications in different fields of engineering and science. In biomedical field NPs have been successfully used for applications like drug delivery, cancer treatment, sunscreen lotion, etc. In chemistry NPs are utilized to synthesize new materials with unique properties for applications like water purification. In engineering field NPs are employed to improve mechanical and thermal properties of materials for different applications like thermal conductivity improvement of heat transfer fluids, strength enhancement for materials used in vehicles and space-crafts, improving lubricating properties of oils, etc. Hence these novel particles have been proved to be equipped with vast potential to solve number of technological and medical issues and have been used in numerous applications [43,44].

2.2 Classification of Nanoparticles:

Nanoparticles can be classified according to different properties. Major classification is as follows:

1. Based on material: metallic, non-metallic, and composite.
2. Based on shape: spherical, rod-shape, elliptical, etc.
3. Based on properties such as: magnetic, charged, and neutral.

2.3 Synthesis of Nanoparticles:

Since their introduction in 1990 different approaches have been developed to synthesize NPs of different sizes and properties using different materials. Some of them are listed below [43,45].

1. Sol-gel Process
2. Wet chemical synthesis
3. Physical vapor deposition
4. Aerosol processing
5. Inert gas condensation method
6. Chemical vapor deposition
7. Mechanical alloying/milling
8. Micro-emulsion
9. Biological methods

Broadly there are two approaches to manufacture nanoparticles and above mentioned methods are one of those types [38,39].

1. Top-down: In this approach material decreases its size from large to nano-scale hence one starts with coarse material and applies forces to disintegrate into the nanosize range. Example: Pearl/ball milling, high-pressure homogenization.

2. Bottom-up: In this approach nanoparticles are produced by assembling atoms or molecules together. It is a classical precipitation method in which molecules in a solution are associated to other molecules to form solid particles of nano-size.

Selection of a synthesis method is governed by size of nanoparticles, amount of nanoparticles required, and economic considerations. For example: bigger size nanoparticles of size 400 nm or high, top-down approach is preferred due to its simplicity and low cost.

2.4 Properties of Copper-oxide Nanoparticles:

As explained earlier in section 1.5, alkanes or paraffins are most suitable material to qualify as a PCM except that their thermal conductivity is poor. Hence nanoparticles are used as a means to enhance thermal conductivity of paraffins. In this research work copper oxide (CuO) nanoparticles have been used due to various reasons [46,47] to improve thermal conductivity of dodecane used as a base fluid [48,49]. The copper oxide (CuO) NPs stabilized by capping with sodium oleate acid (SOA, $C_{18}H_{33}NaO_2$) were synthesized and provided by colleagues from Department of Chemistry and Biochemistry, Auburn University, Auburn, AL. These nanoparticles are prepared using wet chemical method presented in greater detail elsewhere [48,49]. Fig. 2.1 (a) shows TEM image of CuO/SOA which reveals particle size distribution ranging from 3 to 29 nm.

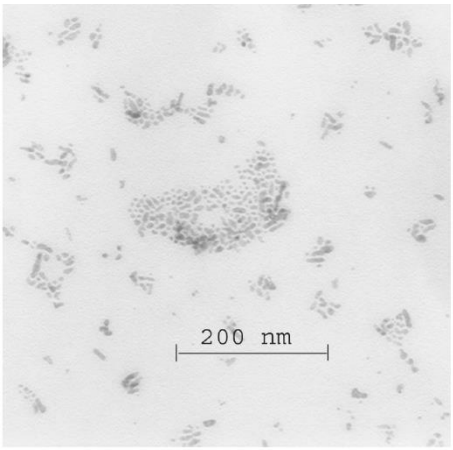

Fig. 2.1(a) TEM image of CuO/SOA Nanoparticles

A histogram presented in Fig.2.1 (b) clearly indicates 90% of the size distribution exists within the range of 5 to 15 nm with dominant size being 9 nm [49].

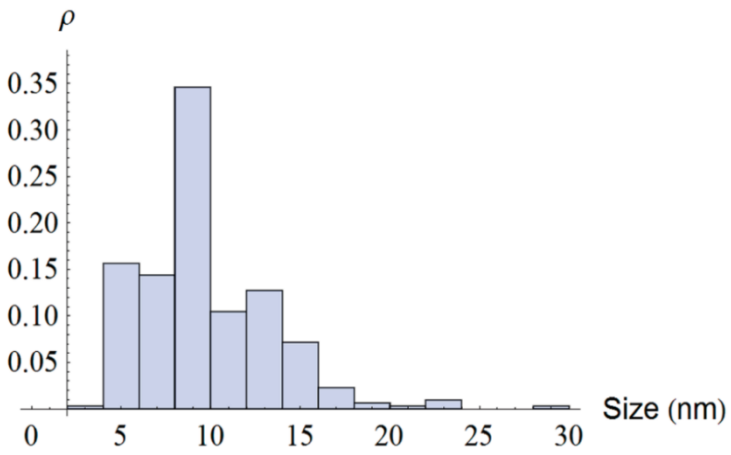

Fig. 2.1(b) CuO particle size distribution assessed over 300 NPs [48,49]

The basic properties of CuO NP can be summarized as:

Size: Peak size distribution at 9 nm with size range 5-15 nm.

Shape: Spherical.

Charge: Not withstanding partial charges, the CuO particles possess no net, permanent charge.

Molecular weight: 79.54 g/mol.

Magnetic Behavior: Non-magnetic.

Color: Black

CHAPTER 3

NANOPARTICLE ENHANCED PHASE CHANGE MATERIALS

3.1 Nanoparticle Enhanced Phase Change Materials

Since the introduction of nanofluids in mid-nineties, it had attracted many applications like energy storage, heat exchangers, refrigeration, lubrication, etc. Nano-materials exhibit unique properties which have been utilized to serve different applications ranging from science, engineering to biology and personal care as explained in previous sections. At nano-level, one of the most prominent feature gets developed is high surface area of the nano-structures, e.g., nano-particles, nano-wires, etc. As heat transfer is a surface phenomenon, addition of nano-structures to heat transfer fluids and mediums enhances their heat transfer capabilities. As explained in section 1.5, though paraffins (alkanes) qualify as an outstanding PCM they lack in heat transfer ability. Hence in order to use paraffins as a PCM, it is required to improve their thermal conductivity which is achieved by embedding or incorporating nanostructures with paraffin. Thermal conductivity improvement by dispersing ultra-fine (nanosize) particles in liquids was first reported in 1993 [50] followed by introduction of term "nanofluids" in 1995 [51] referring to new class of fluids with superior thermal properties. A fluid containing nano-materials with high thermal conductivity tailored specially to store energy is known as nanoparticle enhanced phase change material (NEPCM) [52].

Another term commonly used in exchange with NEPCM is nano-colloid which means nanoparticles are being stabilized to form NEPCM and are colloidal form [48]. Hence adding thermally active nano-particles lead to increase in thermal conductivity of PCM which can hold and release heat at higher rate. Addition of nanoparticles to improve thermal

conductivity of fluids has been reported in numerous articles like: using Cu nanoparticles, nucleate pool boiling heat transfer coefficient of R113/oil was found to be increased by over 23 % by decreasing size of nanoparticles from 80 nm to 20 nm [53], improved thermal conductivity of ethylene glycol based nanofluids using Cu nanoparticles [51,54], volume fraction or concentration of added NPs and specific surface area governs thermal conductivity. For heat transfer applications, effect of different types of nanoparticles metallic, non-metallic with different size variations from 5 nm to several hundred nm in combination with different types of base fluids like water, glycol, etc., have been reported [46,47,55-59].

In this research work dodecane ($C_{12}H_{26}$) was used as a base fluid which is purchased from Vertellus Health & Specialty Products LLC, Indiana, USA [60] and used as is without any further processing. Table 2 presents basic physical and chemical properties of dodecane. For additional information refer Material Safety Data Sheet included in appendix (A). CuO nanoparticles (presented in section 2.4) were used to enhance thermal properties of dodecane.

Table 2: Properties of Dodecane [60]

Physical State	Liquid	**Flash Point:**	74°C
Appearance	Water White (colorless)	**Vapor Pressure: (mm Hg @ 20°C)**	5.9
Relative Density: (Water = 1)	0.753 @ 25°C	**Vapor Density: (Air = 1)**	5.9
Boiling Point:	216°C	**Solubility in Water**	Insoluble
Freezing Point:	-10°C	**Auto Ignition Temperature**	203°C

3.2 Preparation of NEPCM

Nearly homogeneous NEPCM samples were prepared by dispersing desired amount of CuO NPs into the base PCM, i.e., dodecane. The samples were prepared by following a mass fraction approach. In this approach, density of the NPs and dodecane was used to find a required NP concentration (mass) for a particular volume of NEPCM. The amount of CuO

NPs required for preparation of nanofluids is calculated using law of mixtures, which is given by

$$\%\ volume\ conc.\ (\phi_{vol})\ = \frac{W_{CuO}}{\rho_{CuO}} \Big/ \left(\frac{W_{CuO}}{\rho_{CuO}} + \frac{W_{bf}}{\rho_{bf}}\right)$$

where subscripts CuO and bf are referred to NPs and base fluid respectively. In case the corresponding mass fractions are of interest, following relations are used for conversion for a two component system:

$$\phi_{vol} = \phi_{wt}\rho_{bf} / [\phi_{wt}\rho_{bf} + (1 - \phi_{wt})\rho_{CuO}]$$

$$\phi_{wt} = \phi_{vol}\rho_{CuO} / [\phi_{vol}\rho_{CuO} + (1 - \phi_{vol})\rho_{bf}]$$

After determining mass of NPs required, next step followed is dispersing this NP mass in required volume of dodecane, then heating and stirring rigorously at 60°C on a hot-plate magnetic stirrer (SP131325Q, Thermo Fisher, Dubuque, IA) shown in Fig.3.1 for 30 minutes to attain a stable colloidal suspension. This mixing in combination of heating produced a

Fig.3.1 NEPCM Preparation

stabilized NEPCM, which appeared like a black ink and was used for further experiments. Using these sodium-oleate stabilized CuO nanoparticles, long-term stability of colloidal

suspensions in various hydrocarbons (hexane, octane, dodecane, and eicosane) was observed both qualitatively and quantitatively for mass fraction up to 20 wt% corresponding to volume fraction of about 3 vol% [48,49].

In this work, only dodecane was considered as the base fluid to prepare NEPCM and conduct different trials. Using the approach explained above various concentrations (wt %) of NEPCM including 0.5, 1.0, 2.0, 3.0, 5.0 have been utilized to conduct trials using different methods explained in successive sections. Table 3 presents mass of NPs required to prepare 100 ml of NEPCM of different concentrations.

Table 3: Amount of CuO NP required

Sr.No.	NEPCM Volume (mL)	NP wt %	NP mass required (g)
1	100	0.5	0.3798
2	100	1	0.7597
3	100	2	1.5330
4	100	3	2.3202
5	100	5	3.9384

CHAPTER 4

PARTICLE SEPARATION METHODS

Separation of particles/impurities from a solid-liquid mixture has been an age old problem. Various separation methods have been developed for various types of applications over the years. The separation method for a specific class of solid-liquid mixture depends on various factors such as the size of the particles, type/class of the liquid, mass/volume fraction of the particles in the mixture, physical properties of the base liquid and the particles, etc. In this chapter, various available and potential particle separation methods and the associated processes are described. As mentioned earlier, the main objective of this research is to develop efficient, effective, and economical methods for the separation of nanoparticles from colloidal mixture of the nanoparticles in a base fluid. Specifically, separation of CuO nanoparticles from a colloidal mixture in alkanes such as dodecane is considered. This colloid is designated as Nanoparticle Enhanced Phase Change Material (NEPCM).

After extended survey of the existing literature, several particle separation methods have been identified. These are; (i) Filtration, (ii) Distillation, (iii) Centrifugation, (iv) Magnetic Separation, (v) Electrophoresis, (vi) Chromatography, and (vii) Chemical Methods.

4.1 Filtration

Filtration primarily works on size-exclusion principle and has been widely used to separate impurities of different size ranges, e.g., nano, micro, or higher. For micro or bigger size impurities or particles, filtration is basically a sieving mechanism where large size entities get trapped at filter/membrane surface allowing only small entities to pass through depending on filtration membrane pore size rating. However, at nano-level, filtration becomes complex in terms of increased fouling and pressure requirements and is no longer size-exclusion

dependent only. Separation of nanoparticles or nano-size entities from a solution dates back to late 1950's when reverse osmosis (RO) was established as a process primarily for desalination of water. In 1970's relatively low pressure RO membranes were developed yielding higher water flux with added advantages of retaining essential minerals. Such membranes with lower rejections of dissolved components with higher water permeability proved to be great improvement for separation technology. These low-pressure RO membranes are referred as "Nanofiltration" membranes [61,62]. Nanometer-sized particles show unique physical and chemical properties that are different from those of bulk materials depending on their sizes and shapes due to the quantum confinement effect [63-67]. Nano-filtration is a process intermediate between reverse osmosis and ultrafiltration that rejects impurities or molecules which have size in designated nanometer range of membrane. This range of membrane is often specified in terms of molecular weight cut-off ration (MWCO), which is basically a number indicating capacity of membrane to hold 99% of the molecules or particles of size greater than specified MWCO rating. Different membrane suppliers have different rules and guidelines to make selection of membrane for an application. Though different theoretical models have been proposed since its introduction in 1980s, this method of separation mechanism has long been debated as pure convection (sieving) or pure diffusion or combination of both. Some nanofiltration membranes known as "activated membranes" have surface charge to aid in filtration while processing charged solute or solvent in the sample [62,63,68-72]

4.2 Distillation

Distillation is a common and well-known process for separating miscible fluid mixture based on differences in volatility between the components. Apart from conventional distillation systems various other configurations of distillation unit are available like membrane distillation, vacuum distillation, column distillation, etc. Distillation is primarily used in

petrochemical industries for separation and purification purposes [73-76] When size and shape based separation process like filtration, centrifugation, and electrophoresis becomes challenging due to small size of impurities or complexity of solution formation, distillation serves the purpose.

4.3 Centrifugation

Centrifugation is one of the simplest methods for the separation of impurities or particles from a liquid, which works on the principle of density gradient of constituent elements in solution. This is the most convenient method of separation as it does not rely on any liquid-solid phase interactions and specific chemical reactions pertaining to the sample. Due to its simplicity of operation and high efficiency, centrifugation is widely used for chemical and biological applications [77-81].

4.4 Magnetic Separation

Magnetic separation has been studied for many years and is usually applied for metallurgical, wastewater treatment, food processing, chemistry and biological separations in the form of batch or flow through magnetic separators. The basic principle behind magnetic separations is remarkably simple and old. It relies on the simple fact that materials with differing magnetic moments experience different forces in the presence of magnetic fields. Hence the use of this method of separation is straightforward in mixtures where a magnetic component is known to exist [82-89].

4.5 Electrophoresis

Electrophoresis is one of the most powerful separation techniques used to separate a variety of differently sized electrically charged materials. Here, separation mechanism relies upon materials having surface charges; typically charges of nanoparticles arising from the sorption of ions onto the surface of the nanoparticles during their preparation. Different particles

display different specific mobility during electrophoresis under the influence of an external applied voltage because of different charge to size ratios which is utilized for separation. Electrophoresis is available in different configurations like gel, capillary, etc., to serve wide range of applications which makes it suitable for separating, analyzing and characterizing chemical, biological, and metallurgical entities [90-95].

4.6 Chromatography

Chromatography is another process where separation is carried out by difference in physical and chemical properties (size, density, affinity, etc.) of constituents present in the solution. In order to suit different applications, there are different types of chromatography such as gel chromatography, column chromatography, gas chromatography. It is widely used for separation and characterization of polymers, molecules, nanoparticles, and biological entities due to its simplicity and low cost of operation [96-98].Some of these methods have been developed largely for characterization and analysis of bio-medical applications and are limited to handling fluids like water, blood, proteins, etc.

Being a universal solvent with simple molecular structure, water aids simplicity and cost-effectiveness to most of the separation process particularly to nano-filtration. On contrary, for non-aqueous samples nano-filtration becomes highly complex and expensive even for lab scale applications. Also most of these size dependent methods work with high degree of efficiency for larger particles/impurities, e.g., 50 nm (size of biological entities like virus, bacteria, etc.) and higher. For smaller size particles in the range of 1-25 nm, the efficiency of the methods suffer greatly while some of them remains unsuitable. For example, separation of impurities using magnetic separation or electrophoresis demands components to be separated to possess magnetic or electric component, respectively, without which these methods become non-applicable.

As explained earlier the nano-colloid under consideration is a mixture of dodecane as base fluid and copper oxide (CuO) nanoparticles of size 5-15 nm with average size being 9 nm. Producing a stable mixture of the colloidal mixture of the nanoparticles and the base fluid has two fundamental challenges. The first is to prevent particle agglomeration and the second is to prevent gravitational precipitation. Both agglomeration and precipitation decrease the effectiveness of the nanoparticles. In order to keep the nanoparticles suspended and maintain uniform/homogeneous dispersion in the base fluid for a long and effective useful life, they are chemically treated with suitable surfactants before mixing into the base fluid. As the CuO particles do not carry any charge leading to electrically and magnetically neutral behavior the only route to restrict the agglomeration is by placing a barrier between two approaching particles. This is achieved by coating nanoparticles with stabilizing agent/surfactants (Fig. 4.1a) also known as ligand which acts like a cushion between the individual particles. For the present case, the CuO nanoparticles are coated with sodium oleate ($C_{18}H_{33}NaO_2$). This stabilizer/surfactant forms numerous ligands on the particle surface which have a thread or rope like structure as shown in Fig. 4.1a. Thus the nanoparticles have average mass composition of 69% copper oxide and 31% sodium oleate with an uncertainty of ±1.4%. The polar head group of these ligands associates with particle surface whereas non-polar tail interacts with hydrocarbon solvent (dodecane) [49]. Hence under the influence of these ligand nanoparticles form a repulsive matrix as shown in Fig. 4.1b, resulting in highly stable colloid. This form of stabilization is known as steric stabilization.

By comparing process requirements of different separation methods explained before with morphology of nanoparticles and properties of nano-colloid, suitable potential methods can be determined. Being electrically and magnetically immobile, the CuO nanoparticles render electrophoresis and magnetic separation processes unsuitable. As NEPCM under consideration is non-aqueous based colloid, filtration at nano-level becomes highly complex

and cost intensive option. Another approach not explained above is destabilizing the nanoparticles by removing stabilizing ligands from their surfaces. As an order of magnitude difference exists between density of CuO and dodecane, unstable nanoparticles are presumed to precipitate under the action of gravity.

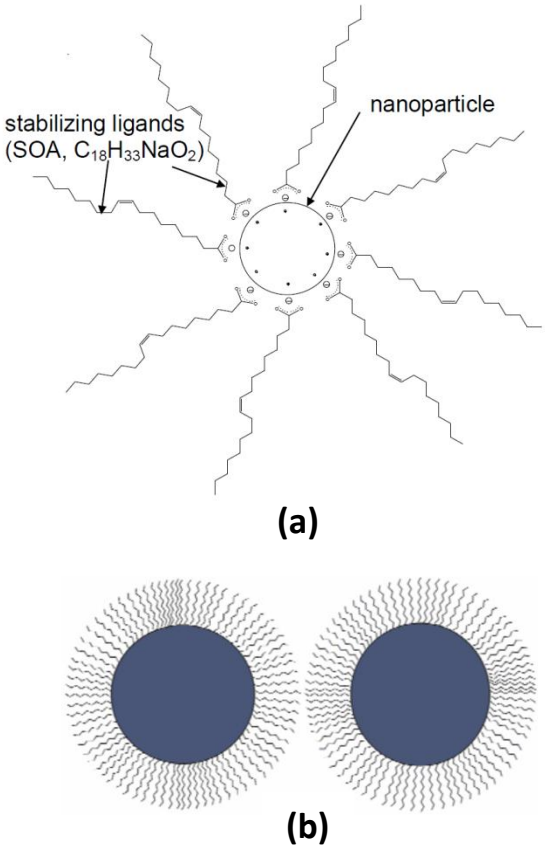

Fig. 4.1. (a) Schematic diagram of a nanoparticle with long ligands coated on its surface serving as the stabilizing cushion layer, (b) Ligands on particle surface to provide a physical barrier (cushion) which prevents particle contact and subsequent agglomeration [49].

Keeping in mind the project objectives, the NEPCM colloidal properties, and process requirements; distillation, centrifugation, chromatography, and destabilization of the nanoparticles were found to be the best suitable methods to achieve the separation of the nanoparticles in an efficient and cost effective manner. Throughout the course of this study, these various nanoparticle separation methods are attempted and tried. Some of the methods

proved to be very successful while others were less or partially successful. Detailed description of the separation methods, the qualitative and quantitative results, and the precise conclusion and recommendations about the suitability of these methods for the separation of the nanoparticles from the base fluid are presented, analyzed, discussed in the following chapter.

CHAPTER 5

RESULTS, ANALYSES, AND DICUSSIONS

5.1 Distillation

Normally, distillation is used to separate a pure liquid from a mixture of a few liquid components of different volatility or boiling point. In its simplest form of distillation [99-104], the liquid mixture is heated in a container until the liquid component with lower boiling point is vaporized followed by condensation in a condenser which is collected as distillate. Distillation has been one of the oldest and primary methods to purify various liquids. The widespread use of distillation is attributed to its operational simplicity and degree of purity offered. It is the best available method for the separation applications where purity is of prime importance. Distillation was invented to purify water to be used for human consumption and reportedly solar energy was employed to carry out distillation. Owing to its low resource requirements and high purification efficiency, eventually it had been established as an attractive alternative for different separation applications including chemical, biological, and petro-chemical processes. Reportedly, distillation is by far the most widely used separation process in chemical process industry. Petroleum refining and chemical industries are two of the most separation-intensive industries which employ distillation as the primary process to carry out separation of olefins from paraffins. Distillation is also used widely in application involving extraction and characterization of hydrocarbons and analysis of hydrocarbons [105-109].

Also distillation is employed to carry out isotope separation like purification of oxygen-18 and other purification applications. Distillation involves both saturated liquid and vapor phase

during operation hence each pressure corresponds to a certain bubble and/or dew point temperature. This means with increasing pressure the temperature also increases accordingly. At atmospheric pressure, several inorganic and light hydrocarbon components have a boiling point well below 0 °C and a larger number of hydrocarbons have boiling points up to and less than 100°C, whereas a great number of important fine chemicals boils well above 200°C. Due to this higher boiling temperature there is a tendency of degradation of component. Hence, to prevent thermal degradation of distilled material, the operating pressure has to be accommodated to allow most economical operation. In case of high-molecular weight (heavy) components this implies distillation under vacuum conditions and for light components distillation under high pressure. Hence, depending on the type of application and material being processed distillation operating requirements vary. Over the period of few decades, various distillation configurations have been invented and are used widely depending upon the application requirements like dry, stream, vacuum, column with straps or without, membrane distillation, etc. [110-113]. Fig. 5.1 shows schematic diagram for atmospheric pressure distillation process.

The distillation process can also be useful to separate suspended solid particles from a solid-liquid mixture. In the present context, the separation of the nanoparticles from the NEPCM can be achieved by taking the base fluid out of NEPCM leaving behind the nanoparticles. This can be accomplished by evaporating the dodecane (base fluid) using a distillation process. Distillation can be conducted at different pressures and temperatures as per requirement. Following sections present distillation of NEPCM conducted to achieve NP separation.

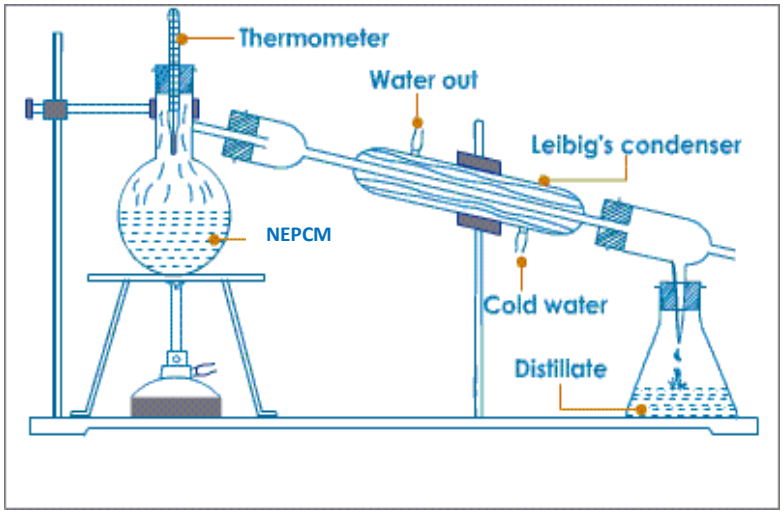

Fig. 5.1 Atmospheric distillation process set up.

5.1.1 Atmospheric pressure distillation trials

A standard distillation unit was used to carry out the distillation process at atmospheric pressure. The standard distillation unit consists of a 1000 ml round bottom heating flask, condenser, collecting flask, and 1000 W heater with power regulator. The distillation unit, along with required accessories such as pipes for condenser; stand, clamps, etc., were purchased from Mountain Home Biological, USA [114]. An energy meter named "Kill-a-Watt" was used to measure the amount of energy consumed during each experiment. All the joints were sealed using sealing tape to minimize the loss of liquid and vapors. Initially, a 100 ml sample of the NEPCM having 1 wt% concentration of CuO nanoparticles was used. The NEPCM was prepared as per the guidelines mentioned in Chapter 3.

The standard safety protocol for distillation was followed to run the experiments. Fig. 5.2a shows the 100 ml NEPCM. The black color of the colloid is due to the presence of black CuO nanoparticles. Fig. 5.2b shows the nanoparticles residue left in heating flask after distillation is complete. Nanoparticles got deposited in the form of a layer at the bottom of the flask. This layer can be removed and collected using glass cleaning agent like acetone. Fig. 5.2c shows

the receiver flask with the distillate which resembles to pure colorless dodecane used to prepare the nano-colloid. Absence of any color clearly indicates that collected distillate is free from any trace of copper oxide. However, as the particles mixed initially were of nanosize, it was required to analyze the distillate microscopically in order to confirm complete removal of the CuO nanoparticles.

a. Before Distillation
Sample: 100 ml
1 % (by mass) NEPCM

b. After distillation:
Flask Bottom showing
nanoparticle residue.

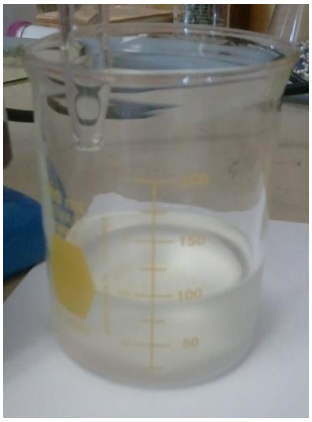

c. After distillation:
Condensate
95 ml

Fig.5.2. Distillation at atmospheric pressure.

Table 5.1 shows the raw data collected for each of the 5 min. time interval during a trial run with 50 ml of NEPCM having 1% (by mass) CuO concentration. A stop watch was used to keep track of time. Fluid temperature inside the flask was monitored using a thermometer of range 0°C – 300°C. Initial boiling and condensation was observed after 5 min. of trial time. This continued further and after 10 min., temperature of the fluid was recorded as 80°C. After 15 min., the temperature was about 212°C which is close to the boiling point of pure dodecane: 216°C [60]. At this point intense vapors at the top of flask rising towards condenser were observed. In next 5 min., the distillate in the form of condensed vapor droplets was observed at the receiver flask and temperature inside the flask reached 250°C. At this point, due to rapid rise in temperature and consequent vaporization of fluid in flask,

vapor amount in the condenser reached to the peak value. This resulted in higher condensation rate producing a continuous stream of distillate. In next 10 min., the temperature inside the flask kept rising as very little amount of liquid was left to absorb the heat energy and get vaporized. This increase in temperate passed well above the range of the used thermometer hence the exact value of the temperature could not be recorded. During this phase of the distillation, the distillate output was decreased to drop by drop and was eventually stopped after 35 min. In order to raise the temperature gradually the power regular of the heater was used. The energy consumed was measured using energy meter connected in series with heater. The water flow rate to the condenser was kept uniform at 2 lpm and tap water with inlet temperature of 21°C was used for cooling. The output collected in the form of distillate was measured to be 48 ml which is 2 ml less than the starting volume. The reduction of distillate is attributed to the loss of fluid on the flask walls.

Table 5.1. Distillation data for 1% concentrated (by mass) 50 ml NEPCM.

Time (mins)	Fluid Temp (0C)	kWhr	Observations
0	22	0	
5	28	0.02	boiling started with churning sound
10	80	0.1	boiling with condensation on flask wall
15	212	0.18	boiling with condensation on flask upper wall
20	218	0.29	output in the forms of initial drops started which turned into a stream
25	250	0.37	output decreased to drop by drop, few drops of liquid at flask bottom
30	over 300	0.5	output decreased further as drop by drop
35	over 300	0.6	no liquid , only smoke was observed in flask

Although the collected distillate resembles pure colorless dodecane and looks free from any CuO nanoparticles, observation with naked eyes does not provide concrete basis to confirm complete removal of nanoparticles. As particles are of nano-size and being very light, there was a possibility of particles being carried away with the dodecane vapor formed during the distillation process. Hence in order to confirm the complete removal of nanoparticles from distillate, an analysis of distillate was required. Scanning Electron Microscopy (SEM) was used for this purpose. All samples for SEM were prepared on a standard nickel grid having carbon coating and were dried for 48 hours before imaging. SEM images of 99% pure dodecane and that of the collected distillate were compared. Fig. 5.3(a) shows the SEM image for the pure dodecane. The structure of carbon coating on the grid is clearly discernible from this image which shows no signs of any nanoparticles present. Same carbon web structure was observed while imaging distillate received after atmospheric distillation as shown in Fig. 5.3 (b). At used SEM settings, any particulate matter would stand out and look very different than carbon web structure. Absence of any NPs gives distillate pure carbon web structure very similar to one observed for pure dodecane. Thus both the images looks similar and provide enough evidence to conclude distillation removes NPs completely from NEPCM and yields 100 % separation efficiency.

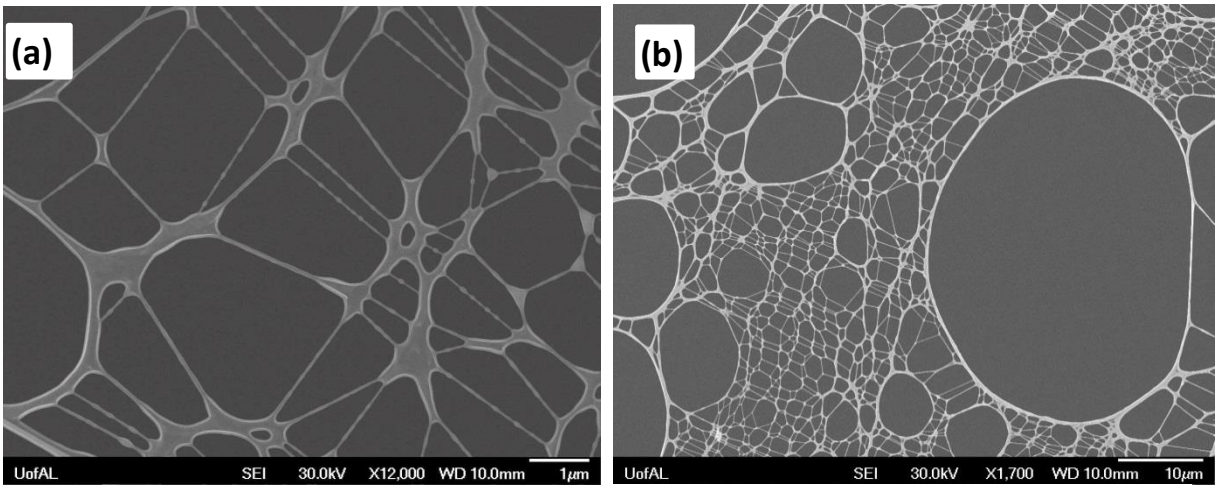

Fig. 5.3. Scanning Electron Microscopy images (SEM); (a) 99 % pure dodecane, (b) collected distillate.

After confirming complete removal of nanoparticles from the NEPCM, numbers of trials were performed to record data about variation of time and energy required, in relation to the amount and NP concentration of NEPCM used for distillation. Table 5.2 shows the summary of the data collected using atmospheric pressure distillation. Total of six trials were performed for different combinations of NEPCM volume and nanoparticles mass concentration. The mass concentration (% wt) of NPs chosen was 0%, 1%, and 3%. A trend was observed for time required and energy consumed in relation to the amount of NEPCM used. Also it was observed that for the same volume, NEPCM with higher concentration of nanoparticles get distilled faster than NEPCM with lower nanoparticle concentration. This confirms the claimed thermal conductivity enhancement of the dodecane with the addition of copper oxide nanoparticles.

Table 5.2. Atmospheric pressure distillation trials summary

Trial Number	NEPCM Volume (ml)	Nanoparticles Mass Fraction (%)	Total Time (min)	Total Energy Consumed (kWh)	Distillate Volume (ml)	Energy/Volume (kWh/ml)
1	100	0	40	0.68	96	0.0068
2	50	1	35	0.6	48	0.0120
3	100	1	40	0.63	95	0.0063
4	150	1	40	0.65	146	0.0043
5	200	1	40	0.66	197	0.0033
6	100	3	32	0.51	97	0.0051

5.1.2 Vacuum distillation trials

Distillation is defined as the separation process based on the tendency of the substances to vaporize in a boiling liquid mixture. And the boiling point of a substance is known as the temperature at which vapor pressure of the liquid equals the pressure surrounding the liquid and the liquid changes into vapor. Hence the boiling point of the liquid varies depending upon the surrounding environmental pressure. A liquid at high pressure has a higher boiling

point than when the liquid is at atmospheric pressure. Conversely, at lower pressure or under vacuum boiling point of liquid is lower than that at atmospheric pressure conditions. Distillation has long been criticized as slow and highly energy intensive process. Hence, in order to make it more energy efficient, distillation at reduced pressure was thought to be a better alternative. This section explains the procedure followed for vacuum distillation trials, results, and analysis.

To perform distillation under reduced pressure a complete new setup was required, as the distillation unit for this purpose has to be airtight and of sufficient strength to withstand the applied vacuum. Hence a new vacuum distillation unit with a vacuum pump was purchased from Mountain Home Biological, USA [114]. The configuration of the distillation system differed slightly than the atmospheric distillation. Here the condenser has the straight passage for incoming vapor which is different than spiral one in atmospheric distillation and also it is held about 20° inclined to the horizontal plane. Vacuum pump of 1/6 HP power rating, 2.4 CFM free air displacement, and 10 Pa ultimate vacuum was used which was capable of creating vacuum from 0 bar (min) to -1 bar (max).All the standard procedures and safety measures were followed while conducting the trials.

Fig.5.4 shows the actual vacuum distillation setup used to conduct trials. Energy meter was used in series with the vacuum pump and heater power lines to record total power consumed. All joints were sealed using sealing tape and airtight performance (to hold constant vacuum) was confirmed by having a trial run for 2 min. In order to have a comparison with atmospheric distillation, vacuum distillation trials were carried out for the same amount and concentrations of NEPCM samples. The vacuum distillation was carried out at 33.6 kPa (vacuum) which is about one-third of the atmospheric pressure.

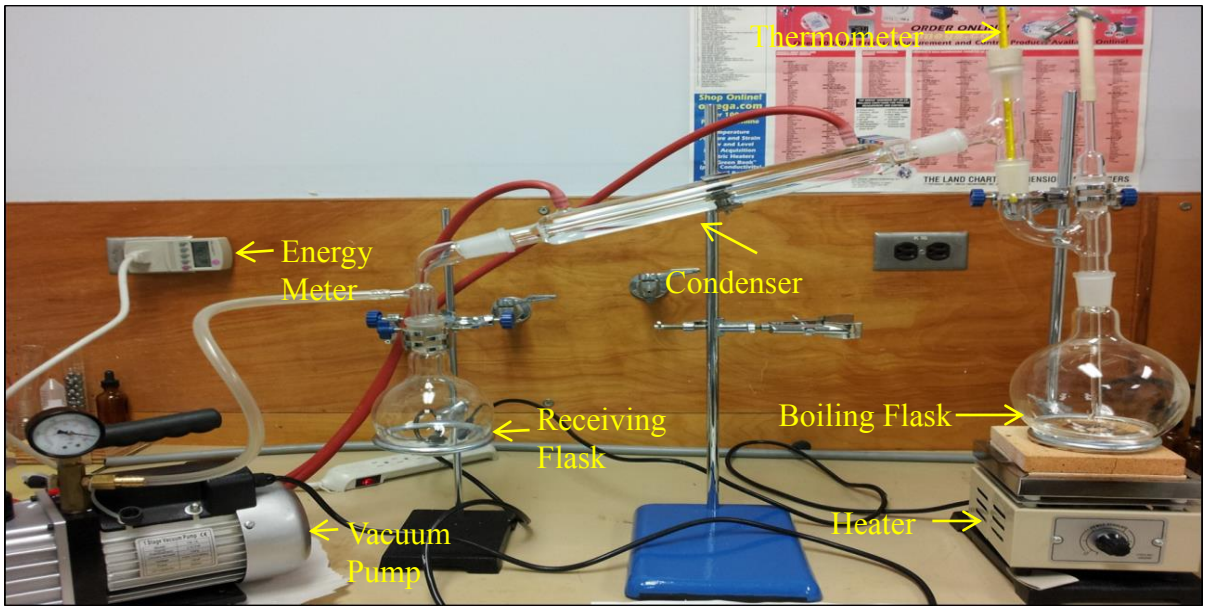

Fig. 5.4. Laboratory vacuum distillation unit.

Table 5.3 shows the vacuum distillation data for 100 ml 1% conc. NEPCM after every 5 min. time interval. Final vacuum applied was -20 inches of Hg (33.6 kPa) which was applied gradually by following consistent steps. Pressure dial mounted on the vacuum pump was used to record the vacuum readings. After initial 5 min. of trial under 33.6 kPa pressures (vacuum), boiling of NEPCM started followed by condensation on lower flask walls.

Table 5.3. Vacuum distillation of 100 ml 1 % conc. NEPCM at 33.6 kPa vacuum.

Time (mins)	Fluid Temp (^{0}C)	kWhr	Observations
0	26	0	
5	26	0.05	Boiling , condensation on lower flask walls
10	162	0.19	Rapid boiling followed by evaporation and condensation. Output started
15	154	0.24	No fluid in heating flask, only black residue of nanoparticles observed

At this point the temperature reading on the thermometer was found to be same as initial value of 26°C. In next 5 min. the temperature raised to 162°C and rapid boiling was observed which resulted in evaporation and condensation leading to the stream of distillate which was

collected as an output in receiving flask. During next 5 min. all of the NEPCM got distilled leaving behind nanoparticle residue in heating flask. The water flow rate to the condenser was kept uniform at 2 lpm and tap water with inlet temperature of 21°C was used for cooling.

In order to establish relation between volumes of NEPCM distilled, power consumed, and time required etc. vacuum distillation was performed for 3 different samples. Table 5.4 shows the data so collected. For 100 ml volume of NEPCM, it was found that, as the amount of NPs increased, time required for vacuum distillation decreased which resulted in less power consumption. This is due to fact that high heat conducting NPs present in NEPCM increases rate of distillation as observed in atmospheric distillation case as well. The final volume of distillate measured was found to be lower than initial volume of 100 ml due to removal of NPs and loss of fluid as vapors.

Table 5.4 Vacuum distillation data summary.

Trial Number	Volume (mL)	NPs Conc. (wt %)	Total Time (min.)	Total Energy Consumed (kWh)	Distillate Volume (ml)	Energy/Volume (kWh/mL)
1	100	0	20	0.35	96	0.0035
2	100	1	15	0.24	97	0.0024
3	100	3	12	0.18	96	0.0018

To verify the nanoparticle removal efficiency of the vacuum distillation process, the NEPCM samples were analyzed on a nickel grid having carbon coating with Scanning Electron Microscope (SEM) of the University of Alabama Central Analytical Facility. Fig. 5.5 shows comparison of SEM images taken for base fluid (pure dodecane), NEPCM before distillation, distillate at atmospheric pressure, and distillate collected by vacuum distillation. Fig. 5.5(a) shows SEM image of the 99% pure technical grade dodecane structure which has been used as a base fluid for the NEPCM preparation. The structure of carbon coating on the grid is clearly visible from this image. Fig. 5.5(b) shows the structure of the NEPCM containing

0.5% (by mass) concentration of the CuO nanoparticles. The lump of nanoparticles sticking to the carbon web structure of the grid is clearly visible in the image. As 0.5 % by mass is a higher concentration especially after preparing SEM sample where it is dried which makes nanoparticles to agglomerate. These two images in Figs. 5.5(a) and (b) were compared with the SEM images of the distillate samples. Fig. 5.5(c) shows the image of the distillate collected from the atmospheric pressure distillation while Fig. 5.5(d) shows the image of the distillate collected from the vacuum distillation. While capturing presented SEM images the whole sample grid was scanned at minimum 8-10 locations to detect any particulate matter in order

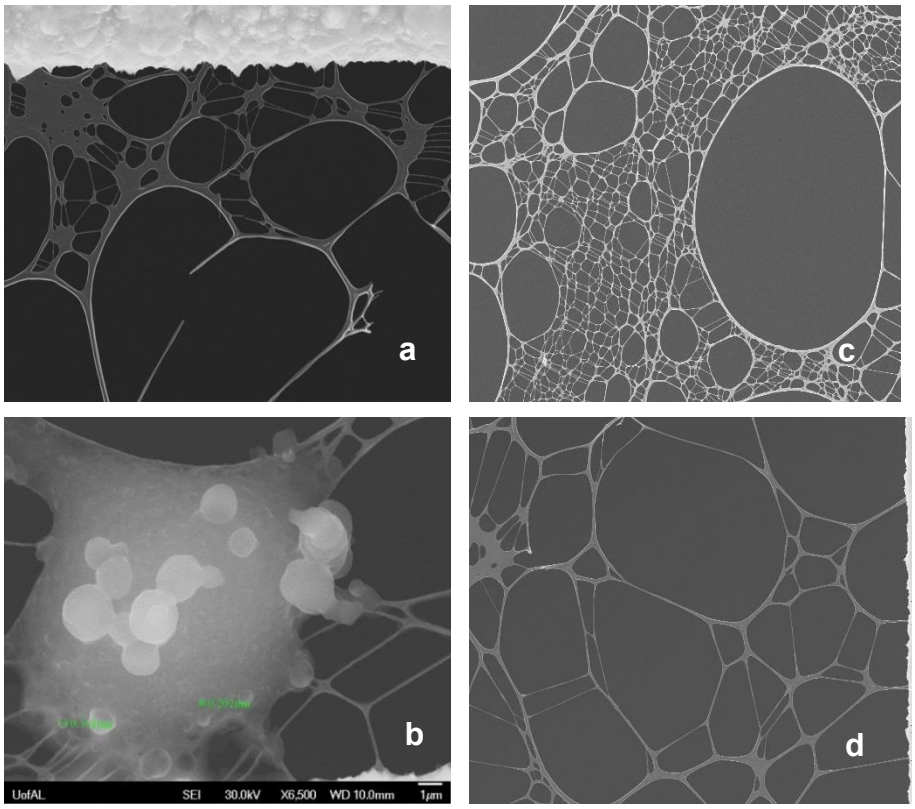

Fig. 5.5. Scanning Electron Microscope (SEM) images of: a) dodecane, b) NEPCM, c) distillate after atmospheric pressure distillation, d) distillate after vacuum distillation.

to capture best image. No trace of the nanoparticle is detected in the distillate in these images asserting that the distillation is a successful process for the separation of nanoparticles from the NEPCM.

Table 5.5 presents distillation data comparison for atmospheric and vacuum pressure distillation experiments. The data is also plotted in Fig. 5.6 on basis of total energy consumption and in Fig. 5.7 on the basis of total time taken. From graphs it is evident that

Table 5.5 Distillation Data Summary for comparison.

NEPCM Volume(ml)	CuO Mass Fraction	Total Time(min.)	Total Power Consumed(kWhr)	Distillate Volume(ml)
Atmospheric Pressure (101.3 kPa) Distillaltion				
100	0%	40	0.68	96
50	1%	35	0.60	48
100	1%	40	0.63	95
150	1%	40	0.65	146
200	1%	40	0.66	197
100	3%	32	0.51	97
Vacuum (33.6 kPa) Distillaltion				
100	0%	20	0.35	96
100	1%	15	0.24	97
100	3%	12	0.18	96

vacuum distillation is much more efficient process to carry out distillation of NEPCM, as it consumes lower energy and takes lesser time than distillation at atmospheric. Based on calculations it is found that for the same volume and nanoparticle concentration of NEPCM distilled, vacuum distillation consumes about 60% less energy as well as time.

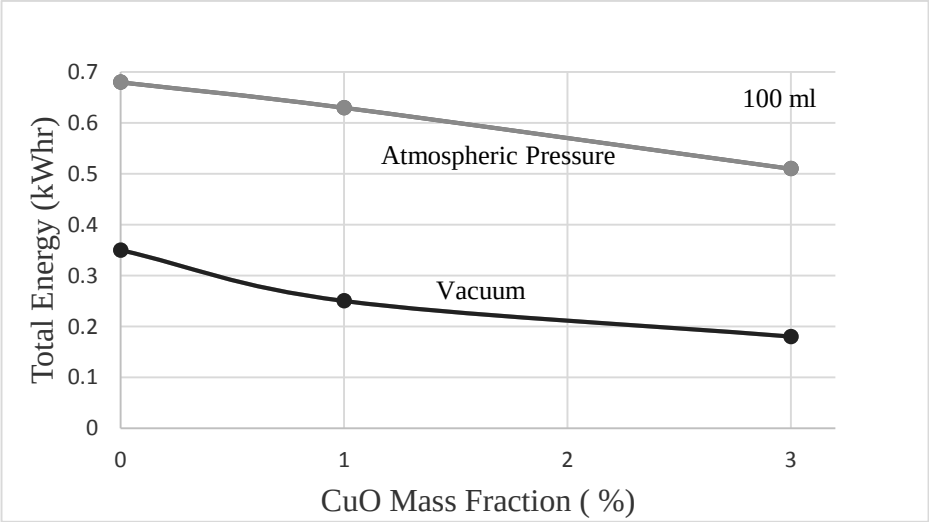

Fig. 5.6. Distillation data comparison on energy basis.

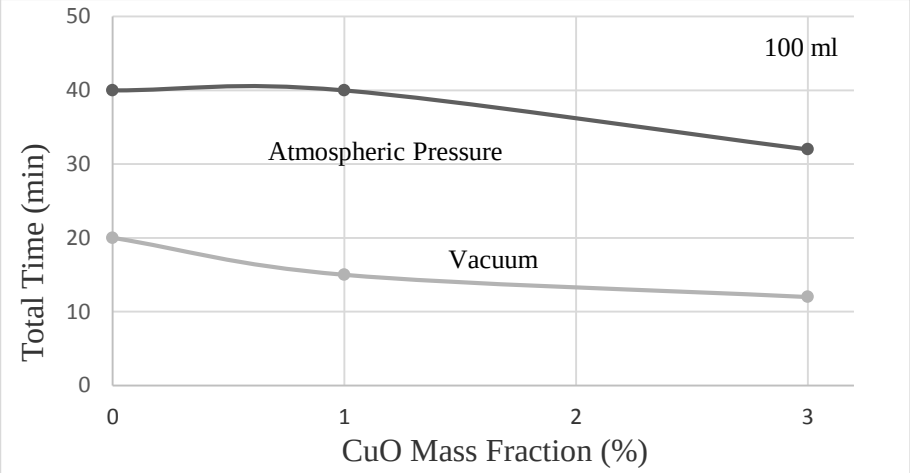

Fig. 5.7. Distillation data comparison on total time basis.

Hence, it can be concluded that vacuum distillation should be preferred over atmospheric distillation in order to separate nanoparticles from NEPCM in an efficient and faster way. Though initial equipment cost for vacuum distillation setup is higher than that for atmospheric distillation the operating cost for vacuum distillation is much lower. This lower

operating cost would make vacuum distillation a cost effective option within a short period of operation in terms of most sought benefit of energy saving. Thus it can be concluded that for long term applications and higher volumes of NEPCM to be processed vacuum distillation is a better alternative.

5.2 Chemical Treatment of the NEPCM

It is hypothesized that, if the NEPCM is mixed with another heavier liquid in which the base fluid is soluble, then a portion of the dodecane in the NEPCM will be dissolved into the heavier liquid and settle down at the bottom leaving a more concentrated NEPCM layer on top. The concentrated top layer can then be separated out and further processed. Based on literature survey and consultation with the experts in chemistry, different heavier solvents were selected to verify the hypothesis. Initial attempts were made using methanol, ethanol, and mixture of methanol and propanol as solvents. Equal volume of NEPCM and solvent were added in a test tube and were shaken for 30 min. at 450 rpm and 34°C using a Controlled Environment Incubator Shaker unit available at University of Alabama Biology Department. Three samples of alcohols containing pure methanol, pure ethanol, and a 50%-50% mixture (by volume) of propanol and methanol were tested. Out of three samples tested the 50%-50% mixture of propanol and methanol showed satisfactory results.

Fig. 5.8 shows the results obtained using the alcohol mixture. During sample preparation and before shaking, it was found that due to high density, the colorless alcohol mixture sits at the bottom of the test-tube occupying half of the filled tube length while the top half is filled by the black colored NEPCM. After shaking, it was observed that the volume of the black colored liquid part shrank while the volume of the colorless liquid part increased substantially. This is because a portion of the colorless dodecane (base fluid) in the NEPCM got dissolved into the colorless alcohol mixture and settled down at the bottom. Thus the process leads to a concentrated NEPCM on top.


Before Shaking After Shaking

Fig. 5.8 NEPCM and alcohol mixture.

To obtain a quantitative data about the amount of dodecane dissolved using the procedure described above, 5 ml of NEPCM (containing 0.5% mass fraction of nanoparticles) was added to 5 ml of alcohol mixture and experiment was repeated. Fig. 5.9 shows the results of first trial after shaking at 450 rpm for 30 min. The concentrated NEPCM on top after shaking was pipetted out and was found to be 3.75 ml in volume. Using this concentrated volume the experiment was repeated again using another 5 ml of alcohol mixture and it was found that the NEPCM got concentrated to 2.5 ml as shown in Fig. 5.9.



Before Shaking **After Shaking** **NEPCM volume ~ 3.75 ml**

Fig. 5.9. NEPCM (5 ml) and alcohol mixture (5 ml); NEPCM volume reduced to 3.75 ml after mixing.

Though visible observations indicate some amount of dodecane has been mixed with alcohol and clear layer shown in Fig.5.9 does not contain any nanoparticles, analytical results are required to support this claim. Hence, in order to confirm complete removal of nanoparticles after processing with alcohol mixture, pipetted out sample was analyzed using UV-visible spectrophotometer.

Before Shaking **After Shaking** **NEPCM volume ~ 2.5 ml**

Fig. 5.10. NEPCM (3.75 ml) and alcohol mixture (5 ml); NEPCM volume reduced to 2.5 ml after mixing.

UV-visible spectrometry was selected to perform analysis over other methods like electron microscopy due to its simplicity, versatility, speed, accuracy and cost-effectiveness. "Varian Cary 100 UV-Vis spectrophotometer" was employed to determine absorption wavelengths. It is a double beam, recording spectrophotometer controlled by a computer operating under Windows 2000 and WinUV software. It hosts tungsten halogen as a visible light source and deuterium arc for ultra-violet light and has wavelength range from 190 to 900 nm. A 1 cm cell was used to feed sample in sample holder. A wavelength range of 300 nm to 800 nm was used to capture data. UV-Vis scan rate was set to 600 nm/min and data interval was 1 nm. Please refer appendix (B) for detailed specifications.

Fig. 5.11 shows UV-Vis spectrum of collected sample, which is compared with baseline (dodecane) spectrum and 0.01 wt% NEPCM spectrum. Due to presence of NPs NEPCM spectrum shows increasing absorbance values as the wavelength is varied from 800 nm to 300 nm, indicating presence of light absorbing NPs. Whereas for sample spectrum (Run1) no

variation of absorbance with respect to wavelength is observed. Also sample absorbance spectrum resemble closely with dodecane spectrum which provides a concrete evidence that sample is free from any NPs after treatment with alcohol mixture.

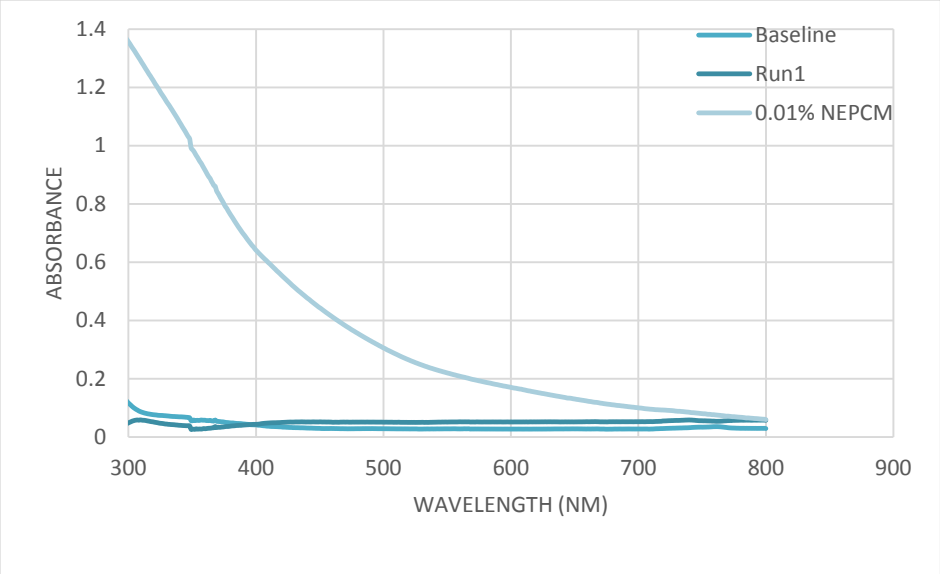

Fig. 5.11 UV-Vis Spectrum of Sample

It can be concluded from these trials that every mixing and shaking step yields about 25% more concentrated nano-fluid. The trial was done with a mixture of alcohol containing 50-50% of methanol and propanol. The concentrated NEPCM collected after a few cycles of mixing and shaking can be further processed by other separation methods such as distillation for complete separation of the nanoparticles with significant reduction in energy and time.

5.3 Centrifugation of the NEPCM

Due to the density gradient between CuO nanoparticles (ρ = 6.31 g/cm^3) and base fluid dodecane (ρ = 0.753 g/cm^3), it was anticipated that centrifugation at higher speeds would sediment the nanoparticles. Initial trials were performed at speed up to 10,000 rpm and no sedimentation was observed for centrifugation duration of 30 min. A micro-centrifuge with maximum speed of 12,000 rpm, typically used by chemists, was utilized for this purpose. However, no deposition of the nanoparticles was observed at this speed due to the fact that the stabilizing ligand threads on the nanoparticle surfaces exert large opposing drag forces on the particles which could not be overcome by the centrifugal forces on the particles. Hence, in order to bring the nanoparticles out of the suspension it is required to apply larger centrifugal forces to overcome the stabilization effect. This force can be applied using higher centrifugation speeds on a large size centrifugation machine.

In order to control the centrifugation precisely, often centrifugation is specified in terms of relative centrifugal force (RCF) which is expressed in units of gravity (times gravity or ×g). Hence, most of the advanced centrifuge machines are equipped with settings for centrifugation speed as well as centrifugal force. In order to have an easy conversion between RPM and RCF, centrifuge manufacturers often supplement the operating instructions with an equation or formula. For the given rotor and RPM specification, using this equation the RCF value can be calculated.

For the centrifuge that have been used to perform the ultra-high centrifugation trials the equation is given as [115] $RCF = (1.118 \times 10^{-5})\, RS^2$ where, R is the radius of rotor in centimeters and S is speed of centrifuge in rpm.

A SORVALL RC6 super-speed centrifuge, which is a floor model, was used to conduct high speed trials. The unit was available at Biology Department at the University of Alabama. Fig.5.12 shows the centrifuge, the rotor which holds the sample via test-tubes or bottles, and the operator interface which allows control of the cabinet temperature, centrifuge speed, and time. For centrifugation trials of the NEPCM at higher speed on SORVALL RC-6, SM-24 rotor was selected which is a fixed angle type. Please refer appendix (C) for detailed technical specifications of SORVALL RC6.

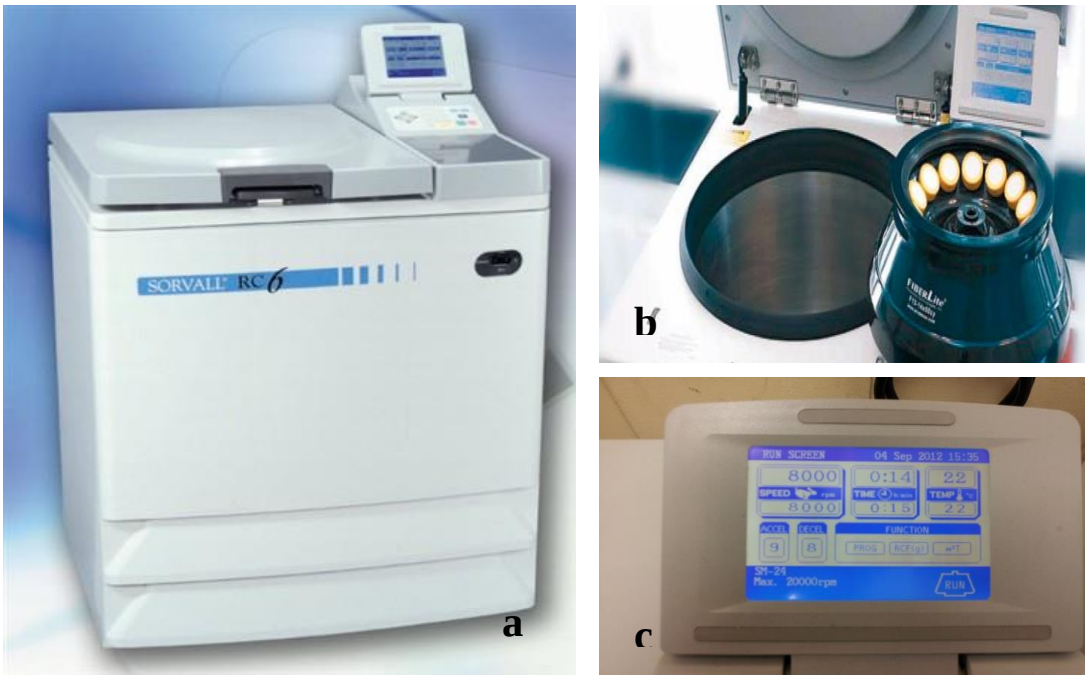

Fig. 5.12. (a) Centrifuge machine, (b), Centrifuge rotor, (c) Operator interface.

SORVALL RC6 is suitable for lower to higher speed applications with wide range of operating conditions in terms of temperature, duration, etc. Depending upon the application requirements, the sample can be operated using one of the different types of rotors this instrument supports, e.g., fixed-angle rotor, swinging bucket rotor, or micro-tube rotor. For different rotors the sample holding size, number of samples to process one time and rpm (or RCF) specification varies. Hence, this instrument facilitates processing of wide range of samples by selecting a correct rotor.

To conduct trials rotor SM-24 was used (please refer appendix C for detailed specifications) which requires sample to be fed in a test-tube with 16 ml capacity. For this purpose, Nalgene Oak Ridge Centrifuge Tubes made up of Polypropylene Co-polymer, were used. The test-tubes were purchased from ThermoScientific and have following dimensions Diameter: 17.9 mm, Length: 106.6 mm, Capacity: 17 mm, Maximum RCF: 50,000 × g. These are the extra strong test-tubes manufactured especially for high centrifugal force applications. While selecting the centrifugation tube to hold sample apart from its size and capacity, diameter and length play a critical role. Any clearance between the tube wall and cavity of the rotor to hold the tube can result in tube bulging and eventual breaking. This is mainly due to the fact that at high speeds, centrifugal force generated is of higher magnitude which results in a force concentration at the lower part of centrifuge tube, essentially at the test-tube bottom as tube is oriented at an outward angle from the axis of rotation. Hence lower part of the tube would get bulged out if any clearance is available. Also length of the tube is crucial as rotor has a top lid which should be secured before operation.

Initial trial was carried out using centrifuge tubes of 16 mm diameter and 12 ml 0.5 wt% NEPCM. The trial duration was 4 hours and speed was maintained at 15,000 RPM (27,820 × g). Fig. 5.13a shows the precipitation of the nanoparticles at the bottom tube wall. But since results show a colored centrifuged solution, it is perceived that centrifugation at this setting could not remove all the nanoparticles. This is mainly due to the insufficient RCF generated at operating rpm to overcome the stabilization. Fig. 5.13b shows the side of the tubes shown in Fig. 5.13a which shows the tube bulging or swelling as a clearance was present between test-tube holding sample and rotor cavity due to use of under-size tubes.

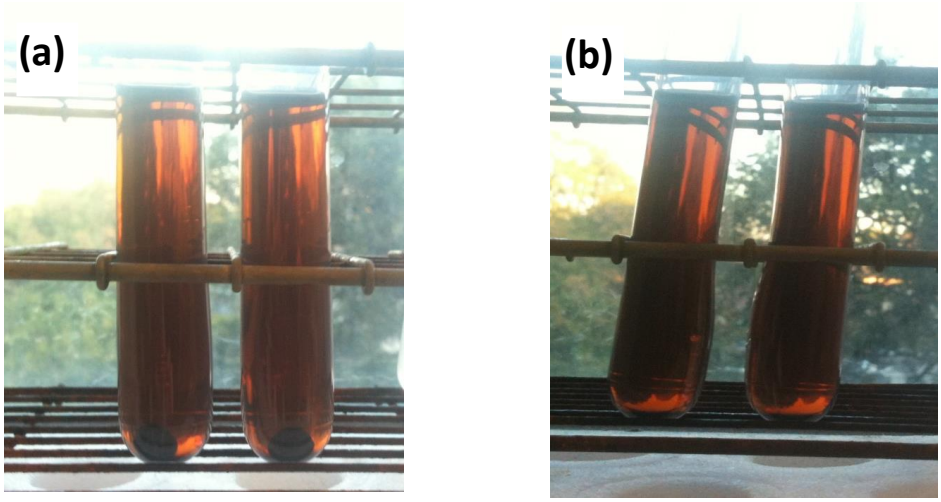

Fig. 5.13. Centrifugation result: first trial, (a) front view, (b) side view.

Further experiments were performed using 17.1 mm diameter centrifuge test tubes which left only enough clearance between the tube and the holder to allow loading and unloading of the tubes in rotor cavity. The tubes used have capacity of 17 ml but as per recommendations only 75% of its volume was utilized. The empty volume of the centrifuge tube allows the movement of the fluid during operation. Fig. 5.14 shows the results of the centrifugation trials for 0.5%, 2%, and 5% concentration for the same operating conditions of 18,000 rpm (40,173 × g) for 19.5 hr.

It is observed that centrifugation could not remove all of the nanoparticles from the given sample volume, as the centrifuged samples have reddish color indicating some of the nanoparticles are still in suspension. As the pure dodecane is colorless fluid hence a non-clear centrifuged sample indicates presence of nanoparticles.

Trial 1: 0.5 % conc. (by mass)

Trial 2: (a) 2 % conc (by mass)
(b) 5 % conc (by mass)

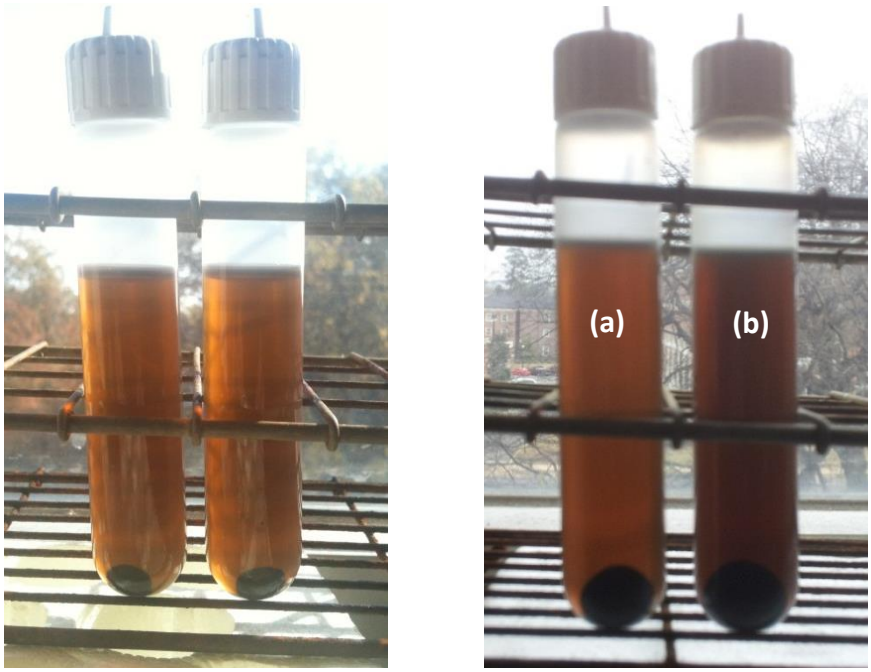

Sample: Volume: 13 ml, Speed: 18,000 rpm, Duration: 19.5 hr.

Fig. 5.14. Nanoparticle precipitation in the test tube after centrifugation trials.

Fig. 5.15a shows SEM image of diluted NEPCM which shows general size distribution of NPs. Fig.5.15b presents SEM image of trial-1 sample after centrifugation. Comparing these two images it is evident that NPs present in centrifuged sample are of less than 10 nm size. Hence the nanoparticles still in suspension after the centrifugation giving the reddish color to the centrifuged samples are of lower size in the nanoparticle size range of 5-15 nm. As the centrifugal force is proportional to the particle mass, the applied centrifugal force of 40,173 × gravity was found to be capable of pulling the larger particles out of NEPCM whereas smaller NPs remained stable.

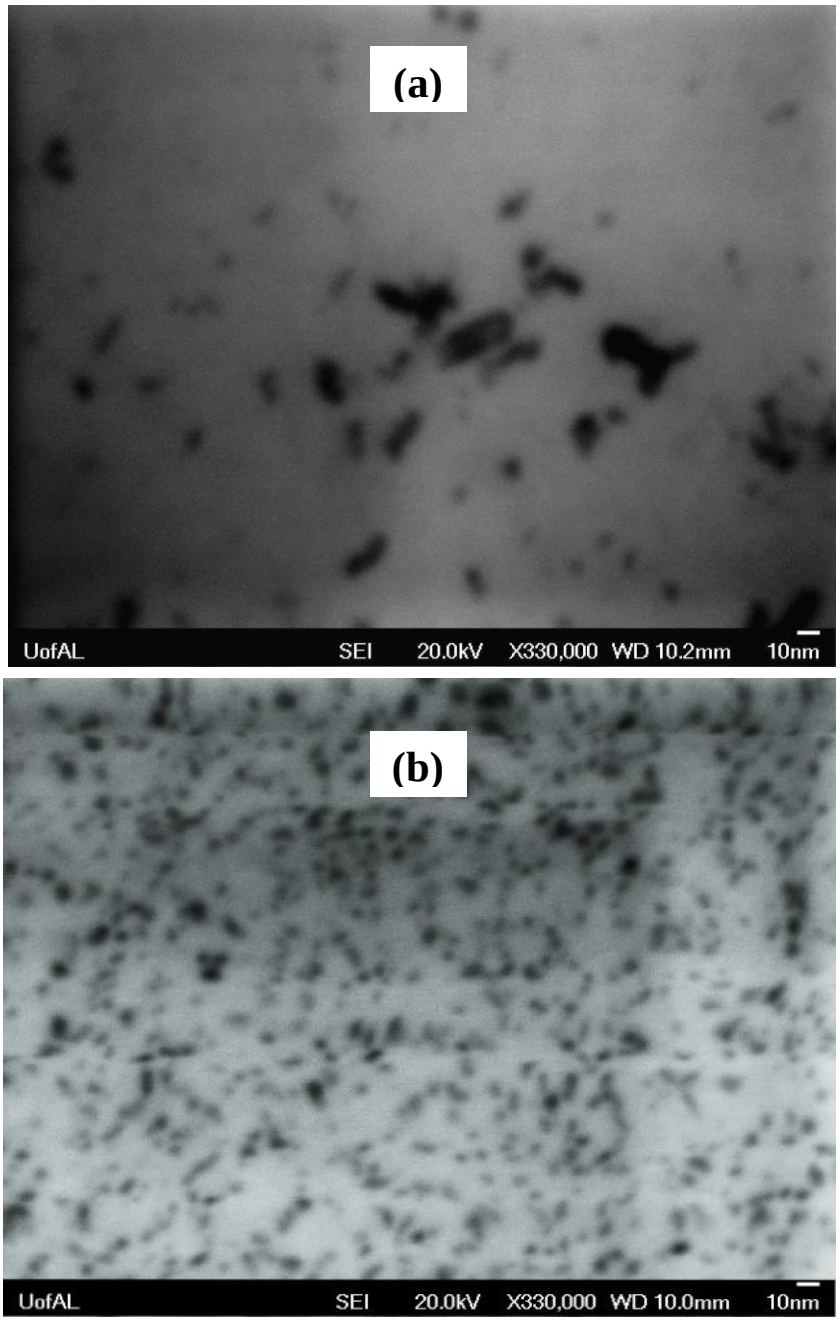

Fig.5.15. (a) SEM image of diluted NEPCM, (b) SEM image of centrifuged sample (Trial-1).

Similar trails were conducted for 0.5, 1 & 2 %wt concentrations of 12 ml NEPCM for 24 hrs. and 48 hrs. at 18000 rpm in order to analyze effect of centrifugation duration (if any). Fig. 5.16 a shows three samples i.e. 1, 2, & 3 of concentration 0.5 %, 1% & 2% respectively before centrifugation trial. After 24 hours of centrifugation at 18000 rpm most of the NPs were precipitated as shown in Fig. 5.16b. At this point 1 mL of centrifuged NEPCM sample

was collected from each of the three samples for comparison purposes. Samples in Fig. 5.16b were centrifuged back for next 24 hours and after end of 48 hours sample conditions are presented in Fig.5.16c.

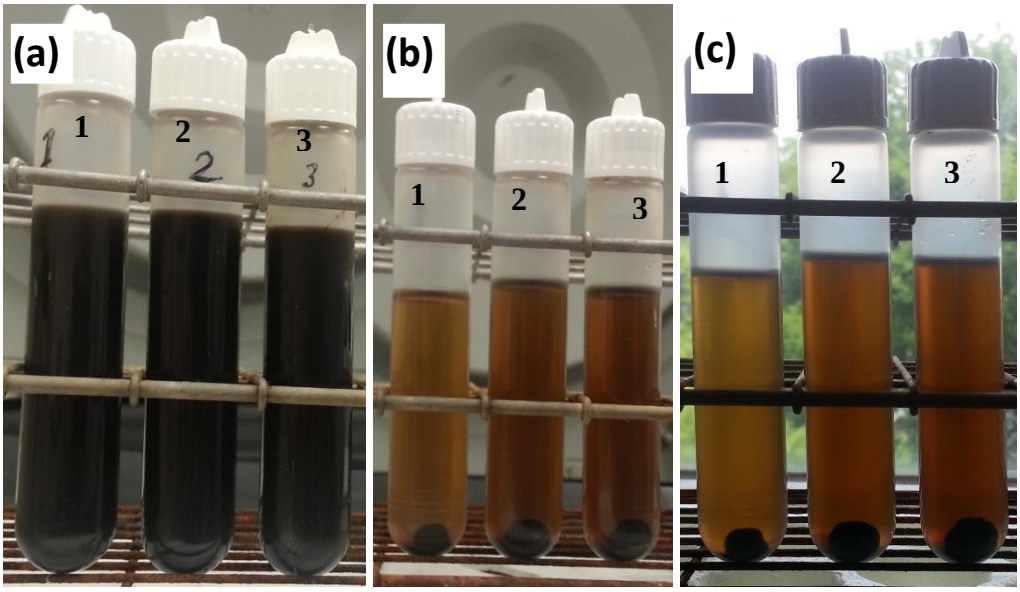

Fig. 5.16. (a) Before centrifugation, (b) after 24 hr. of centrifugation, (c) after 48 hr. of centrifugation.

General visual observation of Fig.5.16c indicates that longer centrifugation duration of additional 24 hours at 18000 rpm results in no further precipitation of NPs because samples in Fig. 5.16 b and c bear same color. In order to quantify the particle removal efficiency of the centrifugation trials and record difference in concentration after duration of 24 and 48 hours (if any), a concentration based analysis was done where concentrations of NEPCM before and after centrifugation were used to calculate efficiency of particle removal by centrifugation. As a known concentration of NEPCM was used initially to conduct trials, concentration of NEPCM was known before centrifugation. In order to determine concentration of NEPCM after trial, “Calibration Curve” or “Internal Standard” approach using UV-Vis photo-spectroscopy was employed. Using UV-Vis spectroscopy concentration of a sample can be determined either by using Beer-Lambert Law (refer appendix (B)) or by

plotting calibration curve. But as Beer-Lambert Law is not applicable to all solutions since solutions can ionize/polymerize at higher concentrations or precipitate to give a turbid suspension that may increase or decrease the apparent absorbance. Further, the Beer-Lambert Law is most accurate between absorbance (Abs) values of 0.05 to 0.70, the measured Abs for higher values tend to underestimate the real Abs. As the NEPCM samples used were of higher concentration and samples of unknown concentration after centrifugation might have higher Abs than the limit of Beer-Lambert Law, Calibration Curve method was preferred. To plot a calibration curve which is a graph of concentration versus absorptivity for the solution, six samples of known concentrations were prepared in addition to the unknown centrifuged sample. Fig. 5.17 & 5.18 shows the samples of known varying NP wt% prepared to determine concentration of centrifuged sample after 24 hours of 2 % concentrated NEPCM and 48 hours of 1 % concentration NEPCM respectively. These known concentrations were selected such that the unknown concentration sample falls in the middle these sample concentration range. The color of centrifuged NEPCM (or NEPCM) sample proved as an aid in preparing these samples with known varying concentrations to bracket unknown sample concentration.

Fig. 5.17. UV-Vis spectrometry samples of 2 wt% NEPCM to find concentration after 24 hours of centrifugation

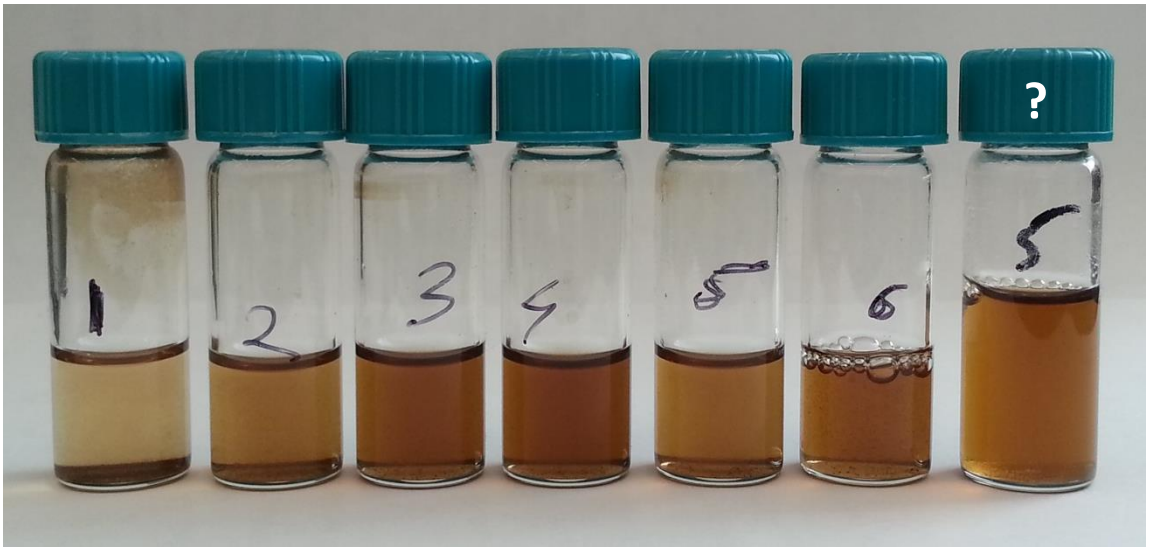

Fig. 5.18. UV-Vis spectrometry samples of 1 wt% NEPCM to find concentration after 48 hours of centrifugation

For each sample, absorbance spectra were recorded using UV-Vis spectrometer and the value of the absorbance of each of the spectrum curves at the highest absorbing wavelength (λ_{max}) is determined. Fig. 5.19(a) & (b) shows absorbance spectra of 2 wt% & 1 wt% respectively of NEPCM samples of different known concentrations & unknown concentration. After determining absorbance values at λ_{max} calibration curves were plotted.

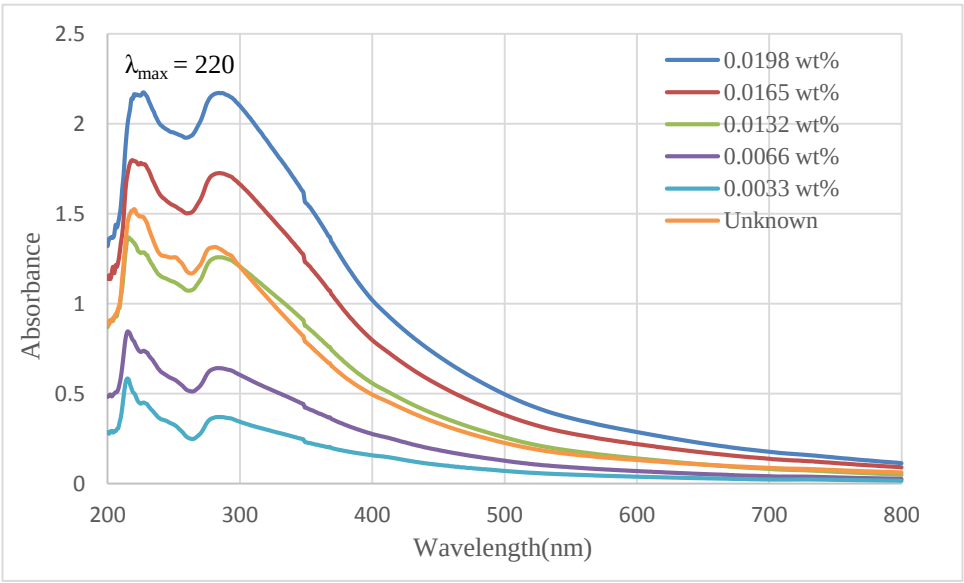

Fig. 5.19(a). UV-Vis spectra of 2 wt% NEPCM and sample 3(After 24 hrs.)

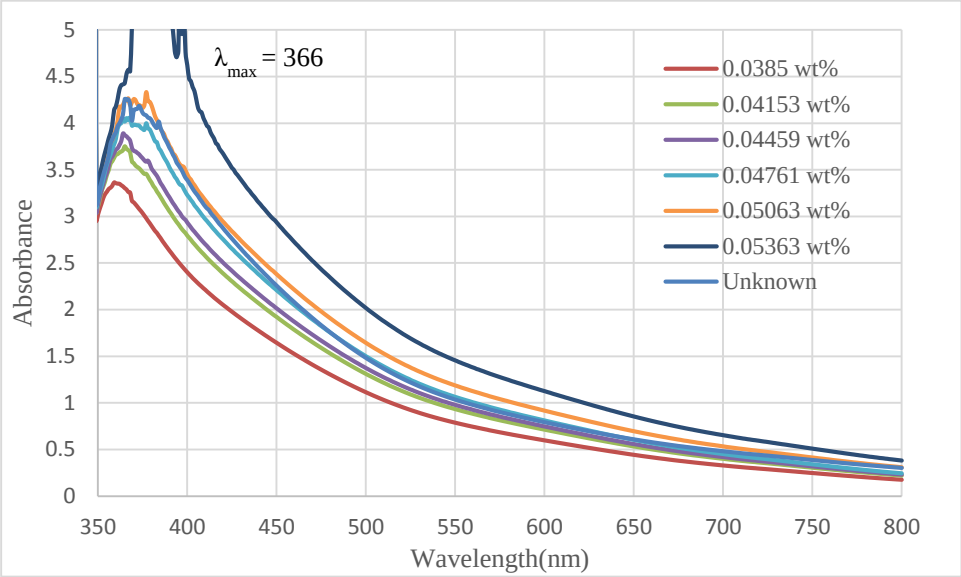

Fig. 5.19(b). UV-Vis spectra of 1 wt % NEPCM and sample 5 (After 48 hrs.)

Fig. 5.20 a and b shows calibration curve for sample 2 (1 wt %) and sample 3 (2 wt %) respectively. As shown absorption spectra was recorded for samples with concentrations varying from 0.0066 %wt to 0.016 %wt for sample 2 and 0.0033 %wt to 0.021 %wt for sample 3. Due to errors introduced during data recording and inconsistent concentration steps of sample, Calibration curve deviates from being a perfect straight line. Using Calibration curve so plotted a curve fit equation was determined to calculate x value (concentration) of centrifuged samples for the known Y-value (Absorbance) determined from absorbance spectrum.

Using Calibration curve concentration (%wt) of NEPCM after centrifugation were determined and compared with initial concentration before centrifugation. Table 5.6 presents summary of data collected for two centrifugation samples. For the same centrifugation speed in this case 18000 rpm equivalent to 40,173 x gravity (which is the maximum attainable speed with the equipment available) , 24 hours period resulted in about 95 % efficiency

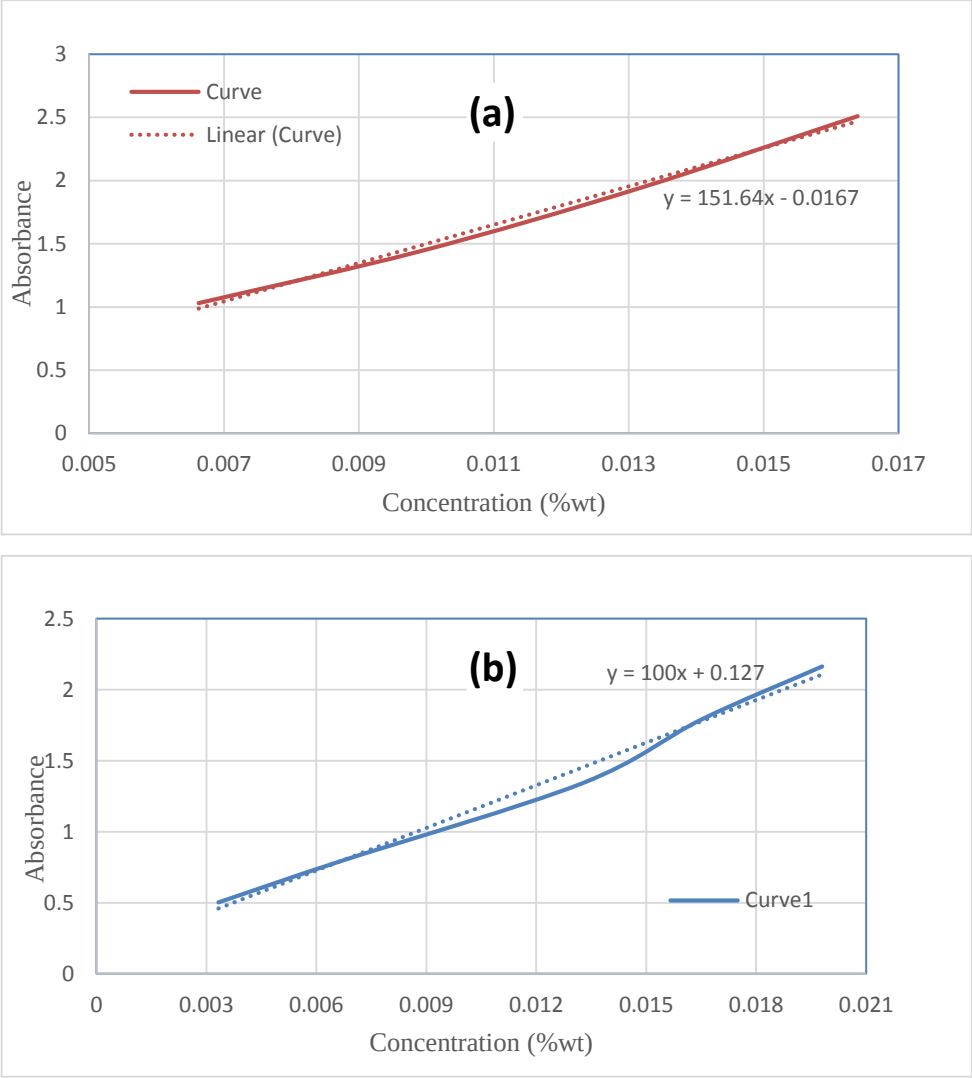

Fig. 5.20. Calibration curve for centrifugation, (a) sample 2, (b) sample 3.

Table 5.6. Centrifugation results.

Sample No.	Initial wt %	Centrifugation rpm (×Gravity)	wt % after 24 hrs	Overall Efficiency (%)	wt % after 48 hrs	Overall Efficiency (%)
2	1	18,000(40,173 × g)	0.044	95.6	0.043	95.7
3	2	18,000(40,173 × g)	0.084	95.8	0.081	95.95

which remained almost same without any significant further improvement for additional 24 hours centrifugation period. This is evident from the overall efficiency values presented.

Referring to Fig. 5.14b remaining NPs are of lower size range (dia < 10 nm), hence they need stronger centrifugation force to bring them out of solution to make them precipitate. The primary hypothesis of by applying same centrifugation force for longer duration should result in improved centrifugation efficiency broke down.

In order to achieve separation of nanoparticles from NEPCM, high-speed centrifugation is a partially successful method. Based on the performed experiments and analysis it can be concluded that centrifugation at higher RCF (25,000× gravity and up) brings separation of nanoparticles from the NEPCM by means of sedimentation. However, for the applied RCF of over 40,000 × gravity for 48 hr., centrifugation was found to be capable of producing around 95% efficient results. With the available centrifuge maximum 2000 ml of NEPCM volume can be processed in a single run using a suitable rotor for the required duration at right speed. Also new advanced centrifuges are available which are known as “continuous centrifugation devices” which allows sample feeding and processed sample collecting during the required the processing cost is very low. Using the available resources and performed experimental analysis, it is evident that centrifugation at further higher RCF values should bring higher and faster precipitation of nanoparticles resulting in more efficient NP separation from NEPCM.

5.4. Destabilization of the Nanoparticle Ligands/Surfactants using Concentrated Base

As explained earlier, nanoparticles in NEPCM are stabilized by means of steric stabilization using oleic acid which is achieved by chemically attaching large and bulky oleic acid ligands on to the particle surface that provide a physical “cushion” between colliding particles and stable suspension of the particles in the base fluid after mixing. In this type of stabilization, ligands have their polar heads attached to the nanoparticle surface and non-polar tails lying in non-polar base fluid (dodecane). This kind of stabilization is proved to be very efficient and

strong due to the fact that being heavier than base fluid (density: 0.753 g/cc), nanoparticles (density: 6.31 g/cc) stay stable for months with no or negligible precipitation [49]. Hence, if ligand end attached to nanoparticle surface gets detached, steric stabilization will break down leading to nanoparticle destabilization and consequential precipitation due to gravity. With this premise, trials were conducted using solvents in which oleic acid is soluble. After conducting several experiments and getting unsatisfactory results, interaction of concentrated potassium hydroxide (KOH) with NEPCM in the presence of ethanol produced desired result. It was observed that KOH interaction with NEPCM results in steric stabilization break down which makes nanoparticles fall down quickly due to gravity.

An initial trail was conducted using 5 ml of 0.5% CuO mass fraction NEPCM, 3 ml of saturated aqueous solution of KOH, and 0.5 ml of ethanol. Saturated KOH solution was prepared by mixing KOH pallets in deionized water till the resulting solution was saturated and no further mixing was observed. All chemicals used were purchased from Sigma Aldrich, USA and used as is without any purification. Glassware used was purchased from VWR international. The 5 ml of NEPCM was taken in a test-tube and 3 ml of KOH solution was added followed by continuous shaking for about 1 min. At this point little mixing was observed with no sedimentation of nanoparticles. Few drops of ethanol were added followed by continuous shaking. NPs were observed to form a dense black layer at the bottom and a colorless top layer.

Fig. 5.21 a shows the end result of trial 1. A schematic chemical reaction between the oleic acid ligands and the KOH is presented in Fig. 5.21b to explain the net effect of KOH on NEPCM stability. It is predicted that KOH saponifies the oleate ester linkage which eventually results in formation of potassium oleate. This results in cancellation of stabilizing

effect by disintegration of ligands from NP surface which makes nanoparticles loose stability and fall down under the action of gravity forming a dense layer at test-tube bottom. The clear layer on top of precipitated nanoparticles is thought of as a mixture of base fluid dodecane and ethanol. Hexane was added to wash the test-tube walls and to make layers look distinct. The removal of the oleate ligands from the CuO nanoparticles is believed to occur via the reaction mechanism is illustrated in Fig. 5.21 b On left hand side, a CuO nanoparticle is shown with the oleate group attached to its surface. We propose that KOH saponifies the oleate ester linkage, resulting in the formation of potassium oleate. The detachment of oleate from the nanoparticle surface makes the particles unstable and results in precipitation as shown in Fig. 5.21a. After the reaction with the KOH, the top clear layer in Fig. 5.21a is expected to contain potassium-based oleate group as shown on right hand side of the equation in Fig. 5.21b.

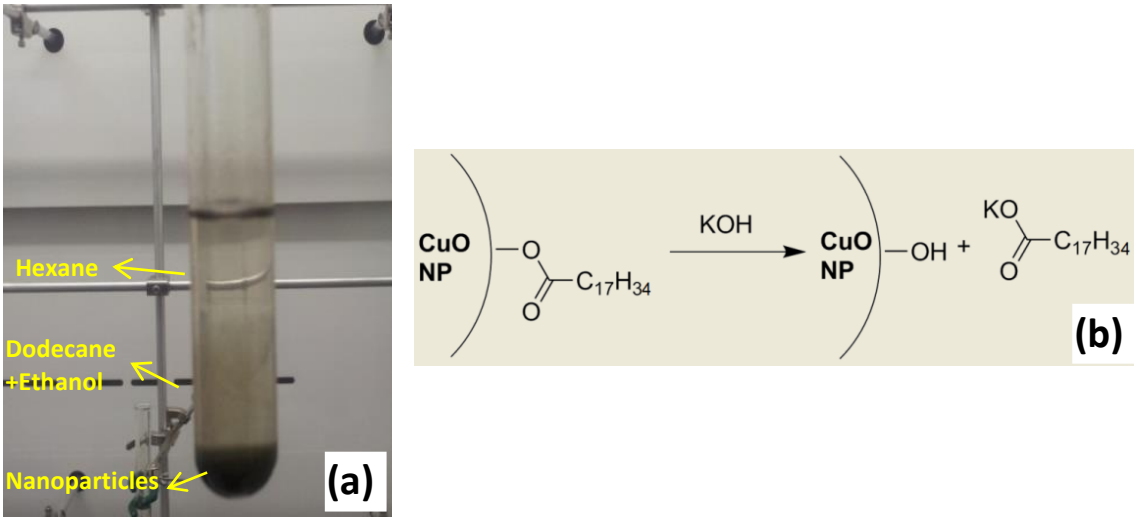

Fig. 5.21. (a) Nanoparticle destabilization using saturated KOH solution, (b) schematic of the chemical reaction between oleic acid and KOH.

In order to confirm complete removal of NPs due to action of conc. base (KOH) top layer of clear fluid (Fig.5.21a) was analyzed optically using UV-Vis spectrometry. UV-Vis spectrometry was chosen due to its simplicity, accuracy, and speed. Pure dodecane (99 %

technical grade) was used as reference sample (baseline). For the same sample two spectra were recorded and compared with baseline spectrum. For the same sample UV –Vis spectrum was recorded and was compared with spectrum of 99 % pure dodecane and 0.0167 wt% NEPCM as shown in Fig. 5.22. Absorbance spectrum of sample i.e. Run 1 resembles to spectrum of baseline where as NEPCM spectrum possess very different behavior with high absorbance values. Hence it can be concluded that treated sample is free from the CuO nanoparticles. This demonstrates that aqueous KOH in the presence of ethanol is capable of removing oleate ligands from the particle surfaces resulting in the precipitation of all of the nanoparticles from the sample NEPCM yielding 100% separation efficiency.

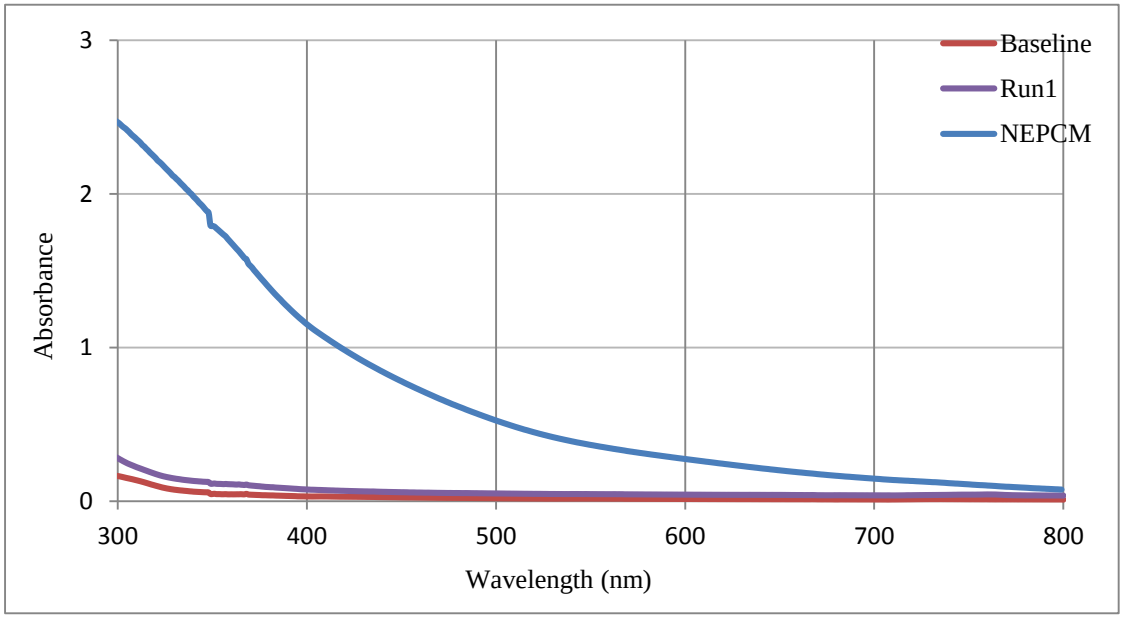

Fig. 5.22. UV-Vis Spectrum of trial 1.

For different volumes and nanoparticle concentrations of the NEPCM, different trials were performed in order to determine the optimum amount of KOH and ethanol required. First experiment was performed using 2 ml of 2 wt % NEPCM as shown in Fig. 5.23a.

One ml saturated aqueous KOH solution was added to sample and solution was shaken followed by addition of 6-8 drops of ethanol. After continuous manual shaking for about 30

seconds nanoparticle precipitation was observed as shown in Fig. 5.23b. Small volume (~1 ml) of hexane was used to wash out nanoparticles sticking to the test-tube wall due to shaking. Top clear layer was pipetted out for qualitative analysis using UV-Vis photo-spectrometry explained before. The volume of precipitated nanoparticles was found to be 0.6 ml (approx.).The nanoparticles are coated with ligands which accounts for about 30% of nanoparticle mass.

After reacting with the KOH this 30% mass of nanoparticle or ligand gets detached from the particle surfaces and forms a separate thin reddish colored layer right over the nanoparticle layer, as shown in Fig. 5.23c. As explained (refer Fig. 5.21b), potassium ion (K) replaces the oleate bond with CuO nanoparticles forming a potassium based oleate which separates out from the NEPCM system forming the thin layer. After a period of 20 hr., further concentration of nanoparticle layer and thickening of reddish oleate layer is observed as shown in Fig. 5.23d. This is due to further agglomeration or precipitation of nanoparticles due to gravity and thereby releasing more solvent into the layer above. The second layer is a mixture of water (density: 1 g/cc), ethanol (density: 0.789 g/cc) and potassium based oleate. Being light dodecane (density: 0.753 g/cc) occupies top layer.

Fig. 5.24a shows separated or precipitated nanoparticles after the top layer has been pipetted out for analysis. In order to check the possibility of dispersing precipitated nanoparticles back into dodecane as well as prove the mechanism of precipitation using KOH, fresh dodecane volume was added to sample shown in Fig. 5.24a and was given a rigorous shaking . One ml of 99 % pure technical grade dodecane was added to precipitated nanoparticles and solution was shaken for 2 mins. It was observed that separated nanoparticles no-longer mix with fresh dodecane as shown in Fig. 5.24b, where clear layer of dodecane on the top and separate black layer of nanoparticles in the bottom is clearly visible. Hence reuse of so separated nanoparticles is not feasible. Above results provide a concrete evidence to support presented

hypothesis where disintegration of KOH and formation of potassium based oleate were considered as the possible steps for nanoparticle destabilization and precipitation.

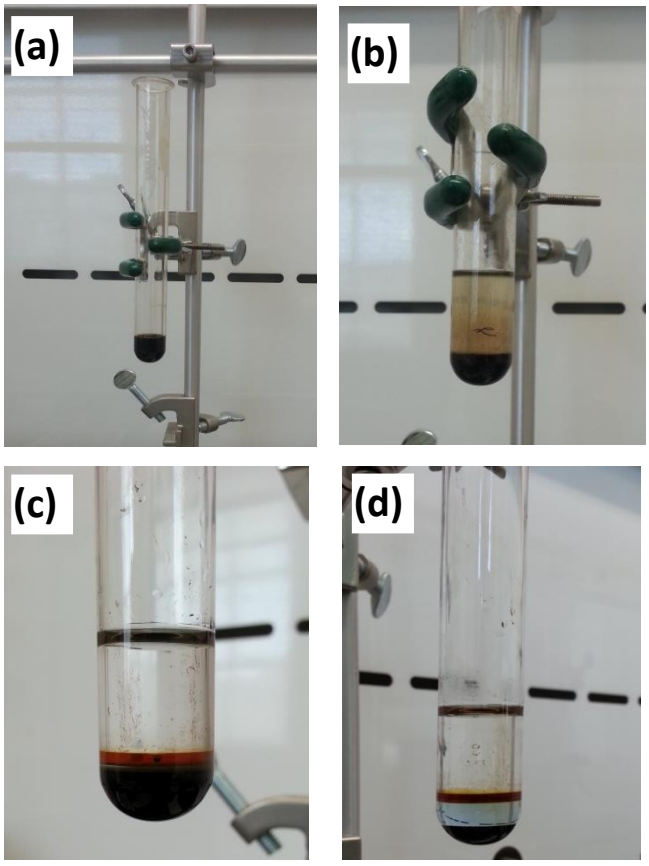

Fig. 5.23. Two ml 2 % conc. NEPCM sample, (a) before trial, (b) after KOH reaction, (c) sample after trial showing 3 separated layers, (d) sample after 20 hours of trial showing 3 separated layers

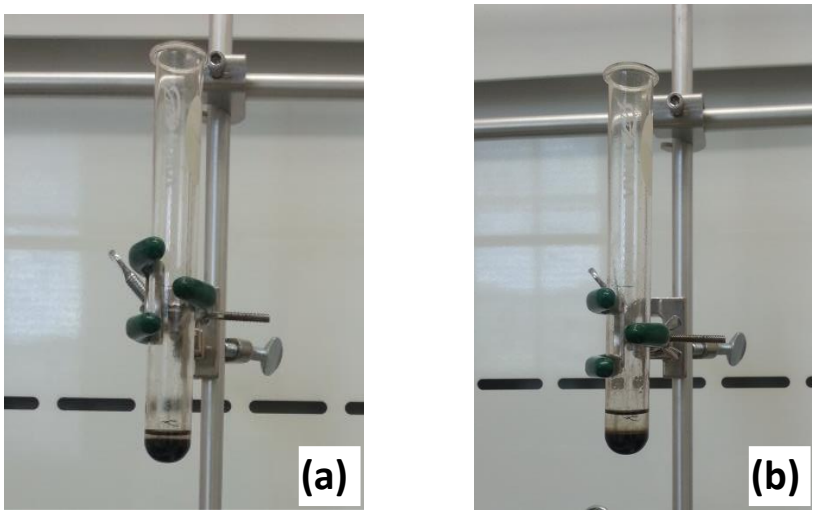

Fig. 5.24. (a) Sample after top layers pipetted out for analysis, (b) Sample showing coating-less nanoparticles and dodecane layer.

Table 5.7 presents the summary of trials performed using different volumes and concentrations of NEPCM. It can be deduced that volume of NEPCM governs the volume of saturated KOH solution required for complete precipitation. This is true for the ethanol amount required as well.

Table 5.7. KOH trails summary.

Trial No.	NP conc. (%)	NEPCM Vol. (ml)	KOH Vol. (ml)	Ethanol Added (drops)
1	0.5	5	3	10
2	2	2	1	6
3	1	3	2	8
4	2	3	2	8

Figs. 5.25a and b shows trial number 4 results. Adding KOH solution to NEPCM with shaking in absence of ethanol results in incomplete mixing as shown in Fig. 5.25a where a clear liquid volume portion with bubbles at the bottom of test-tube is clearly visible. At this stage all NPs are stable and no precipitation was found. However after adding 8-10 drops of ethanol in addition to continuous shaking a phase separation was observed as shown in Fig. 5.25b. It was observed that first few drops of ethanol were capable of initializing separation process and after adding the mentioned amount of ethanol all nanoparticles were accumulated at the bottom of test-tube.

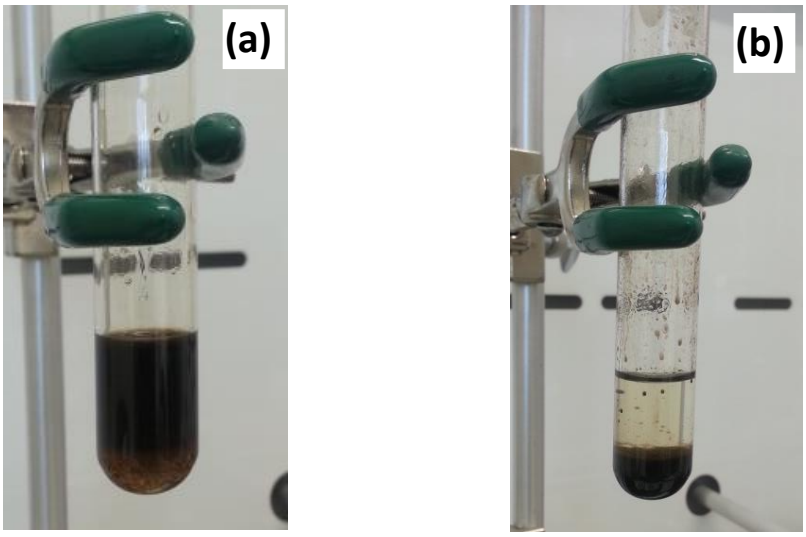

Fig. 5.25. (a) 2 wt % 3 ml NEPCM and KOH before adding ethanol,
(b) 2 wt % 3 ml NEPCM and KOH after adding ethanol.

Effect of additional KOH solution and ethanol was evaluated by adding another 1 ml of KOH solution after observing complete precipitation. It was found that additional KOH has no effect on further precipitation even after adding few more drops of ethanol to facilitate further mixing and precipitation. Additional KOH and ethanol volumes add up to precipitated nanoparticles volume as shown in Fig. 5.26 below.

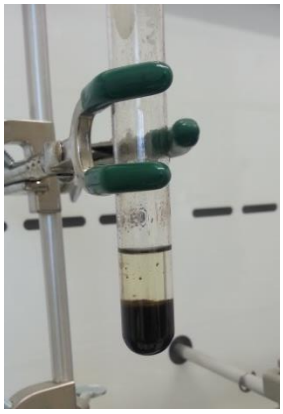

Fig. 5.26 Effect of additional KOH and ethanol

In summary, it can be stated that the NEPCM reaction with saturated aqueous KOH solution in the presence of ethanol results in separation of nanoparticles by means of destabilization. Due to reaction with KOH, oleate group attached to the surface of nanoparticles, which is primarily responsible for stabilization, gets detached resulting in unstable nanoparticles. Being heavier than base fluid dodecane and any other solvent present in solution these unstable particles precipitate due to gravity bringing separation. This is one of the simplest methods where complete separation of the nanoparticles is achieved by attacking stabilizer ligands. As it requires saturated aqueous solution of KOH and ethanol only to carry out separation, it is deemed very safe and economical process. Chemicals formed after completion of reactions are dodecane, mixture of ethanol and water and potassium based oleate which is safe for handling. Based on experiments performed and analysis done it can be concluded that this method can be easily scaled up to suit for large volumes of the NEPCM.

5.5 SILICA COLUMN CHROMATOGRAPHY

Chromatography is a separation process in which sample mixture to be processed is distributed between two phases in the chromatography bed (column or plane). One phase is stationary known as stationary phase while the other phase passes through the chromatography column and is known as mobile phase or eluent. The substances in the mixture to be processed or separated must have different affinities for these two phases. The substance with a relatively higher affinity for the stationary phase moves with a lower velocity through the chromatography column than the substance with lower affinity. This difference in migration velocities of the components of the sample ultimately leads to physical separation of the components [116].

A component of the sample mixture that leaves the stationary phase and moves with mobile phase is said to be eluted in a process known as elution. The stationary phases are either a solid, porous, surface-active material in a small-particle form or a solid support covered with a thin film of liquid. The particle size of the stationary phase governs the efficiency. Column efficiency is inversely related to rate at which sample components elute through the stationary phase.

There are different types of chromatography methods to suit variety of application requirements. Depending on the system design they are classified as column or planer chromatography; according to the physical state of the mobile phase they are defined as gas or liquid chromatography; according to the separation mechanism they are classified as ion-exchange, size-exclusion, or expanded bed adsorption chromatography. Also there are some special techniques like reversed-phase chromatography, two-dimensional chromatography, moving-bed chromatography, Chiral chromatography, etc. Most advanced chromatography systems are computer controlled and are capable of spectrometry analysis and continuous operation.

In the specific application of this research, the separation of nanoparticles from the NEPCM is carried out using the silica column. As silica is classified as probable carcinogen by Hazard Communication Standard (HCS), care should be taken while handling silica. Also a face mask is recommended when performing experiments using silica. A manual column chromatography using powder silicate was used to carry out NEPCM chromatography trials. This type of chromatography is known as silica column chromatography, silica gel chromatography, gel chromatography, or flash chromatography. A glass chromatography column of 10.5 mm internal diameter and 200 mm length was purchased from The Lab Dept, Inc., which came with a straight stopcock with a poly-tetrafluoroethylene(PTFE) plug. A cotton plug, sand (coarse) and silica were used to establish the column. Coarse sand (washed and dried) was purchased from Macron Chemicals (ref. appendix-D for material properties) and was used as is without any treatment. Silica gel with 40-63 μm grain size (230-400 mesh), pore size 60Å in dry form was purchased from SILICYCLE, UltraPure SILICA GELS, Canada and was used as is. As a first step in column preparation, a small piece of the cotton plug was dropped inside column which was adjusted right into the narrow passage above PTFE plug. This cotton plug was used to provide a base for silica column formation. In the next step a small amount of coarse sand was added which occupied about 2 mm of column length. Cotton plug with coarse sand layer accounted for base formation for the silica gel column. Finally, fine grain silica (silica gel) was added to the required column height. After adding silica to required column length, hexane was added to make the entire column wet and bubble free. In this formation silica gel was used as stationary phase and hexane was used as mobile phase.

There is another approach to establish silica gel column generally followed by chemists. In this approach after base formation using cotton plug and coarse sand, silica gel column is formed by using a diluted silica solution or wet silica. Silica is dissolved in hexane and this

saturated solution is added to the chromatography glass column. In order to form a compact column of desired length excess hexane from the silica column is drained by opening PTFF plug. This approach requires a good estimate of the amount of silica required for the desired column length. As excess hexane removal is a slow process this approach takes longer time for a compact column formation. Also any excess hexane left, leads to a loosely packed column which eventually adds up to the elusion length or requires a longer column length to process a given sample when compared to the first approach mentioned previously. Hence to process a given sample using shortest possible silica gel column first approach was followed.

A silica column of 4 inch (approx.) was used for all the trials. Table 5.8 shows the chromatography data for different volume and concentrations of NEPCM. Silica used to build column served as stationary media while hexane was used as eluent. After the column is established, NEPCM sample to be processed was added followed by hexane to aid in elusion process. Hexane was added till the top end of the glass column, this hexane column (5 ml approx.) on the top of NEPCM sample helps in faster elusion. Due to the pressure exerted by the hexane, movement of NEPCM was observed through silica column, which was easier to observe due to its black color. After reaching a certain length of the column the nanoparticle elusion stopped. At this point nanoparticles are considered to be trapped by silica matrix or column allowing only transport of base fluid dodecane under action of hexane as an eluting agent.

Table 5.8. Silica Column Chromatography trial results.

Trial No.	NEPCM Volume (ml)	NP conc. (by mass)	Elusion Length(inch)	Elutant Volume(ml)	Time (min)
1	0.5	0.5%	0.25	15	70
2	1	1%	0.3	15	70
3	1	2%	0.3	15	75
4	2	2%	0.3	10	55

After first elusion was complete, i.e., when the hexane level drops from the top of the glass column to the top of the silica column, hexane was refilled. This process was repeated 2-3 times or until no movement of the nanoparticles was observed. As reported in Table 5.8 for the different concentrations and volumes of NEPCM samples, maximum length to which nanoparticles could travel through silica column (elution length) varies from 0.25 to 0.3 inch. Elution length is a function of concentration of nanoparticles and the compactness of column. Trial 1 for 0.5 % conc. 0.5 ml NEPCM sample was carried out using second approach of column building as well (not reported in Table 5.8), it was observed that elution length in this case was very long when compared to the same with a compact silica gel column formed using the first approach. As shown in Fig. 5.27a, for a less compact column, the elution length was about 2 inch or half of the total column length. Fig. 5.27b shows the trial 2 elusion, where limited travel of the nanoparticles in silica column can be observed. Fig. 5.27c and Fig. 5.27d shows trial 3 and trial 4, respectively, indicating elution length and hexane amount added during each elusion step. The time taken for complete elusion where no further movement of the nanoparticles was observed, was found to vary from 55-75 min., which is a function of volume of the hexane required for elution to have a complete separation of nanoparticles.

A close observation of the silica column after the completion of the experiment reveals that all of the nanoparticles are trapped. This is due to the fact that nanoparticles are black in color and the length of silica column with black color indicates the depth of nanoparticle travel which is only fraction of the total column length. However, there might be a possibility of nanoparticles escaping through the inner core which is not visible from the outer glass surface. In order to confirm complete removal of nanoparticles using silica column, collected eluted mixture of dodecane and hexane was air dried to get rid of most of the hexane and was analyzed using optical characterization.

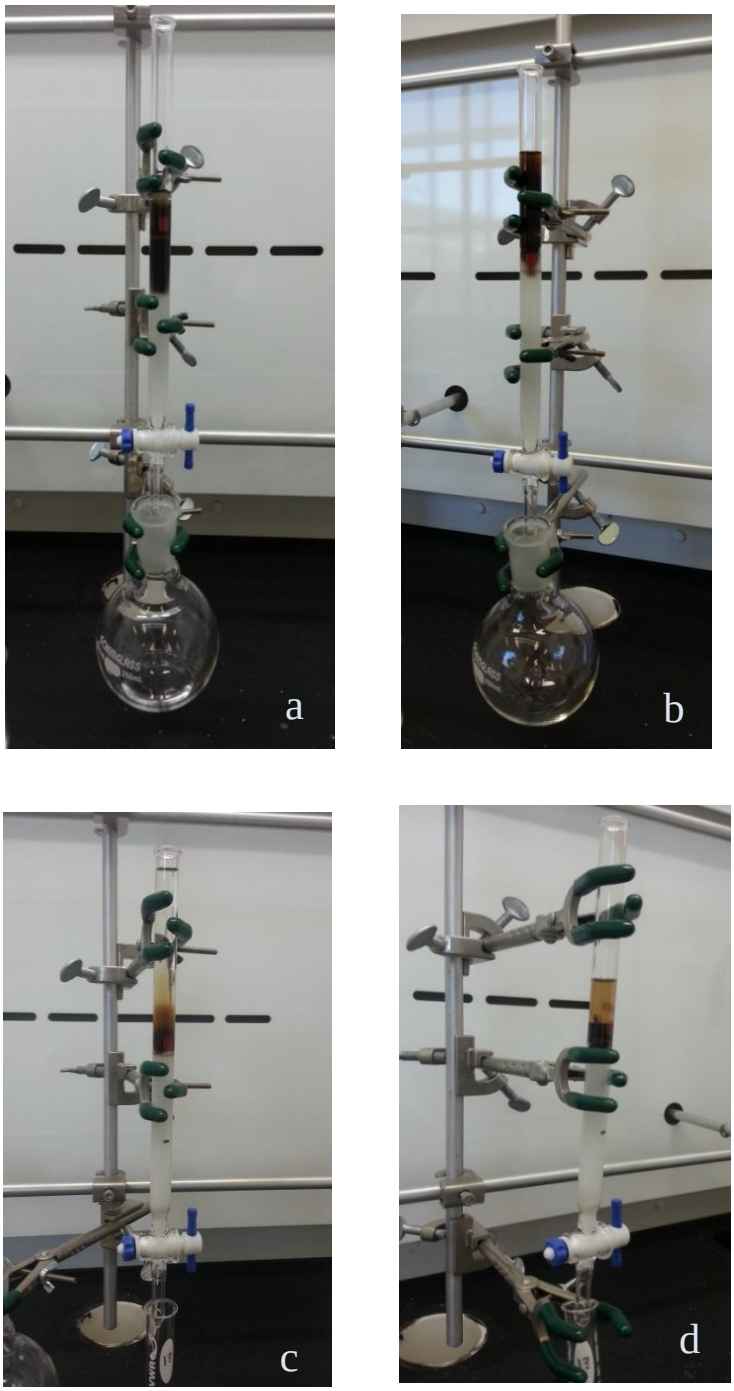

Fig. 5.27 NEPCM Chromatography

Optical characterization using Varian Cary 100 UV-Vis spectrophotometer was used to determine any trace of nanoparticles in the processed samples. UV-visible spectrometry was selected to perform analysis over other methods like electron microscopy due to its

simplicity, versatility, speed, accuracy, and cost-effectiveness. A standard quartz cuvette of size $10mm^{L}$ x $10mm^{W}$ x 40 mm^{H} was used to feed the sample. A wavelength range of 200 nm to 800 nm was used to capture data. UV-Vis scan rate was set to 600 nm/min and data interval was 1 nm. Please refer appendix (B) for additional information about UV-Vis spectrophotometry.

Fig. 5.28 shows UV-Vis spectrum of the elutant obtained after trial 3. To record data a freshly prepared sample of elutant was irradiated at 20°C by a dual source of light in the wavelength range specified before. The solution was removed at fixed times and its UV spectrum recorded until no further spectral changes occurred. To capture the data pure dodecane was used as a base or reference solution. Fig.5.28 shows three spectra namely Baseline as pure dodecane, Run1 as chromatography sample and 0.0167 wt% NEPCM sample. According to UV-Vis spectrometry principle solution containing light absorbing particles or particulate matter should produce absorbance values at specific wavelengths as evident from 0.0167 wt% NEPCM spectrum in Fig.5.28. When compared to the NEPCM spectrum, chromatography sample spectrum revealed it's free from any particles as it shows almost same absorbance values unlike NEPCM absorbance spectrum. Also chromatography sample spectrum shows same trend as that of baseline and resembles very closely to the same. This proves that using silica chromatography all the NPs have been removed from NEPCM sample.

After running silica chromatography trials, an analysis was done to understand the mechanism of nanoparticle separation through silica column. It was anticipated that a packed silica column has sub-nanosize permeability which restricts the transport of nanoparticles. Along with this hypothesis another objective of this analysis was to check the feasibility of dispersing back nanoparticles in fresh dodecane. A small amount of silica from the top part of the silica column capturing nanoparticles is collected in a beaker as a sample. A small volume

of hexane was added followed by manual stirring and shaking for 2 min. No mixing or any color change was observed for two both of the components in solution. Once the stirring/shaking is stopped a two phase solution in beaker was observed, clear hexane as top layer and black silica as bottom layer. It revealed that nanoparticles are being chemically adsorbed on the silica surface. Hence during silica column chromatography nanoparticles did not get trapped in the space between silica grains, and permeability of column was not responsible for nanoparticle capture, instead they are chemically adsorbed on silica grain surface.

Silica gel chromatography was proved to be an efficient, simple, and cost-effective alternative for nanoparticle separation from the NEPCM. Compared to two methods of column formation described, the first method using dry silica for column building, proved to be more efficient and economical as it requires shorter elusion length and is faster to construct. Elusion time required for 5 ml of mobile phase (hexane) was found to be higher due to the compactness of the column. For a less compact column, elusion time will be shorter but elusion length will be longer. Hence there is a tradeoff between elusion time and

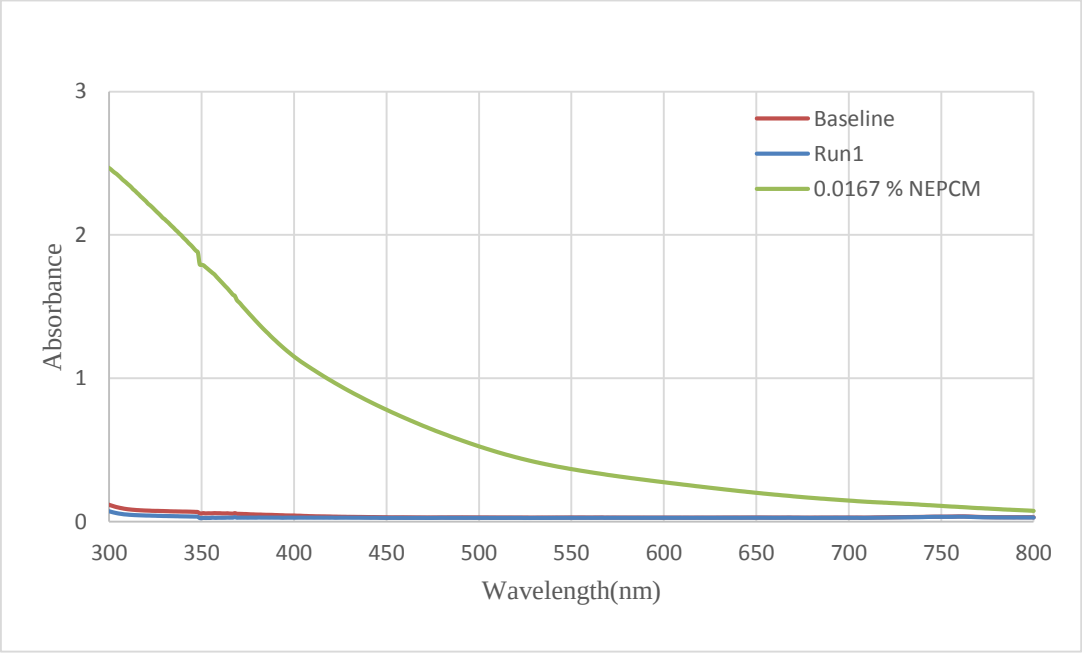

Fig. 5.28 Trial 3 (2 wt %, 1 ml NEPCM) UV-Vis spectrum.

elusion length to be considered while determining the process parameters. To have a faster elusion or shorter elusion time for a compact column additional pressure can be applied to the silica column using a pressure source like compressed air or rubber bulb. Being simple and economical silica gel chromatography can easily be scaled up to process larger amounts of NEPCM.

5.6 NANOPARTICLES ADSORPTION ON SILICA PARTICLE SURFACE

At room temperature silica can be seen coated by a mono-molecular layer of water molecules which tightly cling to its surface via extended hydrogen bonds to adjacent silanols which explains why silica is highly hydrophilic material. Silica has a moderately strong acidity, negligible basicity, and moderately strong di-polarizability. Silanol groups (≡ Si – OH) are formed on the surface by the two processes. First, during silica synthesis, e.g., condensation polymerization of $Si(OH)_4$ where the supersaturated solution of the acid is converted into spherical colloidal particles containing Si – OH (silanol) groups on the surface. Upon drying, hydrogen yields xerogel as the final product which retains some or all of the silanol groups on the surface. Secondly, surface Si – OH groups can form as a result of re-hydroxylation of de-hydroxylated silica when it is treated with water or aqueous solutions. The surface silicon atoms tend to have a complete tetrahedral configuration and in an aqueous medium their free valence becomes saturated with hydroxyl groups. The various surface properties of amorphous silica which is considered to be an oxide adsorbent depend on the presence of silanol groups. The OH groups act as the centers of molecular adsorption during their specific interaction with adsorbates capable of forming a hydrogen bond with OH groups or in general undergo donor-acceptor interaction. It is no surprise that removal of hydroxyl groups from the silica surface leads to a decrease in the adsorption [117-122].

After learning silica is acting as adsorbent for CuO nanoparticles from silica chromatography trials, experiments were performed to determine minimum amount of silica required to separate or adsorb all of the nanoparticles present in a given sample. Silica with 40-63 μm grain size (230-400 mesh), pore size 60Å in dry form was purchased from SILICYCLE, UltraPure SILICA GELS, Canada and was used as is. The black color of the nanoparticles present in NEPCM sample served as an indicator during these trials. For these trials a known volume and concentration of NEPCM was taken as a sample in a test-tube and measured amount of silica was added in a steps of 0.1 gm followed by rigorous manual shaking for 1 min. A digital scale (Mettler Toledo MS204, USA) was employed to measure the weight of silica. Solution was allowed to settle for 15 s followed by addition of more silica in the mentioned measured amount if no settling of nanoparticles with silica was observed. Once enough silica was added to adsorb all of the nanoparticles, once settled two distinct layers were observed in test-tube; a clear top layer of base fluid (dodecane) and black layer at bottom containing silica and adsorbed nanoparticles (Fig. 5.29a).A Whatman grade no. 1 filter paper of diameter 9 cm (Whatman 1001-090) was used to separate the two phases. Fig. 5.29b shows filtration process where a funnel was used in conjunction with Whatman filter. Hexane was used as a washing agent and as an aid in filtration. The filtrate which is basically a mixture of dodecane and hexane was air dried to get rid of excess hexane. The final solution containing dodecane and traces of hexane was analyzed using UV-Vis photo-spectrometry to check and confirm nanoparticles are completely removed.

Table 5.9 presents summary of the trials done for different concentrations and volumes of NEPCM. Same procedure as explained in previous section was followed to record data. Amount of silica required to adsorb all nanoparticles increases almost linearly with

nanoparticle mass concentration as evident from Fig. 5.30. This is in accordance with the adsorption mechanism explained. As concentration of nanoparticles increases silica surface area required for adsorption increases proportionally, hence amount of silica required increases. As adsorption is a surface phenomenon, grain size of silica is a critical factor to determine amount (weight) of silica required. Silica with bigger grain offers less surface area for adsorption as compared to one with smaller grains. Reported results pertains to silica with grain size of 40-63 µm, hence using silica of smaller grains, amount of silica required to capture the nanoparticles in a given NEPCM volume will be lesser in relation to grain size.

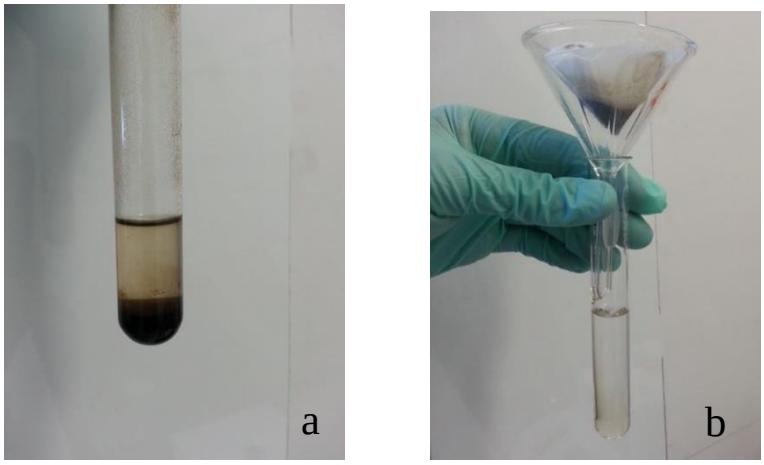

Fig. 5.29 Silica adsorbing Nanoparticles

Table 5.9: Silica adsorption trials summary.

Trial Number	NP conc. (%)	NEPCM Vol. (ml)	Silica required (mg)
1	0.5	5	750.1
2	1	5	2051.2
3	2	5	2854.4

The UV-Vis spectrum of trial 1 sample along with reference dodecane and NEPCM sample is shown in Fig. 5.30. Pure dodecane was used as a reference to capture UV spectrum of sample 1. Resulting spectrum for sample 1 was recorded 3 times and same behavior is observed. Comparing three spectra it is clear that sample 1 shows very similar behavior and absorbance values as that of base fluid dodecane and unlike NEPCM which exhibits higher absorbance values. Hence it can be said that sample 1 does not contain any impurities or particles as such

to absorb UV light. This result confirms that sample so obtained after running trial 1 is free from nanoparticles and all the particles were adsorbed by silica.

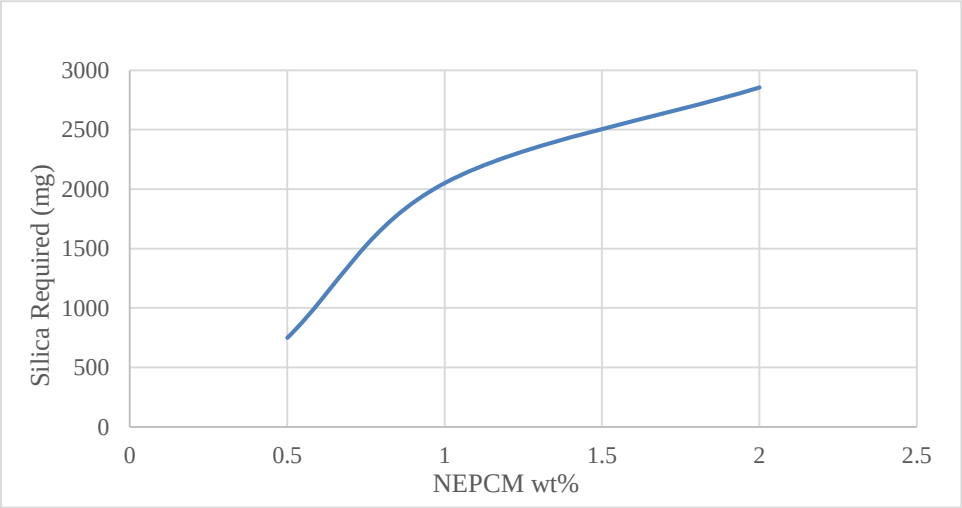

Fig. 5.30. Silica required Vs NEPCM wt%

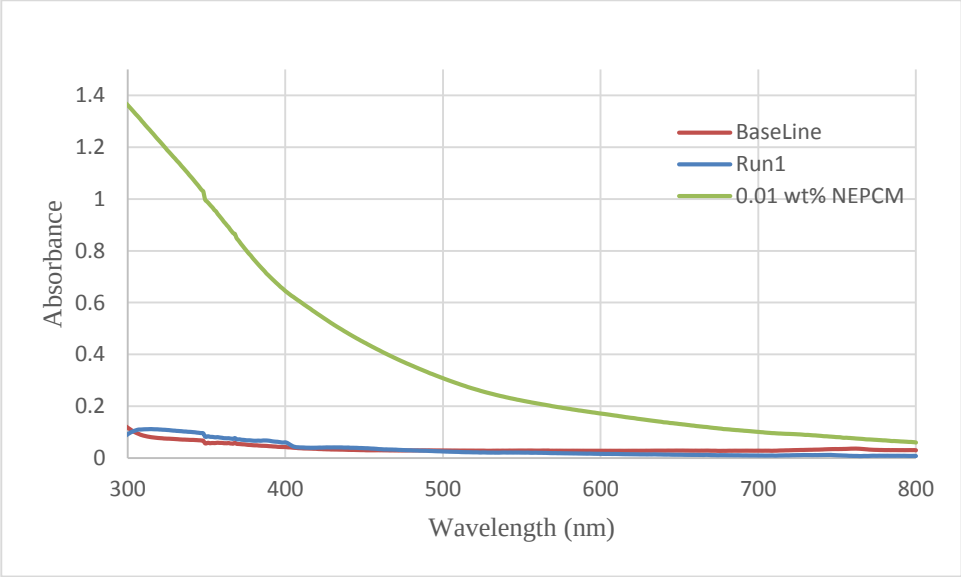

Fig. 5.31. UV Spectrum of trial 1 sample.

Fig. 5.32a shows transmission electron microscopy (TEM) image of silica grains with no nanoparticles which clearly indicates size of silica grains which ranges from 40-63 µm as per manufacturer specifications. Fig. 5.32b shows the surface structure of individual silica grain

without nanoparticles. It can be observed that the selected silica grain has a clean surface with negligible irregularities. Fig. 5.32c, d, and e show silica grains after trial 1 indicating nanoparticles adsorbed on silica grains surface. Fig. 5.32c shows adsorbed nanoparticle at lower magnification of 6,000 whereas Fig. 5.32d shows zoomed in view at a magnification of 35,000 and Fig. 5.32e shows highest possible magnification of 140,000 under applied settings.

It can be observed that even at lower magnification of 6,000 (Fig. 5.32c) the presence of nanoparticles on silica grain surface is visible. Any further close-up view like Fig. 5.32d gives a better picture clearly depicting presence of nanoparticles on the silica surface, though these particles look way bigger than the size of nanoparticles used (5 – 15 nm). Fig. 5.32e provides enough evidence to comment on the adsorption mechanism. On scale of 100 nm, Fig. 5.32e clearly shows cluster of nanoparticles forming bigger size structures which looks like a big nanoparticle as seen in Figs 5.32c and d. This cluster formation results mainly due to the presence of silanol (Si – OH) groups on the silica surface which act as oxide adsorbent. The OH groups here acts as the centers of molecular adsorption during their interaction with adsorbates (i.e., CuO nanoparticles) forming a hydrogen bond. Hence being an oxide adsorbent, silanol groups attracts more and more nanoparticles by forming hydrogen bonds with available OH groups, till saturation is reached. Saturated surface of silica is clearly visible in Fig. 5.32 e.

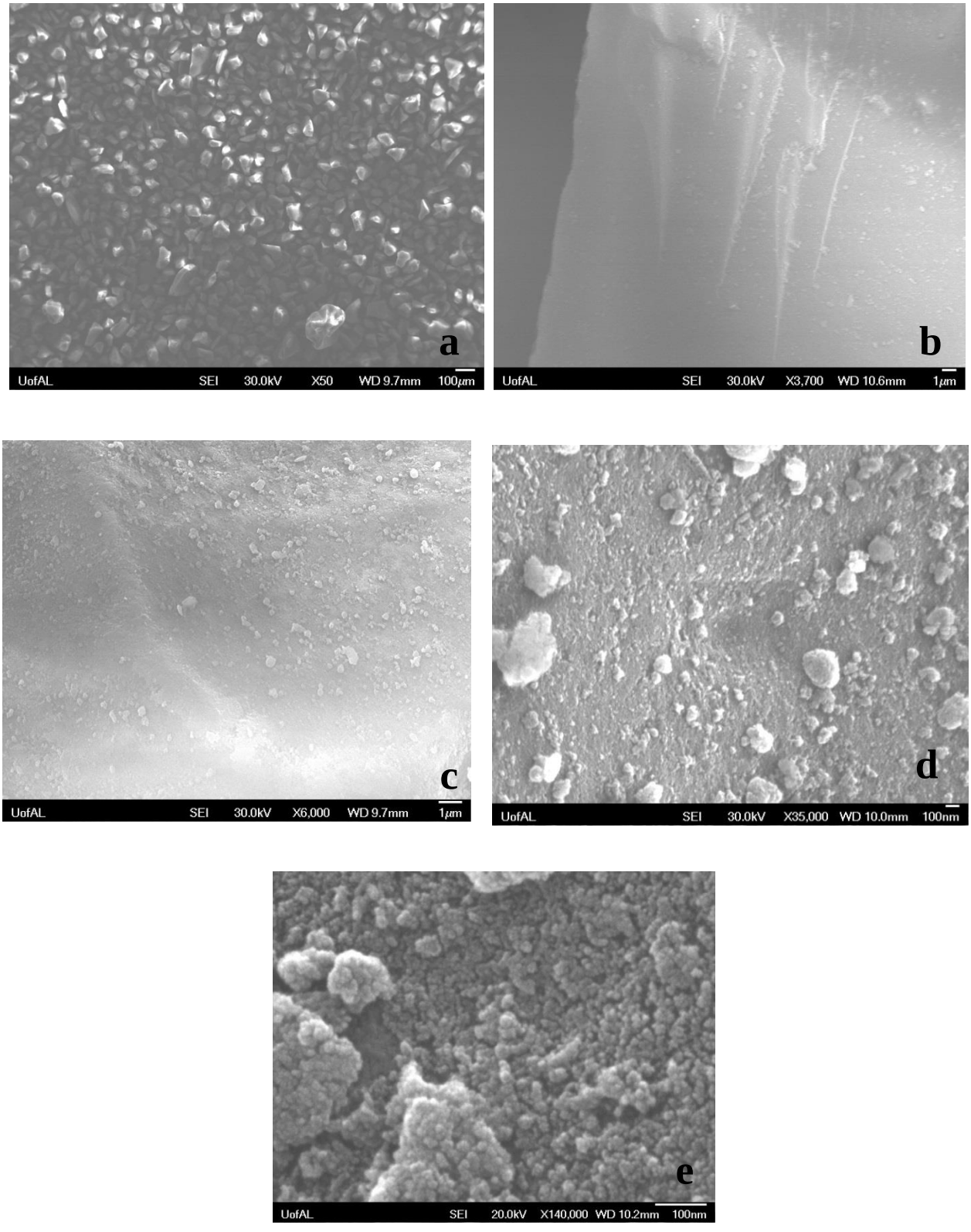

Fig.5.32 Silica Grain surface with Adsorbed Nanoparticles

Nanoparticles separation or extraction from NEPCM using silica is proved to be an efficient and simple process. Silanol groups attached on the silica surface were responsible for adsorbing copper oxide nanoparticles, due to their inherent property. As adsorption is the sole mechanism for nanoparticles extraction, interaction of silica with nanoparticles in NEPCM is the most critical factor. The interaction was achieved using manual shaking in the trials and experiments so presented. If mechanical means like a shaking unit, mixing unit could be utilized for achieving nanoparticles and silica interaction, amount of silica required would be much lesser than that used in these trials. Due to mixing at higher speed more nanoparticles would come in contact with one silica grain and would get attached thereby amount of silica required to extract all of the nanoparticles from a given sample of NEPCM will be less than that required using manual shaking.

Nanoparticles separation or extraction from NEPCM using silica is proved to be an efficient and simple process. Silanol groups attached on the silica surface were responsible for adsorbing copper oxide nanoparticles, due to their inherent property. As adsorption is the sole mechanism for nanoparticles extraction, interaction of silica with nanoparticles in NEPCM is the most critical factor. The interaction was achieved using manual shaking in the trials and experiments so presented. If mechanical means like a shaking unit, mixing unit could be utilized for achieving nanoparticles and silica interaction, amount of silica required would be much lesser than that used in these trials. Due to mixing at higher speed more nanoparticles would come in contact with one silica grain and would get attached thereby amount of silica required to extract all of the nanoparticles from a given sample of NEPCM will be less than that required using manual shaking.

5.7 NANOFILTRATION OF NEPCM

Filtration primarily works on size–exclusion principle and has been widely used to separate impurities of different size ranges, e.g., nano, micro or higher. Separation of nanoparticles or nano-size entities from a solution dates back to late 1950's when reverse osmosis (RO) was used as a process primarily for desalination of water. In 1970's relatively low pressure RO membranes were developed yielding higher water flux with added advantages of retaining essential minerals. Such membranes with lower rejections of dissolved components with higher water permeability proved to be great improvement for separation technology. These low-pressure RO membranes referred as "Nanofiltration" membranes [61,123]. For micro or bigger size impurities or particles, filtration is basically a sieving mechanism where large size entities get trapped at filter/membrane surface allowing only small entities to pass through depending on filtration membrane pore size rating. However, at nano-level, filtration becomes complex in terms of increased fouling and pressure requirements and is no longer size-exclusion dependent only. Nanometer-sized particles show unique physical and chemical properties that are different from those of bulk materials depending on their sizes and shapes due to the quantum confinement effect [63-67].

Nano-filtration is a process intermediate between reverse osmosis and ultrafiltration that rejects impurities or molecules which have sizes greater than designated rating of membrane. This range of membrane is often specified in terms of molecular weight cut-off ratio (MWCO) which is basically a number indicating capacity of membrane to hold 99% of the molecules (refer appendix E for more details) or particles of size greater than specified MWCO rating. Different membrane suppliers have different rules and guidelines to make selection of membrane for an application. Though different theoretical models have been processed since its introduction in 1980s, this method of separation mechanism has long been debated as pure convection (sieving) or pure diffusion or combination of both. Some

nanofiltration membranes known as “activated membranes” have surface charge to aid in filtration while processing charged solute or solvent in the sample [62,68,69,71,72,124].

Due to its higher separation efficiency and comparatively low operating pressures unlike reverse osmosis, nanofiltration had attracted wide variety of applications including biological, chemical, medical, etc., to separate entities like proteins, viruses, and dissolved solvents from aqueous based solutions as shown in Fig. 5.33. Hence Nanofiltration membranes are commercially available to suit wide variety of application where solvents or samples to be processed are aqueous based. Being a universal solvent with a simple chemical structure nanofiltration of water based solutions was simple to accomplish and hence variety of nanofiltration membranes were manufactured for water based solutions. This is mainly due to lower pressure requirements unlike RO and a large molecular size difference between water (dia.:0.275 nm) and entities to be separated like viruses (dia.: 20 -200 nm), and other dissolved compounds (size 1-100 nm) etc. Hence to suit different application requirements NF membranes have been manufactured in different size ratings (MWCO) and are made up of different materials like Cellulose Acetate, Cellulose Ester, mixed Cellulose, regenerated Cellulose, Polyamide, Polysulfone, Polyethersulfone, Polypropylene, etc. For aqueous based solutions, these membrane serves best by producing higher separation efficiency without degradation of membrane structure. However, for non-aqueous solutions, like organics, these membranes have limited applicability mainly due to their lower stability [125].

Hence, as most polymeric membranes have swelling and stability issues, non-aqueous nano-filtration process requires membranes made of crystalline and rigid polymers which are thermally stable, resistant to compaction, inert, and non-swelling in solvents [126-128]. Due to widespread use of non-aqueous solutions like organic solvents, solvent resistant NF membranes have been an extensive research topic since last decade. These membranes are made up from material like ceramic, metals, and solvent resistant polymers. Inorganic

membranes like one made of ceramic have been found to be suitable for extreme conditions

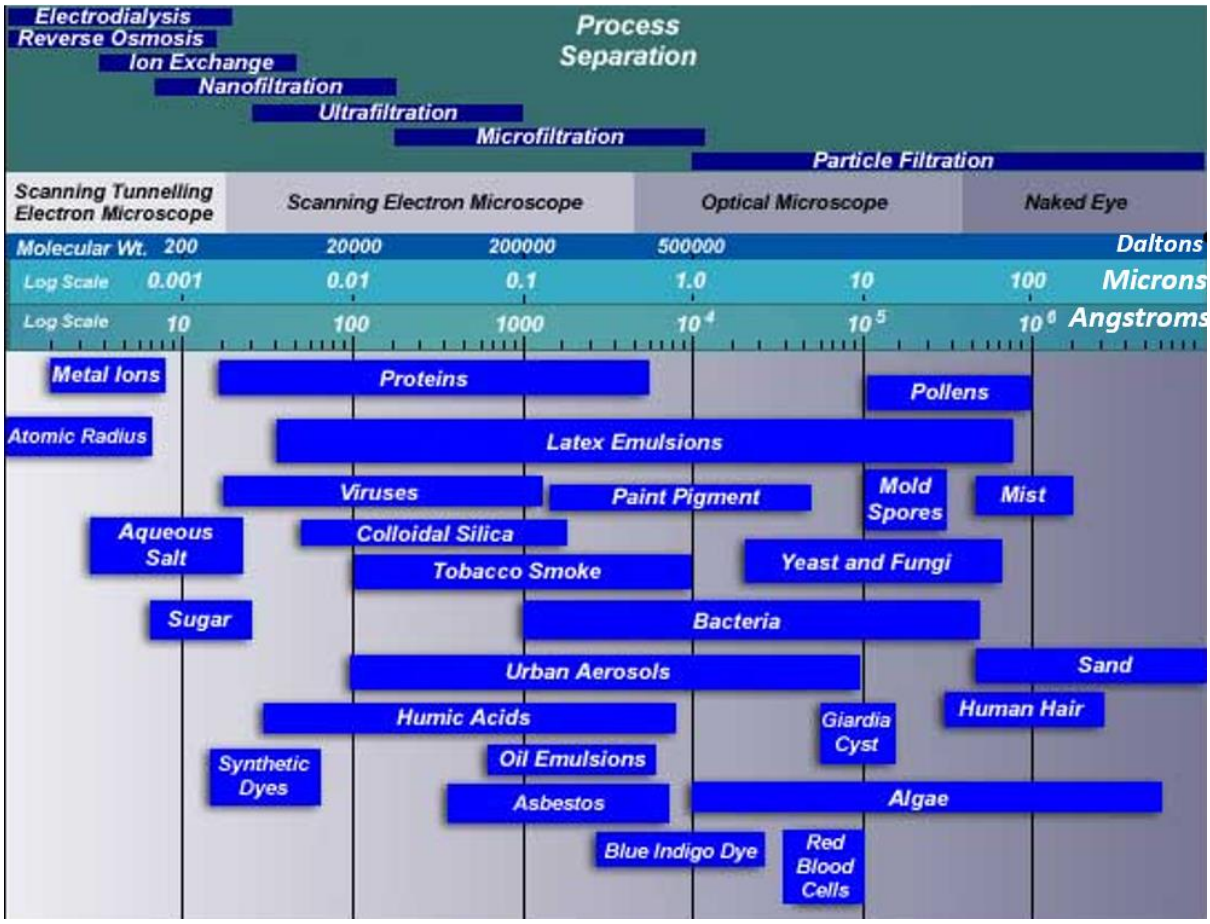

Fig. 5.33 Separation Spectrum

and higher temperature applications where polymeric membranes cannot be used. To separate NPs from NEPCM we used ceramic membrane (Fig. 5.34) purchased from "Sterlitech", Table 5.10 presents properties of the ceramic membrane.

Table 5.10 Ceramic Membrane Specifications

Manufacturer	Sterlitech
Size	47 mm dia, 2.5 mm thickness
Pore Size Range	1 kDa to 1.4 µm
Maximum Operating Pressure	4 bar (58 psi)
Operating Temperature	< 350 °C (662 °F)
pH Range	0 – 14 , 2-14 (Nanofiltration)
Sterilization	Chemical or Autoclavable

Fig. 5.34 Membrane

Nanofiltration and filtration in general can be conducted in one of the two configurations: Dead End filtration and Cross-flow (Tangential) filtration [129] as shown in Fig. 5.35. Dead end filtration works at high pressure, and depending on the concentration of solute (retentate), has inherent issue of membrane block over a period of time whereas tangential filtration is comparatively low pressure application and does not pose risk of quick membrane blockage due to retentate accumulation, hence tangential filtration is preferred for commercial applications. For lab scale applications to process small volumes of sample, cross-flow filtration is more suitable due to its limited source requirements and lower cost as compared to tangential flow filtration system. The dead-end filtration system commonly consists of membrane in combination with membrane holder or stirred cell as shown in Fig. 5.35. An in-house filter holder was designed and manufactured at university glass shop to analyze separation efficiency of ceramic membranes. Fig. 5.36 shows in-house designed and manufactured nanofiltration set-up in dismantled form. This is designed for dead-end filtration trials by incorporating features of both: membrane holder and stirred cell shown in Fig. 5.35.

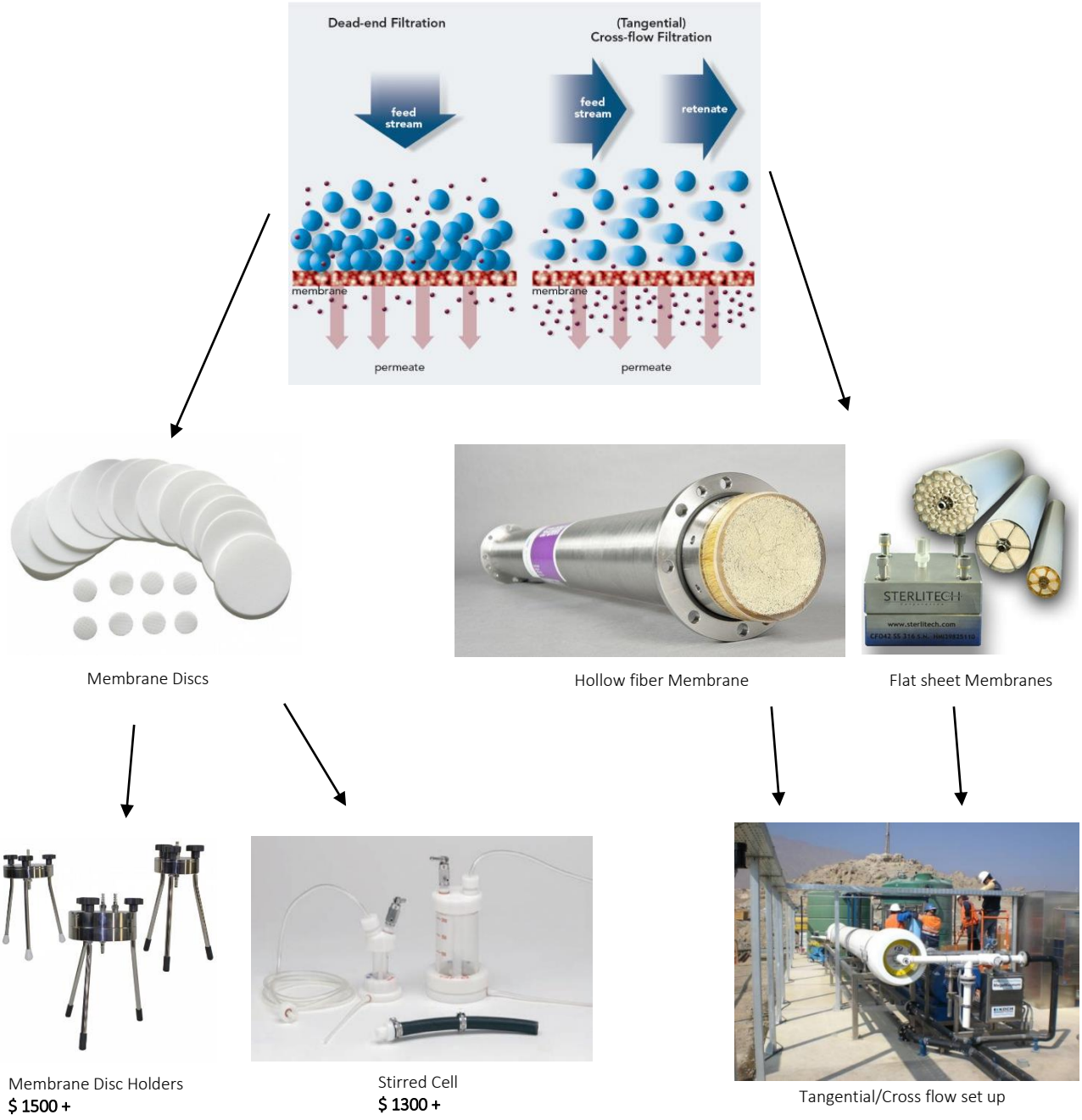

Fig. 5.35 Filtration Configuration

As shown, it consists of two glass parts: top and bottom to hold the filtration membrane in between, a pair of gaskets to provide necessary sealing and pair of clamps to hold these parts together by means of 3 bolts. Top part of the set-up is designed with two inlets to apply pressure while bottom part contains one inlet to apply vacuum (if required) or to collect filtrate. To manufacture top and glass parts of the set-up Pyrex glass tubing of size 38.1 mm

OD and 2.5 mm thickness was used which can withstand maximum internal pressure of 9 bar (131.2 psi). Glass was preferred to make the top and bottom parts of the nanofiltration set-up primarily due to its lower material and machining cost. Fig. 5.37 shows set-up in assembled form where assembly was done using 7/16 size spanner/wrench. Fig. 5.38 shows experimental set-up used to carry out trials. As shown top part is subjected to pressure using pressurized nitrogen through one of the inlet while other inlet served as a stopper or pressure relief port. Vacuum was applied at the bottom part which was required during filtration trials to improve the filtration rate.

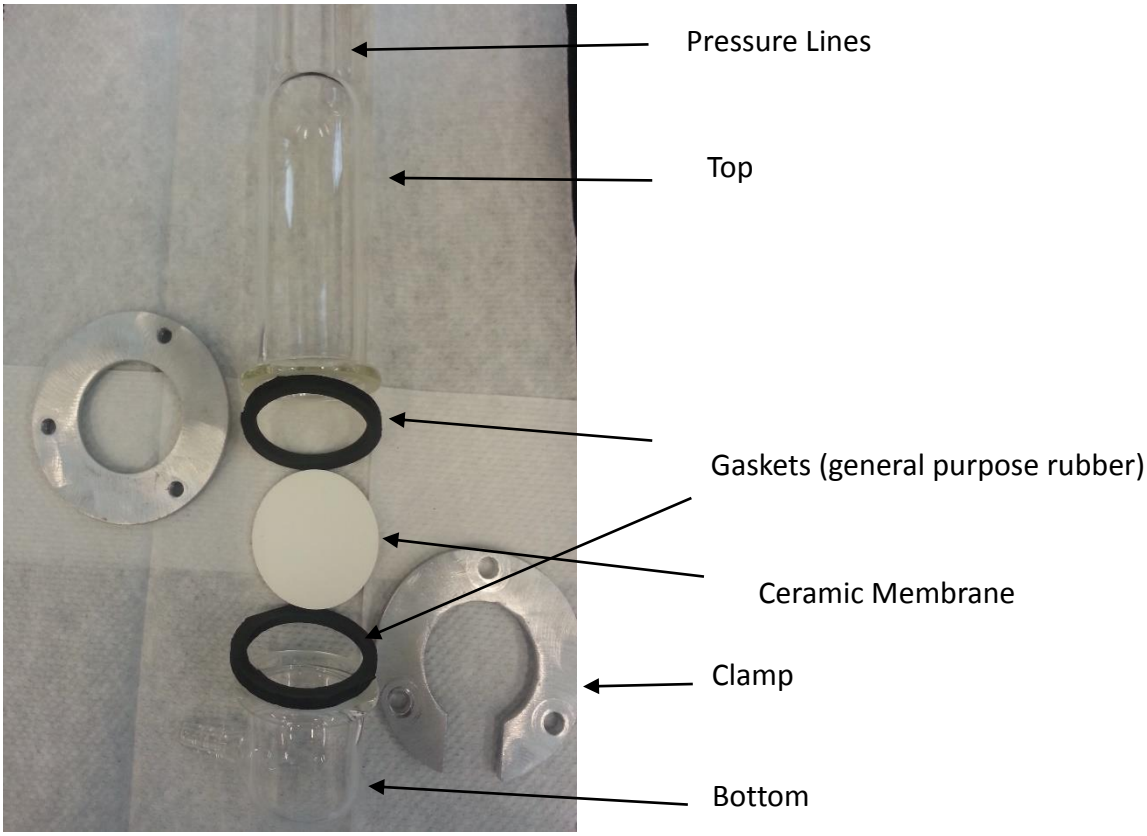

Fig. 5.36 Designed Filter Holder Parts

For dead end filtration design, there is always a possibility of membrane clogging due to capture of solute (nanoparticles) which can be minimized by stirring the solution at the membrane interface. This is one of the inbuilt feature of stirred cells shown in Fig. 5.35. Being a dead-end filtration, stirring in the present set-up is incorporated by having a stir bar on membrane interface and stirring solution during filtration operation by holding set-up on the magnetic stir plate as shown in Fig.5.38.

Fig. 5.37 Designed Filter Holder Assembly

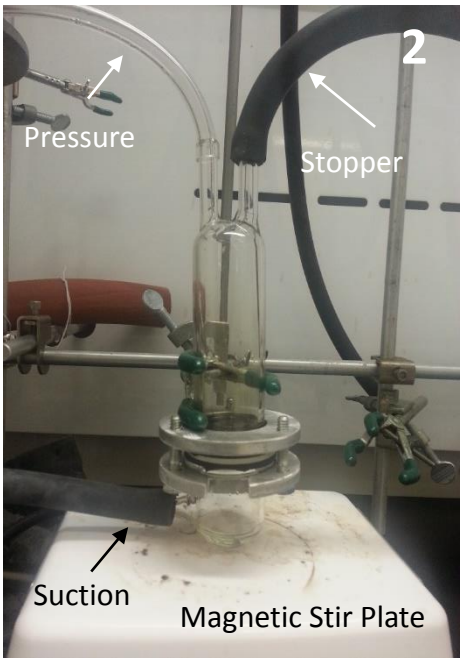

Fig. 5.38 Filtration Set-Up

The separation mechanism behind basic NF operation is ambiguous and topic of debate among researchers around the world. NF membranes are rated according to molecular weight cut-off (MWCO) (refer appendix E for details) [130-132].This rating is determined using solutes like globular proteins like albumin, bacitracin, etc., in aqueous based solutions. Hence the ratings of these membranes do not serve as a legitimate selection criteria when the entities to be separated is of non-biological type and solvent itself is non-aqueous. This was observed and confirmed after finishing initial NF trials using Ultrafiltration disk membranes of size 30 kDa and 100 kDa and Centrifugal filtration devices of pore size 3 kDa an 10 kDa of

regenerated cellulose. As per manufacturer (Pall Life Sciences) specifications, these membranes are capable of retaining particles of lower nanosize range of 1-2 nm. For the average CuO nanoparticle of size 5 nm, its molecular or particle weight was calculated as 248 kDa, whereas molecular weight of dodecane is 170.33 Da. Hence being highly tighter for NPs all these membranes should retain NPs by allowing dodecane to easily pass through. Because of their basic design filtration trials for 3 kDa and 10 kDa membrane were conducted under a centrifugal force of 8920 x gravity whereas for 30 KDa and 100 kDa trials were conducted under a vacuum of 33.6 kPa. It was observed that 3 kDa membrane could not produce any filtrate, whereas 10 kDa, 30 kDa and 100 kDa membranes could not retain most of the nanoparticles and produced black colored filtrate. Repeating above trials using the same set of membranes revealed the membrane structure had been distorted. Hence selection of membranes based on their size ratings had produced highly irrelevant results primarily due to non-aqueous application and alteration of membrane structure due to reaction with dodecane (alkane).

Experimental:

Fig. 5.39 shows filtration set-up. Top part of the filtration cell was kept under pressure using pressurized nitrogen at 1.4 bar – 2.75 bar, whereas vacuum of 0.02 mbar was applied at the bottom while the additional port at the top part served as stopper/pressure relieving port. To initiate filtration, it was required to have a vacuum on the filtrate side of membrane.

First trial was conducted for 10 ml of pure dodecane in order to study porosity or diffusing ability of the membrane which is rated as 1 kDa according to manufacturer. The set-up and procedure followed was same as explained before. Filtration started by producing filtrate in a consistent drops and was observed to be very slow. After 70 min trial time experiment was stopped which produced about 5 ml of filtrate. When compared, the collected filtrate carried

some color and looked very different from the pure dodecane feed sample (Fig. 5.40a) which bears a clear water like appearance. A close observation has shown presence of black particles around the inner perimeter of the top glass part on the surface of the filter membrane. This provided an indication that these black particles are of rubber gasket being generated due to reaction with dodecane. As rubber gaskets are supporting the ceramic membrane and providing sealing from both the sides of membrane, filtrate comes in contact with rubber gaskets before and after filtration. Due to slower filtration rate, filtrate on the downstream or permeate side gets enough time to come in contact with rubber gasket which results in generation of particles and subsequent colored filtrate as shown in Fig. 5.40b. This was further confirmed by checking chemical compatibility of organic fluids like alkane with rubber material. General purpose rubber was selected as a gasket material due to its lower cost and easy availability.

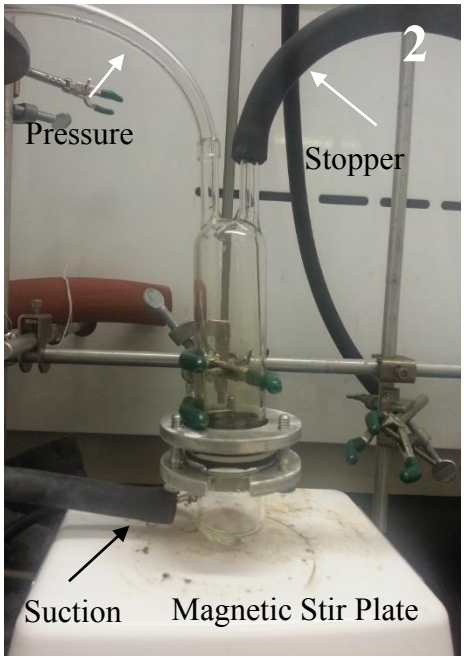

Fig. 5.39 Filtration Set-Up

Second trial was conducted using 10 ml of 0.5 wt% NEPCM by using same set up and following same procedure. Filtration is observed drop by drop and the rate of filtration was also slow for NEPCM. After a period of 70 min trial was stopped, and the filtrate collected is shown in Fig. 5.40c which bears the same color as that of dodecane filtrate due to presence of rubber particles. By visual observation of samples shown in Fig. 5.40, it can be concluded that ceramic membrane is capable of capturing all the NPs from NEPCM sample. In order to confirm the presented hypothesis these samples were analyzed using UV-Vis spectroscopy.

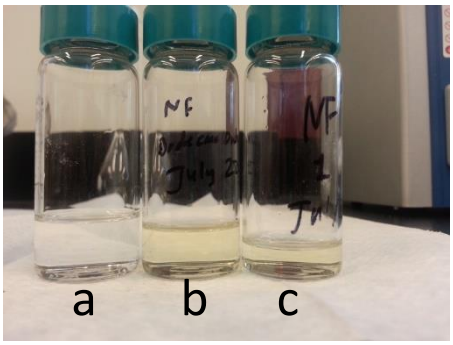

Fig. 5.40 Filtration Results

UV-Vis spectroscopy was used to analyze samples mainly due to its simplicity, speed and lower cost. Fig. 5.41 (a) shows four UV-Vis spectra presented to compare NF samples with the base fluid dodecane and concentrated NEPCM. As shown in Fig. 5.40, NF samples of dodecane and 0.5 wt% NEPCM exhibit the same color due to presence of rubber gasket particles, this is also confirmed by their respective spectra (Fig. 5.41a). This further confirms that both the filtrate sample contain same size and type of particular matter which is generated due to reaction of dodecane with gasket material (rubber). Also comparing these filtrate spectra with that of 0.0033 wt% NEPCM and dodecane reveals that filtrate spectra follows same trends as that of dodecane. Fig. 5.41b presents zoomed view of the spectra for wavelength range of 400-800 nm which clearly indicates filtrate samples are free from NPs.

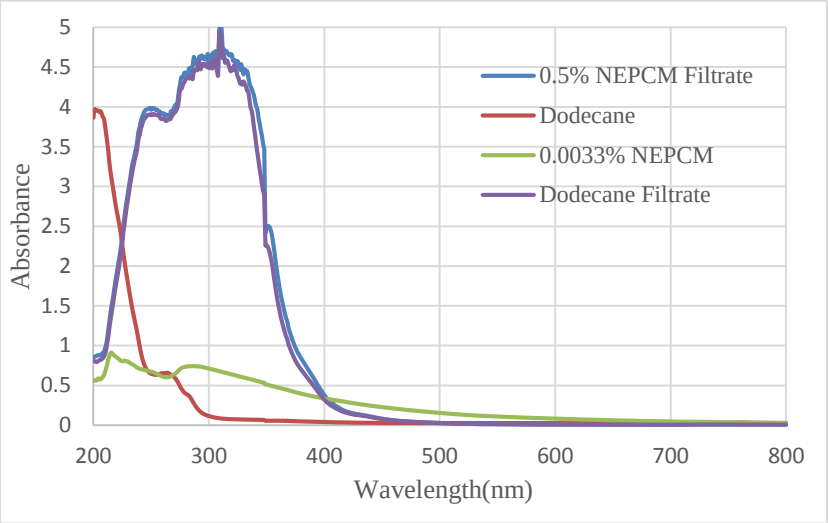

Fig. 5.41(a) UV-Vis Spectra Comparison

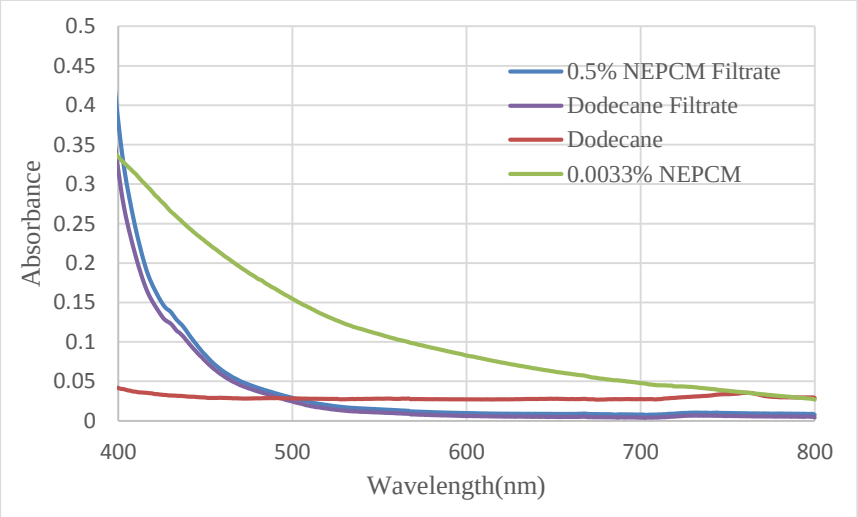

Fig. 5.41(b) UV-Vis Spectra Comparison (Zoomed In view)

Hence, based on the trial results and analysis, it can be concluded that NF using solvent resistant membrane, i.e., ceramic membrane of 1 kDa rating is capable of separating NPs by yielding 100 % separation efficiency. For the type of cost-optimized in-house designed set up and under maximum applied pressure differential of 3.75 bar (approx.) across membrane, NF was found to be a slow process. Higher filtration rates can be achieved by using membrane manufacturer recommended membrane holder in conjunction with pressurized feed.

CHAPTER 6

SEPARATION METHODS COMPARISON AND CONCLUSION

After laying project objectives, studying NEPCM morphology and literature surveys various methods looked promising to bring separation of nanoparticles from NEPCM. Using available resources keeping project objectives in mind various methods were attempted to seek separation of nanoparticles. The methods which produced positive results have been reported in Chapter 5. The methods which did not work or did not produce desired results which are not reported are: Electrophoresis, heating-thawing, reaction with strong acid, reaction with heavier alcohols, syringe filtration, vacuum filtration & centrifuge-filtration

6.1 Comparison:

Based on the experiments conducted, analysis performed and presented in chapter 5, separation methods have been compared on the basis of economical and functional parameters. Table 6.1 presents comparison summary. The comparison has been done strictly referring to the equipment used and practices followed to conduct trials. Referring to table 6.1 following conclusions can be drawn:

Table 6.1 Separation Methods Comparison

Separation Method	Equipment Cost	Material Requirement	Processing Volume	Separation Efficiency	NP Reclamation
Atm. Pressure Distillation	Low	None	Moderate	High	No
Vacuum Distillation	Moderate	None	Moderate	High	No
Chemical (alcohol) treatment	High	Low	Low	High	Yes
Centrifugation	High	None	Low	Moderate	Yes
KOH-treatment	Low	Low	Low	High	No
Silica Chromatography	Low	Moderate	Low	High	No
Silica Adsorption	Low	Moderate	Low	High	No
Nanofiltration	High	None	Moderate	High	No

1. As evident from the results presented distillation at atmospheric pressure is one of highly efficient process to separate nanoparticles from NEPCM. For the set-up used to conduct trials equipment costs was low and it did not require any material during operation other than sample. Also it was able to handle moderate volumes of NEPCM to process, which resulted in high overall efficiency. For larger NEPCM volumes to process, distillation units on industrial scale are available and has been used successfully for different applications. Hence distillation at atmospheric pressure qualifies as one of the best method to separate NPs from NEPCM. However it has one inherent limitation of slow speed and comparatively high energy consumption.
2. Vacuum distillation demands negative pressure set-up which adds to the equipment cost. However while conducting experiments it was observed that operating costs in terms of energy consumed and time taken to process a given NEPCM sample was much lower when compared to distillation at atmospheric pressure. This mode of distillation also does not exhibit any additional material requirements. Moderate volumes (about 1000 mL) of NEPCM can be easily processed using the lab scale unit utilized in this work. For higher NEPCM volume industrial scale units can be utilized. Similar to distillation at atmospheric pressure vacuum distillation yields 100 % efficiency.
3. Chemical (alcohol) treatment was proved to be another highly efficient process to separate NPs from NEPCM. This method does not demand any special set-up as only test-tubes and beakers were used to conduct experiments. However it requires a shaking unit capable of producing required momentum to attain desired result which adds to the equipment cost. As only mixture of inexpensive alcohols is required its material requirement cost is low. Presented trials were conducted to prove the functionality of the approach and record the data to provide grounds for further

research. Hence low volumes of NEPCM were processed, however using appropriate equipment this approach can be used to process higher NEPCM volumes. This method does not destabilize NPs per se by dissolving surfactants rendering NPs able to form stable NEPCM if re-dispersed back.

4. Centrifugation is another potential method to achieve NPs separation from NEPCM. Referring to the data presented in chapter 5, it can be concluded that for the maximum relative centrifugation force used (40,173 x gravity) this method yields 95% efficiency. This also clarifies that for NEPCM separation efficiency of centrifugation is factor of centrifugal force and not of duration. This method bears high equipment cost and does not demand any additional materials for NEPCM processing. Trials were conducted using low volumes of NEPCM, however advanced centrifuges offer high volume processing capabilities. Hence for higher centrifugal force centrifugation may result in higher efficiency. One of the biggest advantage of centrifugation over distillation is NPs so separated in the form of precipitation can be re-dispersed back hence centrifugation facilitates NP reclamation.
5. Separation of NPs from NEPCM via removal of surfactant using aqueous KOH is one of the most efficient and economical methods. This method does not require special equipment or expensive material to process NEPCM thus keeping equipment and material costs low. Based on the trials presented for low volumes of NEPCM, it can concluded that this method of separation can be easily scaled up to suit large NEPCM volumes.
6. Silica chromatography is capable of removing all of the NPs from NEPCM sample using low cost equipment. It demands a fine grain silica to build column which add up to material requirement cost. A lab scale unit was used to prove the concept, however chromatography columns to handle large sample volumes are readily available which

makes it suitable to process high NEPCM volumes with ease. As elusion of sample takes place solely due to gravity, this method is comparatively slower.

7. Separation of NPs form NEPCM via their adsorption on silica is one of the best methods that have been discovered during this research work. It needs fine grain silica alone to process the NEPCM sample and achieve separation. Being economical, simple and safe this method also yields high separation efficiency. Silica amount required to process a sample is directly proportional to volume and concentration of NEPCM sample. Due to its operational simplicity and safety it can be easily scaled up to process larger NEPCM volumes.
8. Nanofiltration: This is one of the separation methods which yield 100 % separation efficiency. Due to process complexity its equipment cost is high whereas material cost is low as it does not need additional materials. For the set-up used to conducted nanofiltration trails using NEPCM, processing volume was found as moderate. However using commercially available set-up nanofiltration can easily process large NEPCM volumes. All the nanoparticles so captured remains adhered to the filtration membrane rendering them un-suitable for reuse.

Hence presented methods fulfill most of the benchmarked objectives of this research work, i.e., simplicity, safety, economic, and suitability of scaling up. Every method has its advantages and disadvantages in terms of characteristics and requirements and provide a guideline to make a selection as per application objectives. Based on the observation and analysis, Vacuum distillation and Silica Adsorption proves to be the best approaches to separate NPs from NEPCM completely (with no reclamation plan). Whereas, to preserve the surfactant and re-disperse NPs, treatment of NEPCM with alcohol mixture deems best.

6.2 Future Work:

In presented research work NEPCM was prepared using dodecane as a base fluid and copper oxide nanoparticles to enhance its thermal conductivity. However depending upon application requirements which demands different phase change temperature, alkanes with a different number of carbon atoms should be used, as explained in section 1.5 of Chapter 1. Similarly instead of copper oxide, nanoparticles of materials like Ag, Cu, AlO_3 can also be utilized, choice of which is primarily governed by NEPCM stability and economic considerations. Hence, the presented work can be extended to determine the nanoparticles separation efficiency for a different base fluid or different type of nanoparticles or for a completely different NEPCM. Due to the variety of operating conditions pertaining to each separation process presented, change in NEPCM configuration might demand alterations in the processes parameters. For example; eicosane exists as a waxy solid at room temperature, hence to separate nanoparticles from an eicosane based NEPCM using one of the presented separation methods, it is required to change eicosane based NEPCM state from solid to liquid, perhaps using heating. This is due to the fact that all the presented methods are capable of processing NEPCM in liquid form. Hence future work can be directed to adjust the presented methods to suit different NEPCM configurations.

REFERENCES

(1) Kuznik F, David D, Johannes K, Roux J. A review on phase change materials integrated in building walls. Renewable and Sustainable Energy Reviews (2011) 1;15(1):379-391.

(2) Nomura T, Okinaka Ni, Akiyama T. Impregnation of porous material with phase change material for thermal energy storage. Mater Chem Phys (2009) 6/15;115(2–3):846-850.

(3) Meng Q, Hu J. A poly(ethylene glycol)-based smart phase change material. Solar Energy Mater Solar Cells (2008) 10;92(10):1260-1268.

(4) Fang G, Li H, Chen Z, Liu X. Preparation and characterization of flame retardant n-hexadecane/silicon dioxide composites as thermal energy storage materials. J Hazard Mater (2010) 9/15;181(1–3):1004-1009.

(5) Lu D, Di Y, Dou J. Crystal structures and solid–solid phase transitions on phase change materials (1−CnH2n+1NH3)2CuCl4(s) (n=10 and 11). Solar Energy Mater Solar Cells (2013) 7;114(0):1-8.

(6) Oró E, de Gracia A, Castell A, Farid MM, Cabeza LF. Review on phase change materials (PCMs) for cold thermal energy storage applications. Appl Energy (2012) 11;99(0):513-533.

(7) Salunkhe PB, Shembekar PS. A review on effect of phase change material encapsulation on the thermal performance of a system. Renewable and Sustainable Energy Reviews (2012) 10;16(8):5603-5616.

(8) Liu M, Saman W, Bruno F. Review on storage materials and thermal performance enhancement techniques for high temperature phase change thermal storage systems. Renewable and Sustainable Energy Reviews (2012) 5;16(4):2118-2132.

(9) Mehling H, Cabeza LF. Heat and cold storage with PCM:An up to date introduction into basics and applications. Germany: Springer; (2008).

(10) Gu X, Xi. P, C. B, Niu S. Synthesis and characterization of a novel solid?solid phase change luminescence material. Polym Int (2010);59(6):772-777.

(11) Xi P, Xia L, Fei P, Zhang D, Cheng B. Preparation and performance of a novel thermoplastics polyurethane solid–solid phase change materials for energy storage. Solar Energy Mater Solar Cells (2012) 7;102(0):36-43.

(12) Aydın AA, Okutan H. High-chain fatty acid esters of myristyl alcohol with odd carbon number: Novel organic phase change materials for thermal energy storage—2. Solar Energy Mater Solar Cells (2011) 8;95(8):2417-2423.

(13) Zhang Y, Wang S, Rao Z, Xie J. Experiment on heat storage characteristic of microencapsulated phase change material slurry. Solar Energy Mater Solar Cells (2011) 10;95(10):2726-2733.

(14) Farid MM, Khudhair AM, Razack SAK, Al-Hallaj S. A review on phase change energy storage: materials and applications. Energy Conversion and Management (2004) 6;45(9–10):1597-1615.

(15) Li H, Fang G-. Experimental Investigation on the Characteristics of Polyethylene Glycol/Cement Composites as Thermal Energy Storage Materials. Chem Eng Technol (2010);33(10):1650-1654.

(16) Chen C, Wang L, Huang Y. Crosslinking of the electrospun polyethylene glycol/cellulose acetate composite fibers as shape-stabilized phase change materials. Mater Lett (2009) 2/28;63(5):569-571.

(17) Kousksou T, Jamil A, Rhafiki TE, Zeraouli Y. Paraffin wax mixtures as phase change materials. Solar Energy Mater Solar Cells (2010) 12;94(12):2158-2165.

(18) Hasnain SM. Review on sustainable thermal energy storage technologies, Part I: heat storage materials and techniques. Energy Conversion and Management (1998) 8/1;39(11):1127-1138.

(19) Meshgin P, Xi Y, Li Y. Utilization of phase change materials and rubber particles to improve thermal and mechanical properties of mortar. Constr Build Mater (2012) 3;28(1):713-721.

(20) Feng L, Zheng J, Yang H, Guo Y, Li W, Li X. Preparation and characterization of polyethylene glycol/active carbon composites as shape-stabilized phase change materials. Solar Energy Mater Solar Cells (2011) 2;95(2):644-650.

(21) Zalba B, Marín JM, Cabeza LF, Mehling H. Review on thermal energy storage with phase change: materials, heat transfer analysis and applications. Appl Therm Eng (2003) 2;23(3):251-283.

(22) Cabeza LF, Mehling H, Hiebler S, Ziegler F. Heat transfer enhancement in water when used as PCM in thermal energy storage. Appl Therm Eng (2002) 7;22(10):1141-1151.

(23) Qureshi WA, Nair NC, Farid MM. Impact of energy storage in buildings on electricity demand side management. Energy Conversion and Management (2011) 5;52(5):2110-2120.

(24) Farid MM, Khalaf AN. Performance of direct contact latent heat storage units with two hydrated salts. Solar Energy (1994) 2;52(2):179-189.

(25) Abhat A. Low temperature latent heat thermal energy storage: Heat storage materials. Solar Energy (1983);30(4):313-332.

(26) Cabeza LF, Castell A, Barreneche C, de Gracia A, Fernández AI. Materials used as PCM in thermal energy storage in buildings: A review. Renewable and Sustainable Energy Reviews (2011) 4;15(3):1675-1695.

(27) Li M, Wu Z, Kao H, Tan J. Experimental investigation of preparation and thermal performances of paraffin/bentonite composite phase change material. Energy Conversion and Management (2011) 10;52(11):3275-3281.

(28) Peng S, Fuchs A, Wirtz RA. Polymeric phase change composites for thermal energy storage. J Appl Polym Sci (2004);93(3):1240-1251.

(29) Huang L, Noeres P, Petermann M, Doetsch C. Experimental study on heat capacity of paraffin/water phase change emulsion. Energy Conversion and Management (2010) 6;51(6):1264-1269.

(30) An evaluation of microencapsulated PCM for use in cold energy transportation medium. Energy Conversion Engineering Conference, 1996. IECEC 96., Proceedings of the 31st Intersociety; (1996).

(31) Web-1. www.wikipedia.com. (2012); Available at: www.wikipedia.com. Accessed 06/22, 2013.

(32) Web-2. www.sigmaaldrich.com. (2012); Available at: www.sigmaaldrich.com. Accessed 06/22, 2013.

(33) Web-3. www.us.vwr.com. (2005); Available at: www.us.vwr.com. Accessed 06/22, 2013.

(34) Ramírez-Garnica MA, Schacht-Hernández P, Mamora DD. Experimental and Analytical Studies of Hydrocarbon Yields under Dry, Steam, and Steam-Propane Distillation. - Petroleum Science and Technology (2008);26(4):369.

(35) Fan L, Khodadadi JM. An experimental investigation of enhanced thermal conductivity and expedited unidirectional freezing of cyclohexane-based nanoparticle suspensions utilized as nano-enhanced phase change materials (NePCM). International Journal of Thermal Sciences (2012) 12;62(0):120-126.

(36) Khodadadi JM, Fan L, Babaei H. Thermal conductivity enhancement of nanostructure-based colloidal suspensions utilized as phase change materials for thermal energy storage: A review. Renewable and Sustainable Energy Reviews (2013) 8;24(0):418-444.

(37) Fan L, Khodadadi JM. Thermal conductivity enhancement of phase change materials for thermal energy storage: A review. Renewable and Sustainable Energy Reviews (2011) 1;15(1):24-46.

(38) Hosokawa M, Nogi K, Naito M, Yokoyama T. Nanoparticle Technology Handbook . Netherlands: Elsevier B.V.; (2008).

(39) Charinpanitkul T, Faungnawakij K, Tanthapanichakoonb W. Review of Recent Research on Nanoparticle Production in Thailand. Advanced Powder Technology (2008);19(5):443-457.

(40) Sweet MJ, Chessher A, Singleton I. Chapter Five - Review: Metal-Based Nanoparticles; Size, Function, and Areas for Advancement in Applied Microbiology. Advances in Applied Microbiology: Academic Press; (2012). p. 113-142.

(41) Kumar P, Robins A, Vardoulakis S, Britter R. A review of the characteristics of nanoparticles in the urban atmosphere and the prospects for developing regulatory controls. Atmos Environ (2010) 12;44(39):5035-5052.

(42) Pignataro B. Ideas in Chemistry and Molecular Sciences: Advances in Nanotechnology . Weinheim: Wiley-VCH; (2010).

(43) Hornyak GL, Moore JJ, Tibbals HF, Dutta J. Fundamentals of Nanotechnology. : CRC Press; (2008).

(44) Hornyak GL, Dutta J, Tibbals HF, Rao A. Introduction to Nanoscience **
**. : CRC Press; (2008).

(45) Moudgil HK. Textbook of Physical Chemistry. India: PHI Learning Private Ltd.; (2010).

(46) Liu M,S., Lin MC,C., Huang I,T., Wang C,C. Enhancement of Thermal Conductivity with CuO for Nanofluids. Chem Eng Technol (2006);29(1):72-77.

(47) Lee S, Choi SU-, Li S, Eastman JA. Measuring Thermal Conductivity of Fluids Containing Oxide Nanoparticles. Journal of Heat Transfer (1999) May 1;121(2):280-289.

(48) Clary D, Mills G. Preparation and Thermal Properties of CuO Particles. - J Phys Chem C (2011)(- 5):1767-1775.

(49) D. Clary. The Extension of Colloid Chemistry from Aqueous to Non-Aqueous Media with Application to Nanofluid Research. Auburn,Alabama.: Auburn University; (2011).

(50) Masuda H, Ebata A, Teramae K, Hishinuma N. Alteration of Thermal Conductivity and Viscosity of Liquid by Dispersing Ultra-Fine Particles
3. - 熱物性 (1993);7(- 4):227-250.

(51) Choi USS, Eastman JA. Enhancing thermal conductivity of fluids with nanoparticles, . ASME: Developments and Application of Non-Newtonian Flows, (1995);231/66:99-105.

(52) Khodadadi JM, Hosseinizadeh SF. Nanoparticle-enhanced phase change materials (NEPCM) with great potential for improved thermal energy storage. Int Commun Heat Mass Transfer (2007) 5;34(5):534-543.

(53) Peng H, Ding G, Hu H, Jiang W. Effect of nanoparticle size on nucleate pool boiling heat transfer of refrigerant/oil mixture with nanoparticles. Int J Heat Mass Transfer (2011) 4;54(9–10):1839-1850.

(54) Eastman JA, Choi SUS, Li S, Yu W, Thompson L,J. Anomalously increased effective thermal conductivities of ethylene glycol-based nanofluids containing copper nanoparticles. (2001);78(6):718-720.

(55) Xie H, Wang J, Xi T, Liu Y, Ai F, Wu Q. Thermal conductivity enhancement of suspensions containing nanosized alumina particles. Journal of Applied Physics (2002);91(7):4568-4572.

(56) Xie H, Wang J, Xi T, Liu Y. Thermal Conductivity of Suspensions Containing Nanosized SiC Particles. International Journal of Thermophysics 2002;23(2)(- 2):571-580.

(57) Anoop KB, Sundararajan T, Das SK. Effect of particle size on the convective heat transfer in nanofluid in the developing region. Int J Heat Mass Transfer (2009) 4;52(9–10):2189-2195.

(58) Mirmasoumi S, Behzadmehr A. Effect of nanoparticles mean diameter on mixed convection heat transfer of a nanofluid in a horizontal tube. Int J Heat Fluid Flow (2008) 4;29(2):557-566.

(59) Lee S, Choi SU,S., Li S, Eastman JA. Measuring Thermal Conductivity of Fluids Containing Oxide Nanoparticles. Journal of Heat Transfer (1999) May 1;121(2):280-289.

(60) Web-1. http://www.vertellus.com/Documents/MSDS/N-Dodecane%20English.pdf. (2005); . Accessed 06/30, 2013.

(61) Lu X, Bian X, Shi L. Preparation and characterization of NF composite membrane. J Membr Sci (2002) 12/1;210(1):3-11.

(62) Van der Bruggen B, Mänttäri M, Nyström M. Drawbacks of applying nanofiltration and how to avoid them: A review. Separation and Purification Technology (2008) 10/22;63(2):251-263.

(63) Kim SH, Medeiros-Ribeiro G, Ohlberg DAA, Williams RS, Heath JR. Individual and Collective Electronic Properties of Ag Nanocrystals. - J Phys Chem B (1999);103(47):10341-10347.

(64) Burda C, Chen X, Narayanan R, El-Sayed MA. Chemistry and Properties of Nanocrystals of Different Shapes. - Chem Rev (2005);205(4):1025-1102.

(65) Collier CP, Saykally RJ, Shiang JJ, Henrichs SE, Heath JR. Reversible Tuning of Silver Quantum Dot Monolayers Through the Metal-Insulator Transition. Science (1997) September 26;277(5334):1978-1981.

(66) Henglein A. Physicochemical properties of small metal particles in solution: "microelectrode" reactions, chemisorption, composite metal particles, and the atom-to-metal transition. - J Phys Chem (1993);97(21):5457-5471.

(67) Heath JR, Sampaio JF, Heath JR. Effects of Size Dispersion Disorder on the Charge Transport in Self-Assembled 2-D Ag Nanoparticle Arrays. - J Phys Chem B (2002);106(9):2131-2135.

(68) Wang X, Shang W, Wang D, Wu L, Tu C. Characterization and applications of nanofiltration membranes: State of the art. Desalination (2009) 1/31;236(1–3):316-326.

(69) Nyström M, Kaipia L, Luque S. Fouling and retention of nanofiltration membranes. J Membr Sci (1995) 1/31;98(3):249-262.

(70) Hilal N, Al-Zoubi H, Darwish NA, Mohamma AW, Abu Arabi M. A comprehensive review of nanofiltration membranes:Treatment, pretreatment, modelling, and atomic force microscopy. Desalination (2004) 11/5;170(3):281-308.

(71) Lin Y, Sung M, Sanders PF, Marinucci A, Huang CP. Separation of nano-sized colloidal particles using cross-flow electro-filtration. Separation and Purification Technology (2007) 12/1;58(1):138-147.

(72) Payán MDR, Li B, Petersen NJ, Jensen H, Hansen SH, Pedersen-Bjergaard S. Nano-electromembrane extraction. Anal Chim Acta (2013) 6/27;785(0):60-66.

(73) Hou D, Wang J, Sun X, Ji Z, Luan Z. Preparation and properties of PVDF composite hollow fiber membranes for desalination through direct contact membrane distillation. J Membr Sci (2012) 7/1;405–406(0):185-200.

(74) Khayet M. Membranes and theoretical modeling of membrane distillation: A review. Adv Colloid Interface Sci (2011) 5/11;164(1–2):56-88.

(75) Adiche C, Sundmacher K. Experimental investigation on a membrane distillation based micro-separator. Chemical Engineering and Processing: Process Intensification (2010) 4;49(4):425-434.

(76) Lam KF, Sorensen E, Gavriilidis A. Towards an understanding of the effects of operating conditions on separation by microfluidic distillation. Chemical Engineering Science (2011) 5/15;66(10):2098-2106.

(77) Wu W, Huang J, Wu L, Sun D, Lin L, Zhou Y, et al. Two-step size- and shape-separation of biosynthesized gold nanoparticles. Separation and Purification Technology (2013) 3/14;106(0):117-122.

(78) Ansón-Casaos A, González-Domínguez JM, Martínez MT. Separation of single-walled carbon nanotubes from graphite by centrifugation in a surfactant or in polymer solutions. Carbon (2010) 8;48(10):2917-2924.

(79) Hinton RH, Al-Tamer Y, Mallinson A, Marks V. The use of density gradient centrifugation for the separation of serum lipoproteins. Clinica Chimica Acta (1974) 6/28;53(3):355-360.

(80) Xiong B, Cheng J, Qiao Y, Zhou R, He Y, Yeung ES. Separation of nanorods by density gradient centrifugation. Journal of Chromatography A (2011) 6/24;1218(25):3823-3829.

(81) Palmer SR, Sivanandan S, Huggett W. Separation of fly ash using density gradient centrifugation. Coal Science and Technology: Elsevier. p. 1999-2002.

(82) Ambashta RD, Sillanpää M. Water purification using magnetic assistance: A review. J Hazard Mater (2010) 8/15;180(1–3):38-49.

(83) Chen H, Kaminski MD, Ebner AD, Ritter JA, Rosengart AJ. Theoretical analysis of a simple yet efficient portable magnetic separator design for separation of magnetic nano/micro-carriers from human blood flow. J Magn Magn Mater (2007) 6;313(1):127-134.

(84) Dunlop EH, Feiler WA, Mattione MJ. Magnetic separation in biotechnology. Biotechnol Adv (1984);2(1):63-74.

(85) Yavuz CT, Prakash A, Mayo JT, Colvin VL. Magnetic separations: From steel plants to biotechnology. Chemical Engineering Science (2009) 5/15;64(10):2510-2521.

(86) Suwa M, Watarai H. Magnetoanalysis of micro/nanoparticles: A review. Anal Chim Acta (2011) 4/1;690(2):137-147.

(87) Liu Y, Chen M, Yongmei H. Study on the adsorption of Cu(II) by EDTA functionalized Fe3O4 magnetic nano-particles. Chem Eng J (2013) 2/15;218(0):46-54.

(88) Sun J, Xu R, Zhang Y, Ma M, Gu N. Magnetic nanoparticles separation based on nanostructures. J Magn Magn Mater (2007) 5;312(2):354-358.

(89) Ngomsik A, Bee A, Draye M, Cote G, Cabuil V. Magnetic nano- and microparticles for metal removal and environmental applications: a review. Comptes Rendus Chimie (2005) 0;8(6–7):963-970.

(90) Liu F, Ko F, Huang P, Wu C, Chu T. Studying the size/shape separation and optical properties of silver nanoparticles by capillary electrophoresis. Journal of Chromatography A (2005) 1/7;1062(1):139-145.

(91) Liu F, Tsai M, Hsu Y, Chu T. Analytical separation of Au/Ag core/shell nanoparticles by capillary electrophoresis. Journal of Chromatography A (2006) 11/10;1133(1–2):340-346.

(92) Reay D, Ramshaw C, Harvey A. Chapter 6 - Intensification of Separation Processes. Process Intensification (Second edition) Oxford: Butterworth-Heinemann; (2013). p. 205-249.

(93) Rodriguez MA, Armstrong DW. Separation and analysis of colloidal/nano-particles including microorganisms by capillary electrophoresis: a fundamental review. Journal of Chromatography B (2004) 2/5;800(1–2):7-25.

(94) Xu X, Caswell KK, Tucker E, Kabisatpathy S, Brodhacker KL, Scrivens WA. Size and shape separation of gold nanoparticles with preparative gel electrophoresis. Journal of Chromatography A (2007) 10/5;1167(1):35-41.

(95) ZHU S, ZHANG J, LI Q, LI H, JIN H, SONG Q. Separation of Metallic Single-Walled Carbon Nanotubes and Semiconducting Single-Walled Carbon Nanotubes by Agarose Gel Electrophoresis. Chinese Journal of Analytical Chemistry (2012) 12;40(12):1839-1844.

(96) Gaborieau M, Nicolas J, Save M, Charleux B, Vairon J, Gilbert RG, et al. Separation of complex branched polymers by size-exclusion chromatography probed with multiple detection. Journal of Chromatography A (2008) 5/9;1190(1–2):215-223.

(97) Liu F. Using micellar electrokinetic chromatography for the highly efficient preconcentration and separation of gold nanoparticles. Journal of Chromatography A (2009) 3/20;1216(12):2554-2559.

(98) Yang X, Pin C, Fane AG. Hollow fiber membrane chromatography: A novel analytical system for trace metal separation. Anal Chim Acta (1998) 8/10;369(1–2):17-20.

(99) Stichlmair JG, Fair JR. Distillation: Principles and Practices. : Wiley-VCH; (1998).

(100) Coker AK. Chapter 10 - Distillation: Part 1: Distillation Process Performance. Ludwig's Applied Process Design for Chemical and Petrochemical Plants (Fourth Edition) Boston: Gulf Professional Publishing; (2010). p. 1-268.

(101) Yang D, Martinez R, Fayyaz-Najafi B, Wright R. Light hydrocarbon distillation using hollow fibers as structured packings. J Membr Sci (2010) 10/15;362(1–2):86-96.

(102) Sánchez LMG, Meindersma GW, Haan AB. (2009)Potential of Silver-Based Room-Temperature Ionic Liquids for Ethylene/Ethane Separation. - Ind Eng Chem Res ;48(-23):10650-10656.

(103) Shi-chang W. Ten years' development on distillation in China. Desalination (1987);64(0):211-215.

(104) Dumitrache DC, Schutter BD, Huesman A, Dulf E. Modeling, analysis, and simulation of a cryogenic distillation process for 13C isotope separation. J Process Control (2012) 4;22(4):798-808.

(105) Alkhudhiri A, Darwish N, Hilal N. Membrane distillation: A comprehensive review. Desalination (2012) 2/15;287(0):2-18.

(106) Olujić Ž, Jödecke M, Shilkin A, Schuch G, Kaibel B. Equipment improvement trends in distillation. Chemical Engineering and Processing: Process Intensification (2009) 6;48(6):1089-1104.

(107) Sampathkumar K, Arjunan TV, Pitchandi P, Senthilkumar P. Active solar distillation—A detailed review. Renewable and Sustainable Energy Reviews (2010) 8;14(6):1503-1526.

(108) Vinoth Kumar K, Kasturi Bai R. Performance study on solar still with enhanced condensation. Desalination (2008) 9/30;230(1–3):51-61.

(109) Tiwari GN TA. Solar distillation practice for water desalination systems. : Anamaya Publishers; (2008).

(110) Tiwari GN, Dimri V, Chel A. Parametric study of an active and passive solar distillation system: Energy and exergy analysis. Desalination (2009) 6;242(1–3):1-18.

(111) Glindemann D, Maskow T, Browarzik D, Kehlen H, Kutscha J. Role of azeotropy in characterization of complex hydrocarbon mixtures by true-boiling-point distillation. Fluid Phase Equilib (1997) 8;135(2):149-167.

(112) Ligon Jr. WV. Azeotropic distillation as an enrichment strategy for determination of aromatic hydrocarbons. Anal Chim Acta (1993) 4/15;276(1):167-171.

(113) López FA, Centeno TA, Alguacil FJ, Lobato B. Distillation of granulated scrap tires in a pilot plant. J Hazard Mater (2011) 6/15;190(1–3):285-292.

(114) Web-4. Mountain Home Biological. (2011); Available at: www.pelletlab.com. Accessed 06/15, 2012.

(115) Web-5. www.thermoscientific.com. (2012); Available at: www.thermoscientific.com. Accessed 06/12, 2012.

(116) Bryant CH, Adam A, Tayior DR, Rowe RC. A review of expert systems for chromatography. Anal Chim Acta (1994) 11/10;297(3):317-347.

(117) Conference on Adsorption:Surface chemical compounds and their role in adsorption phenomena. Moscow, U.S.S.R.: Moscow University Press; (1957).

(118) Iler RK. The Chemistry of Silica: Solubility, Polymerization, Colloid and Surface Properties and Biochemistry of Silica. : Wiley-Interscience; (1979).

(119) Meier A, Gamsjäger H. Characterisation of the surface of a new amorphous microporous silica. Reactive Polymers (1989);11(0):155-163.

(120) Righetti PG, Gelfi C, Sebastiano R, Citterio A. Surfing silica surfaces superciliously. Journal of Chromatography A (2004) 10/22;1053(1–2):15-26.

(121) Zhuravlev LT. Surface characterization of amorphous silica—a review of work from the former USSR. Colloids Surf Physicochem Eng Aspects (1993) 7/6;74(1):71-90.

(122) Zhuravlev LT. The surface chemistry of amorphous silica. Zhuravlev model. Colloids Surf Physicochem Eng Aspects (2000) 11/10;173(1–3):1-38.

(123) Van der Bruggen B, Vandecasteele C. Removal of pollutants from surface water and groundwater by nanofiltration: overview of possible applications in the drinking water industry. Environmental Pollution (2003) 4;122(3):435-445.

(124) Hilal N, Al-Zoubi H, Darwish NA, Mohamma AW, Abu Arabi M. A comprehensive review of nanofiltration membranes:Treatment, pretreatment, modelling, and atomic force microscopy. Desalination (2004) 11/5;170(3):281-308.

(125) Yang XJ, Livingston AG, Freitas dos Santos L. Experimental observations of nanofiltration with organic solvents. J Membr Sci (2001) 8/31;190(1):45-55.

(126) Veríssimo SM, Silva P, Livingston AG. MEMBRANE SEPARATIONS | Nanofiltration in Organic Liquids. In: Editor-in-Chief: Ian D. Wilson, editor. Encyclopedia of Separation Science Oxford: Academic Press; (2007). p. 1-8.

(127) Silva P, Peeva LG, Livingston AG. Organic solvent nanofiltration (OSN) with spiral-wound membrane elements—Highly rejected solute system. J Membr Sci (2010) 3/1;349(1–2):167-174.

(128) Bruggen BV, Geens J, Vandecasteele C. (2002)Influence of organic solvents on the performance of polymeric nanofiltration membranes. - Separation Science and Technology ;37(4)(- 4):783-797.

(129) Bhanushali D, Kloos S, Bhattacharyya D. Solute transport in solvent-resistant nanofiltration membranes for non-aqueous systems: experimental results and the role of solute–solvent coupling. J Membr Sci (2002) 10/1;208(1–2):343-359.

(130) White LS. Transport properties of a polyimide solvent resistant nanofiltration membrane. J Membr Sci 2002 8/1;205(1–2):191-202.

(131) Silva P, Livingston AG. Effect of solute concentration and mass transfer limitations on transport in organic solvent nanofiltration — partially rejected solute. J Membr Sci 2006 9/1;280(1–2):889-898.

(132) Wijmans JG, Baker RW. The solution-diffusion model: a review. J Membr Sci (1995) 11/15;107(1–2):1-21.

APPENDIX-A

MATERIAL SAFETY DATA SHEET

Protective Clothing	NFPA Rating (USA)	EC Classification	WHMIS (Canada)	Transportation
		 Harmful	 B3 D2B	Not Regulated

Section 1: Product and Company Information

Product Name: n-Dodecane

Product Code: A-12, A-12T

Product Use: Not Available

Chemical Family: Alkanes

Synonyms: Dodecane

Manufacturer: Vertellus Health & Specialty Products LLC
300 North Meridian Street, Suite 1500
Indianapolis, Indiana 46204

Phone Number: (616) 772-2193
Fax: (616) 772-7344
24-hour Emergency: CHEMTREC: (800) 424-9300; (703) 527-3887

Section 2: Composition and Ingredient Information

Hazardous Ingredients of Product Code A-12

Common Name	Chemical Name	CAS No.	Wt.%	EINECS / ELINCS	Symbol	Risk Phrases
n-Dodecane	n-Dodecane	112-40-3	99-100	203-967-9	Xn	R36/37/38; R65

Hazardous Ingredients of Product Code A-12T

Common Name	Chemical Name	CAS No.	Wt.%	EINECS / ELINCS	Symbol	Risk Phrases
n-Dodecane	n-Dodecane	112-40-3	95-100	203-967-9	Xn	R36/37/38; R65

Note:
See Section 8 of this MSDS for exposure limit data for these ingredients.
See Section 16 for the full text of the R-phrases above.

MATERIAL SAFETY DATA SHEET

Section 3: Hazards Identification

Preparation Hazards and Classification:

Combustible liquid and vapor. Mild central nervous system depressant. Aspiration hazard. May be irritating to eyes, skin and respiratory tract.

USA: This product is a hazardous material as defined by 29 CFR1910.1200, OSHA Hazard Communication Evaluation.

Canada: This is a controlled product under WHMIS.

European Communities (EC): This substance is not classified in the Annex I of Directive 67/548/EEC. This substance is considered dangerous and has been classified according to Directive 1999/33/EC and its adaptations. Classification: Harmful.

Appearance, Color and Odor: Colorless liquid with a slight gasoline-like odor.

Primary Route(s) of Exposure: Inhalation, Ingestion, Eye contact, Skin contact

Potential Health Effects:

ACUTE (short term): see Section 8 for exposure controls

Inhalation: Because of low vapor pressure and low saturated vapor concentration of decanes, it is unlikely to produce a sufficiently high vapor concentration to cause effects unless material is heated or mists are formed. In this case depression of the central nervous system may result in drowsiness, dizziness, confusion and incoordination. Concentrated vapor may cause nose and throat irritation.

Ingestion: Decanes in general have very low oral toxicity and large amounts would have to be ingested to cause depression of the central nervous system as described for inhalation above. Based on physical properties, decanes can be easily aspirated following ingestion or vomiting. This could result in potentially fatal lung damage (pulmonary edema). Ingestion is not a typical route of occupational exposure.

Skin: Direct skin contact with decanes may cause moderate to severe irritation.

Eyes: Eye contact will probably cause moderate to severe irritation with redness and pain. Concentrated vapor is probably irritating to the eyes.

CHRONIC (long term): see Section 11 for additional toxicological data

Prolonged or repeated skin exposure may cause irritation and dermatitis (inflammation, reddening and swelling).

Medical Conditions Aggravated by Exposure: Not available

Section 4: First Aid Measures

Inhalation: Remove source of contamination or move victim to fresh air. If breathing has stopped, trained personnel should begin artificial respiration or, if the heart has stopped, cardiopulmonary resuscitation (CPR) immediately. Obtain medical attention immediately.

Eye Contact: Quickly and gently blot or brush away excess chemical. Immediately flush the contaminated eye(s) with lukewarm, gently flowing water for 5 minutes or until the chemical is removed, while holding the eyelid(s) open. Obtain medical advice immediately.

Skin Contact: Remove contaminated clothing, shoes and leather goods. Gently blot or brush away excess chemical quickly. Wash gently and thoroughly with water and non-abrasive soap for 5 minutes or until the chemical is removed. If irritation persists, obtain medical advice immediately. Completely decontaminate clothing, shoes and leather goods before re-use or discard.

Ingestion: Never give anything my mouth if victim is rapidly losing consciousness, is unconscious or convulsing. DO NOT INDUCE VOMITING. Have victim drink 240 to 300 mL (8 to 10 oz.) of water. If vomiting occurs naturally, have victim lean forward to reduce risk of aspiration. Repeat administration of water. Obtain medical attention immediately.

MATERIAL SAFETY DATA SHEET

Section 5: Fire Fighting Measures

Extinguishing Media:

Carbon dioxide, dry chemical powder, alcohol foam or polymer foam, water spray or fog.

Unusual Fire and Explosion Hazards:

Sensitivity to mechanical impact: Not sensitive
Sensitivity to static discharge: n-Dodecane can accumulate static charge by flow or agitation due to its low electrical conductivity.

Combustible liquid. Vapor can form flammable or explosive mixtures with air at, or above 74°C. Liquid can float on the top of water and travel long distances and/or spread fire. During a fire, irritating/toxic gases may be generated. Vapors from heated liquid can accumulate in confined spaces, resulting in a flammability hazard. Closed containers may rupture violently when heated.

Fire Fighting Instructions:

Evacuate area and fight fire from a safe distance. Approach fire from upwind to avoid hazardous vapors and toxic decomposition products. Stop leak before attempting to stop the fire. If the leak cannot be stopped, and if there is no risk to the surrounding area, let the fire burn itself out. If a leak or spill has not ignited, use water spray in large quantities to disperse the vapors and to protect personnel. Closed containers may explode in the heat of the fire. Fire-exposed containers should be cooled by application of hose streams. For a massive fire in a large area, use unmanned hose holder or monitor nozzles; if this is not possible withdraw from fire area and allow fire to burn. Firefighters may enter the area if positive pressure self-contained breathing apparatus (MSHA/NIOSH approved or equivalent) and full Bunker Gear is worn.

Hazardous Combustion Products:

During a fire, irritating and toxic gases, fumes and vapors may be generated. Products of combustion may include carbon monoxide, carbon dioxide and dense smoke.

Section 6: Accidental Release Measures

Personal Precautions:

Wear all proper personal protective equipment as indicated in Section 8. Prevent skin and eye contact. Avoid inhaling vapors and mists of this product. Remove all sources of ignition and heat.

Environmental Precautions:

Prevent material from contaminating soil and from entering sewers or waterways.

Methods for Containment:

Isolate the spill area. Stop the leak if it is safe to do so. Contain the liquid immediately using a suitable inert absorbent (sand, clay, vermiculite or commercial hydrocarbon absorbents).

Methods for Clean-up:

Small spills: Soak up liquid with absorbent material which does not react with spilled chemical. Put material in suitable, covered, labeled containers. Flush area with water.

Large spills: Contact fire and emergency services and supplier for advice.

Section 7: Handling and Storage

Handling

Combustible liquid. Use with adequate ventilation. Avoid generating mists and vapors. It is good practice to use combustible liquids in the smallest possible amounts, in a well-ventilated area, separate from the storage area. Avoid contact with skin and eyes. Wash thoroughly after handling. Empty containers may retain product residues.

Storage:

Store in a cool, dry area, out of direct sunlight and away from ignition sources. Keep containers closed when not in use.

MATERIAL SAFETY DATA SHEET

Section 8: Exposure Controls and Personal Protection

Exposure Limits

Ingredient	ACGIH TLV (8-hr. TWA)	U.S. OSHA PEL (8-hr. TWA)	Ontario (Canada) TWAEV	UK OEL (8-hr. TWA)
n-Dodecane	Not established	Not established	Not established	Not established

Exposure Controls

Engineering Controls: Use process enclosures, local exhaust ventilation, or other engineering controls to control sources of dust, mist or vapor.

Personal Protection:

Respiratory Protection: Not required for normal use. Wear an approved organic vapor respirator as needed to control exposure. Wear a positive pressure supplied air respirator for uncontrolled releases or when the organic vapor respirator limitations may be exceeded.

A respiratory protection program that meets OSHA's 29 CFR 1910.134 and ANSI Z88.2 requirements or European Standard EN 149 or Canadian Standards Association (CSA) Standard Z94.4-93 must be followed whenever workplace conditions warrant a respirator's use.

Skin Protection: Wear chemical protective gloves and body-covering clothing to prevent skin exposure.

Eye Protection: Wear chemical goggles. Wear a face-shield when necessary to prevent contact with skin and eyes.

Other Protective Equipment: Have a safety shower and eye-wash fountain readily available in the immediate work area.

Hygiene Measures: Remove contaminated clothing promptly. Keep contaminated clothing in closed containers. Launder contaminated clothing before re-wearing or discard. Do not eat, drink or smoke in work areas. Wash hands thoroughly after handling this material. Maintain good housekeeping. Avoid skin and eye contact. Avoid inhaling mists and vapors.

MATERIAL SAFETY DATA SHEET

Section 9: Physical and Chemical Properties

Physical State:	Liquid	**Vapor Pressure: (mm Hg @ 20°C)**	0.3 mm Hg
Appearance:	Water white (colorless)	**Vapor Density: (Air = 1)**	5.9
pH:	Not available	**Solubility in Water:**	Insoluble
Relative Density: (water = 1)	0.753 @ 25°C	**Water / Oil distribution coefficient:**	Not available
Boiling Point:	216 °C (421 °F)	**Odor Type:**	Slight gasoline-like odor
Freezing Point:	-10 °C (14 °F)	**Odor Threshold:**	Not available
Viscosity:	Not available	**Evaporation Rate: (n-Butyl Acetate = 1)**	Not available
Oxidizing Properties:	Not available	**Auto Ignition Temperature (°C):**	203 °C (397 °F)
Flash Point and Method (°C):	74 °C (165 °F) CC	**Flammability Limits (%):**	LEL: 0.6 % UEL: Not available

Section 10: Stability and Reactivity

Stability: Stable under normal temperatures and pressures.

Conditions to Avoid: Avoid heat, open flames, static discharge, sparks and other ignition sources.

Incompatible Materials: Strong oxidizing agents.

Hazardous Decomposition Products: Products of incomplete combustion may include carbon monoxide, carbon dioxide and dense smoke.

Possibility of Hazardous Reactions: Hazardous polymerization will not occur.

MATERIAL SAFETY DATA SHEET

Section 11: Toxicological Information

Acute Toxicity Data

Ingredient	LD_{50} Oral (mg/kg)	LD_{50} Dermal (mg/kg)	LC_{50} Inhalation (mg/m^3, 4 hrs.)
n-Dodecane	Not available	Not available	Not available

Chronic Toxicity Data

Carcinogenicity: The table below indicates whether each agency has listed any ingredient as a carcinogen.

Ingredient	ACGIH	IARC	NTP	OSHA
n-Dodecane	Not listed	Not listed	Not listed	Not listed

Carcinogenicity Designations:
ACGIH: American Conference of Governmental Industrial Hygienists
IARC: International Agency for Research on Cancer
NTP: National Toxicity Program
OSHA: Occupational Safety and Health Administration

Irritation: May cause eye, skin and respiratory irritation.

Sensitization: Not applicable

Neurological Effects: Not applicable

Teratogenicity: Not applicable

Reproductive Toxicity: Not applicable

Mutagenicity (Genetic Effects): Negative results have been obtained with mammalian cells in vitro.

Toxicologically Synergistic Materials: Not available

Section 12: Ecological Information

Ecotoxicity: Not available

Mobility: Not available

Persistence and degradability: Not available

Bioaccumulative potential: Not available

Other adverse effects: Not available

MATERIAL SAFETY DATA SHEET

Section 13: Disposal Considerations

Waste Disposal Method:	Do NOT dump into any sewers, on the ground or into any body of water. Store material for disposal as indicated in Section 7 Handling and Storage.
USA:	Dispose of in accordance with local, state and federal laws and regulations. RCRA Waste numbers: None listed
Canada:	Dispose of in accordance with local, provincial and federal laws and regulations.
EC:	Waste must be disposed of in accordance with relevant EC Directives and national, regional and local environmental control regulations. For disposal within the EC, the appropriate code according to the European Waste Catalogue (EWC) should be used.

Section 14: Transport Information:

U.S. Hazardous Materials Regulation (DOT 49CFR):	Not regulated
Canadian Transportation of Dangerous Goods (TDG):	Not regulated
ADR/RID:	Not regulated
IMDG:	Not regulated
Marine Pollutants:	None
ICAO/IATA :	Not regulated

MATERIAL SAFETY DATA SHEET

Section 15: Regulatory Information

NFPA Hazard Rating

Category	NFPA
Acute Health	1
Flammability	2
Instability	0

HMIS Hazard Rating

Category	HMIS
Acute Health	1
Flammability	2
Physical Hazard	0

USA

TSCA Status: This substance is listed on the TSCA inventory.

SARA Title III:
Sec. 302/304: None
Sec: 311/312: None
Sec. 313: None
CERCLA RQ None

Canada

This product has been classified in accordance with the hazard criteria of the *Controlled Products Regulations* and the MSDS contains all the information required by the *Controlled Products Regulations*.

WHMIS Classification: B3 – Combustible liquid
D2B – Material Causing Other Toxic Effects [Skin/eye irritation]

NSNR Status (New Substance Notification Regulations): This substance is listed on the Canadian Domestic Substance List (DSL).

NPRI Substances (National Pollutant Release Inventory): None

List of Volatile Organic Compounds (VOCs) Present on List of VOCs (Ontario)

EC Classification for the Substance/Preparation:

Symbol:

Harmful

Risk Phrases: R36/37/38: Irritating to eyes, respiratory system and skin.
R65: Harmful: may cause lung damage if swallowed.

Safety Phrases: S24/25: Avoid contact with skin and eyes.
S26: In case of contact with eyes, rinse immediately with plenty of water and seek medical advice.
S62: If swallowed, do not induce vomiting; seek medical advice immediately and show this container or label.

European Inventory of Cosmetic Ingredients Directive (INCI) (76/768/EEC) – Perfume and Aromatic Materials: The substance n-Dodecane is present on the INCI.

European Flavoring Substances Regulation (1999/217/EC) –Register of Flavouring Substances: The substance n-Dodecane is listed as Chemical Group 31.

MATERIAL SAFETY DATA SHEET

Denmark:	Advisory List for Self-Classification of Dangerous Substances – N;R51/53 This classification is not based on actual testing of the substance but from predictions of Quantitative Structure Activity Relationship (QSAR) models.
Australia:	Present on Inventory of Chemical Substances (AICS).
China:	Present on China Inventory.
Japan:	Existing and New Chemical Substances (ENCS): 2-10
Korea:	Existing and Evaluated Chemical Substances (KE-12826)
Philippines:	Present on inventory of Chemicals and Chemical Substances (PICCS).
New Zealand:	Present on Composite List of Single Component Substances Considered for Transfer (Dangerous Good).

Section 16: Other Information

Full Text of R-phrases appearing in Section 2:	R36/37/38: Irritating to eyes, respiratory system and skin. R65: Harmful: may cause lung damage if swallowed.

Preparation Information

Prepared by:	LEHDER Environmental Services Limited 704 Mara Street, Suite 210 Pt. Edward, ON N7V 1X4 www.lehder.com
Phone:	(519) 336-4101
Preparation Date:	December 23, 2005
Revision Date:	Not applicable
Revision Summary:	Not applicable
Disclaimer:	While LEHDER Environmental Services Limited believes that the data set forth herein is accurate, as of the date hereof, LEHDER makes no warranty with respect thereto and expressly disclaims all liability for reliance thereon. Such data is offered solely for your consideration, investigation and verification.
Manufacturer Disclaimer:	This information is furnished without warranty, expressed, or implied, except that it is accurate to the best knowledge of Vertellus Health & Specialty Products LLC. The data on this sheet relates only to the specific material designated herein. Vertellus Health & Specialty Products LLC assumes no legal responsibility for the use or reliance upon these data.
Printed Date:	September 18, 2006
Printed Summary:	Changed manufacturer from Zeeland, A Division of Rutherford Chemicals LLC to Vertellus Health & Specialty Products LLC. Changed Section 16 Manufacturer Disclaimer. Added printed date to Section 16.

APPENDIX-B

UV-Vis Spectrometry

UV-Vis Spectroscopy Principle: When a beam of electromagnetic radiation strikes an object one of the following phenomenon will result: it will be absorbed, transmitted, scattered, reflected or it will excite fluorescence. The processes concerned in absorption spectroscopy are absorption and transmission. The conditions under which absorption of the sample is examined are chosen to keep reflection, scatter and fluoresces to a minimum. Ultraviolet and visible spectroscopy is used for quantitative analysis of the samples. An optical spectrometer records the wavelengths at which absorption occurs together with the degree of absorption at each wavelength.

UV-visible analysis could be performed on metal nanoparticles dispersed in a solvent or embedded in the insulator matrix. In such cases, absorption of incident radiation takes place due to surface Plasmon resonance (SPR) of the metal nanoparticles. Surface plasmons are essentially the light waves that are trapped on the surface because of their interaction with free electrons of the metals. When metal nanoparticles are embedded in dielectric media and specimen are exposed to the electromagnetic radiation, SPR absorption band is observed at a specific wavelength depending upon the nature of the metal, matrix, size of the particles and their distribution.

Varian cary100 was used to record absorption spectra. It is a double beam, recording spectrophotometer controlled by a computer operating under MS-Windows data acquisition system Cary WinUV. It hosts tungsten halogen as a visible light source and deuterium arc for ultra-violet light and has wavelength range from 190 to 900 nm while range of visual bulb is approximately 350-900 nm. The standard procedure for initial setup and data acquisition was

followed as mentioned in device user manual. A standard quartz cuvette of size $10mm^{L}$ x $10mm^{W}$ x 40 mm^{H} was used to feed the sample. A wavelength range of 200 nm to 800 nm was used to capture data. UV-Vis scan rate was set to 600 nm/min and data interval was 1 nm.

The absorption of radiation in a sample follows the Beer-Lambert law which states that the concentration of a substance in sample (thin film/solution) is directly proportional to the 'absorbance' which is also referred as optical density or extinction. , A, of the solution.

Absorbance, A=absorptivity coefficient X concentration X cell length …….eq.1

Hence if absorptivity coefficient of a solution at a particular wavelength is known and absorbance of the solution at that wavelength is measured then using eq.1 concentration of any particulate matter can be determined. It is known that nanoparticles like silver, gold, copper which possess unique optical properties have peak plasmon resonance which varies as a function of particle diameter. For example for sub-nano size particle peak plasmon resonance occurs for lower values of wavelength with a high absorption peak while for larger diameter (>50 nm) particles plasmon resonance occurs for higher values of wavelengths with a low absorption peak.

APPENDIX-C

SORVALL RC-6 Specifications

Maximum speed(RPM)	21,000
Maximum (RCF)	x g 51,430
Maximum capacity	4 x 1,000 ml
Drive	Brushless high frequency motor
Accel/decel rates	9/10
Speed range (RPM)	300 – 21,000
Speed control accuracy(RPM)	± 25
Temperature set range °C	-20 to +40 in 1°C increments
Temperature control °C	+2 to +40
Temperature accuracy °C	±2
Ambient temperature range °C	+15 to +40
Dimensions (H x W x D) mm (inch)	1132 x 752 x 835 (44.5 x 29.6 x 32.8)
Weight kg (lb)	350 (770)
Control	Microprocessor
Programmability	30 programs
Functions	Automatic RCF; ω^2dt Integrator; Real Time Control; Pre-Cool
Run time hr/min	99/59
Electrical V (Hz)	200/208/220/230/240 (50/60), 30 A, single phase; 400 (50), 25 A, 3 phase

SM-24 Rotor Specifications

Capacity (place × ml)	24 × 16
Max. Speed (rpm)	20,000
Max. RCF (× g)	49,460

APPENDIX-D

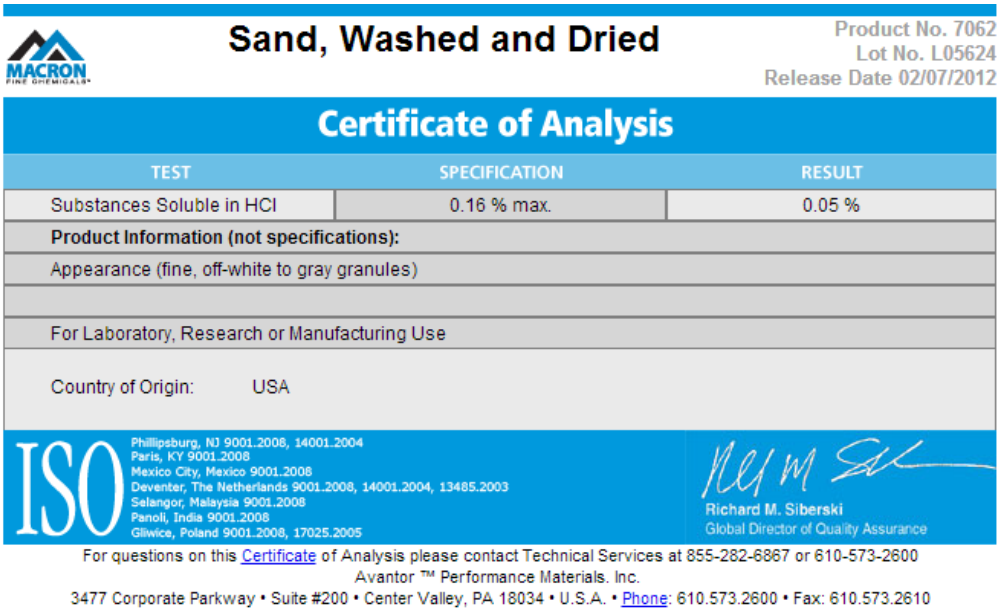

Sand, Washed and Dried

Product No. 7062
Lot No. L05624
Release Date 02/07/2012

Certificate of Analysis

TEST	SPECIFICATION	RESULT
Substances Soluble in HCl	0.16 % max.	0.05 %
Product Information (not specifications):		
Appearance (fine, off-white to gray granules)		
For Laboratory, Research or Manufacturing Use		
Country of Origin: USA		

ISO
Phillipsburg, NJ 9001.2008, 14001.2004
Paris, KY 9001.2008
Mexico City, Mexico 9001.2008
Deventer, The Netherlands 9001.2008, 14001.2004, 13485.2003
Selangor, Malaysia 9001.2008
Panoli, India 9001.2008
Gliwice, Poland 9001.2008, 17025.2005

Richard M. Siberski
Global Director of Quality Assurance

For questions on this Certificate of Analysis please contact Technical Services at 855-282-6867 or 610-573-2600
Avantor ™ Performance Materials. Inc.
3477 Corporate Parkway • Suite #200 • Center Valley, PA 18034 • U.S.A. • Phone: 610.573.2600 • Fax: 610.573.2610

APPENDIX-E

The MWCO of a membrane is defined as the molecular weight of hypothetical globular solutes (proteins) that will be 90% rejected by the membrane. For example a 10000 MWCO ultra filter will nominally reject 90% of molecules with a molecular weight of 10,000 Da. Because rejection is actually a function of physical size, shape and electrical characteristics of the molecule the MWCO is only a convenient indicator based on model solutes. Linear molecules, such as polysaccharides will tend to slip through a membrane that would reject globular molecules of the same molecular weight. There is currently no industry standard for the determination of MWCO and as such they are not always comparable amongst manufacturers. The MWCO cut-off specification is most commonly used to characterize ultrafiltration and nanofiltration membranes.

Although two membranes can be claimed to have the same cutoff, they can exhibit quite different rejection behaviors because of distribution of pore diameters. Solute retention is not absolute. A "sharp" cutoff membrane will have minimal retention for species below its nominal MWCO rating. A "diffuse" cutoff membrane can significantly retain species of a size below the nominal MWCO or allow passage of some species above its cutoff. For concentration of retained species, either sharp or diffuse cutoff membranes will generally work equally well, but where the permeate is of interest, the final product may be markedly different (*Protein Purification Protocols* by Paul Cutler).

Choosing the Correct MWCO Rating:

Once sample volume is determined, the next step is to select the appropriate MWCO (for ultrafiltration) or pore size (for microfiltration). MWCOs are nominal ratings based on the ability to retain > 90% of a solute of a known molecular weight (in Kilodaltons). For proteins, it is recommended that a MWCO be selected that is 3 to 6 times smaller than the molecular weight of the solute being retained. If flow rate is a consideration, choose a membrane with a MWCO at the lower end of this range (3X); if the main concern is retention, choose a tighter membrane (6X).

It is important to recognize that retention of a molecule by a UF membrane is determined by a variety of factors, among which its molecular weight serves only as a general indicator. Therefore, choosing the appropriate MWCO for a specific application requires the consideration of a number of factors including molecular shape, electrical charge, sample concentration, sample composition, and operating conditions. Because different manufacturers use different molecules to define the MWCO of their membranes, it is important to perform pilot experiments to verify membrane performance in a particular application (www.pall.com).